MULTIDIMENSIONAL OPTIMAL CONTROL OF WIND TURBINE GENERATOR

by

Abdulrazig Y. Alarabi

Submitted in partial fulfillment of the
requirements for the degree of
Doctor of Philosophy

at

Dalhousie University
Halifax, Nova Scotia
December 2016

To my family and friends

Table of Contents

List of Tables

List of Figures

Abstract

Small differences in wind speed can lead to huge differences in energy capture. In wind turbines, the received wind speed determines the power generation and output torque. However, as wind speed, direction and inflow angle vary across time and terrain, power systems need the ability to accurately predict wind power output from wind farms. Due to sudden variations in wind speed, direction and inflow angle, the value of the power output becomes a challenge that demands extensive study. In this thesis work, wind direction and pitch angle are used to control the performance of a wind turbine. The thesis is divided into two main parts. The first focuses on the dynamic analysis and control of a variable wind turbine rotor angle, which is represented by the rotor yaw angle and rotor angular deflection. Both the rotor yaw and rotor angular deflection control of horizontal and vertical axis wind turbine rotor are new control techniques. For dynamic analysis, rotor yaw and rotor angular deflection model techniques and experimental setup mechanisms are done step by step. The second part of the thesis describes the overall model of the multidimensional control of the wind turbine rotor. The model proposed in this research simulates the variable wind turbine rotor angle. The effects of changes in wind speed, direction and inflow angle on wind turbine generators are also considered in the proposed model, and an experimental setup is developed to evaluate acceptable changes in these factors. Three kinds of controllers were chosen to improve system stability: an integral plus pole placement, an integral plus Linear Quadratic Regulator, and a Linear Quadratic Gaussian for each actuation direction of the rotor angle. The controllers outputs indicate robust control of the rotor angle actuators and power output. Furthermore, to demonstrate the differences in energy capture, two types of wind turbines are used fixed and variable wind turbine rotor angles. The findings of this thesis regarding the impact of inflow angle on wind turbines can be applied to improve energy capture, reduce fatigue load, increase product lifetime, and improve overall performance.

List of Abbreviations

WTG	Wind Turbine Generator
WT	Wind Turbine
DC	Direct-Current
WTR	Wind Turbine Rotor
H	Generator Inertia Constant
B	Frequency Bias Factors
D	Frequency Sensitive Load Coefficient
R	Speed Regulation
RYA	Rotor Yaw Angle
RAD	Rotor Angular Deflection
PID	Propositional Integral Derivative
HAWT	Horizontal Axis Wind Turbine
VAWT	vertical Axis Wind Turbine
WD	Wind Direction
RA	Rotor Angle

List of Symbols

P_d	Wind turbine power deviation
T_d	Total aerodynamic torque deviation
ω_d	Rotor speed deviation
T_θ	Wind Direction Time Constant [sec]
T_φ	Rotor Yaw Time Constant [sec]
T_ϕ	Rotor Angular Time Constant [sec]
T_{wtg}	Wind turbine time constant [sec]
P_{mech}	Mechanical Power of Wind Turbine Generator [kW]
$P_{mech}(hat)$	Proposed Mechanical Power of Wind Turbine Generator [kW]
T_{wtg}	Turbine Time Constant [sec]
P_{wind}	Wind Power of Wind Turbine Generator [kW]

C_P	Power Coefficient
$C_P(hat)$	proposed Power Coefficient
V_w	Wind Speed [m/s]
ρ	Air Density [kg/m^3]
β	Pitch Angle [degree]
λ	Tip Speed Ratio [-]
ø	Rotor Angular Deflection [degree]
φ	Rotor Yaw Angle [degree]
ω	Turbine Rotor Speed [rad/sec]
θ	Wind Turbine Direction Angle [degree]
T_θ	Wind Direction Time Constant [sec]
T_φ	Rotor Yaw Time Constant [sec]
T_ϕ	Rotor Angular Time Constant [sec]
ΔP_L	Differential Load
K	Torque constant [N_m/A]
R_G	Terminal resistance [Ω]
L_G	Terminal inductance [H]
N	Gear ratio [-]
J_G	Generator inertia [$K_g * m^2$]
J_{GG}	Inertia of generator and gears [$K_g * m^2$]
J_r	Inertia of blades [$K_g * m^2$]
J_{tot}	Total inertia of system [$K_g * m^2$]
B	Viscous friction coefficient [$N_m/(rad/s)$]
ω_{ref}	reference rotor speed [(rad/s)]
ω_r	rotor speed output [(rad/s)]
ω_m	measured speed [(rad/s)]
R	Radius of the Wind Turbine Blade [m]
A	Swept Area of Rotor [m^2]
sec	second [s]
TF_θ	yaw direction transfer function
TF_φ	Rotor yaw angle transfer function

TFf_{ϕ}	Rotor angular deflection transfer function

Aknowledgements

I express my deepest gratitude to my supervisor and my guidance DR. Mohamed El-Hawarry, for his encouragement, valuable guidance and precious suggestions throughout the period of the research work and also for his kind co-operation in completing the research project successfully. I express my sincere thanks to my country Libya for their sponsoring me during this search I am very much grateful to my committee Dr. Jason.Gu and Dr. William , Phillips for their timely help and advice during the period of research work. I would like to thank staff in mechanical work shop for helping me fixing my experimental set-up model. I express my sincere thanks to staff in electrical and computer department, for giving me the opportunity to carry out my experimental set-up model for my research work as a Ph. D. candidate. I am very much grateful to my friend Mofth Mahmod, Ph. D. candidate for helping me in my experimental set-up. I am very much grateful to my friend Umar Farooq, Ph. D. student for helping me in choose type of controller used. I would like to thank for Dr. Hamed Aly for their support and encouragement. I also like to thank my colleagues and friends for their support and encouragement. Last but not the least, I wish to express my gratitude to my parents Mr. Younis Omar and Mrs. Fathe Mohamed , my wife Mrs. Saida Gazie and my daughter Karema for their patience, constant support and encouragement throughout the period of this research work.

Abdulrazig Younis Alarabi

Chapter 1

INTRODUCTION

1.1 Motivation

Wind energy technology has made huge strides over the past few decades. This progress has been helped along by continuously rising oil prices as well as the need to develop clean and renewable forms of energy. Large wind turbine farms are now producing electricity on a large scale, with wind energy representing the fastest growing renewable energy source (e.g., the growth has reached 30% in Europe). While the cost of wind energy was not always cheaper than that of other energy resources, it has experienced regular reductions since the early 1970s. Cost reduction continues to constitute a main concern in the field of wind energy, with research and development programs considering it a top priority. The objective is to increase the amount of energy captured from the wind with high quality specifications but reduced wind turbine costs and servicing expenses [7].

1.1.1 Economics of Wind Power Systems

One of the main advantages of generating electricity from a wind system is that wind is free, which means that the wind system is a one-time cost. Nevertheless, the success of any type of energy generation ultimately depends on the costs involved. The cost of wind power generation has been falling in recent years and is already competitive with fossil fuel and nuclear power in some countries, if social and environmental costs are also considered. The installation cost of a wind system is the capital cost of a wind turbine. Figure 1.1 shows the normalized contribution of an individual sub-system towards the total capital cost of a wind turbine, land, tower and its accessories, demonstrating that it accounts for less than any state or federal tax credits. Moreover, the maintenance cost of the wind system is normally very low, with annual maintenance fees usually running about 2% of the total system cost. However, arranging financing to purchase a wind system is significant to the overall cost of the wind system, along with extra costs such as property tax, insurance, and accidents

caused by the wind system [3]. Much effort has been made to reduce the cost of wind power

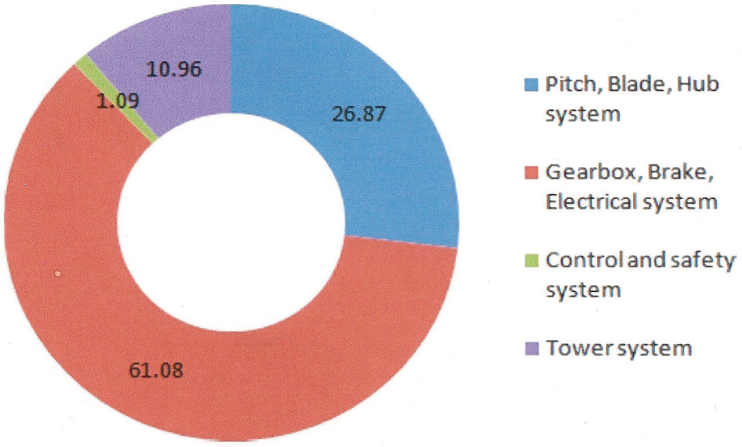

Figure 1.1: Contribution of various sub-systems towards capital cost of wind turbine [3]

through design improvements. These include developing better manufacturing technologies, finding new sites for wind systems, instituting better control strategies (output and power quality control), developing policies and instruments, and human resource development. The cost of commercial-scale, competitively-sourced wind energy has already been found to be similar to traditional sources of energy, such as fossil fuels when those prices spike on global markets, and is less expensive than most other forms of renewable energy.

1.2 Motivation for using wind turbines

The use of wind turbines is a good method for generating electricity from a clean and renewable resource. Energy derived from wind turbines has several advantages, such as [9]:

1) Harnessing a plentiful energy source: the wind.
2) Reducing our carbon footprint (i.e., the total amount of greenhouse gases used to support human activity) because it does not release any harmful gasses or pollutants in the process of generating electricity.
3) Reducing our electricity bills because wind is free and thus after the initial installation, electricity costs will be minimal.
4) Having the ability to store energy even on a calm day, so that if our houses are not connected to the National Power Grid, we can store the excess electricity produced from the wind turbine in batteries and use it even when there is no wind.

5) Having the option to sell electricity back to the grid, meaning if our wind system is producing more than we need, we can sell it to someone else.

1.3 Growing contribution of renewable energy in Canada′s electricity supply mix

Canada is a world leader in the production and use of renewable energy, with renewable energy representing 17% of its total primary energy supply. In the electricity sector, hydro-electricity is the largest renewable energy source in Canada, accounting for approximately 60% of the countrys electricity generation. Other non-hydro renewable energy sources, such as biomass, wind, tidal and solar, contribute to increasing this share by 3% to over 63%. When adding nuclear energy, over 77% of Canadas electricity generation does not emit greenhouse gases. Canada is the worlds third largest producer of hydroelectricity, and it is positioned ninth globally in terms of wind energy-installed capacity. Canada also has one of the largest tidal barrage power plants in the world the 20-megawatt (MW) Annapolis tidal power plant in Nova Scotia [3].

1.3.1 Development of renewable energy

In 2011, Canadas total electricity generation was 618 terawatt-hours (TWh) with Quebec and Ontario producing about 57% of the electricity generated in the country. The generation mix varies by province and territory, with many jurisdictions meeting over 90% of their electricity demand with renewable electricity (as shown in the map Canadas Electricity Supply Mix, 2011), while others rely on a mix of renewable, fossil fuels and nuclear generation. On a regional basis, renewable electricity generation accounts for over 52% of Western Canadas energy generation, over 65% of central Canadas energy generation, and 72% of Atlantic Canadas energy generation.

Over the last decade, renewable electricity generating capacity has expanded at a rapid pace. Hydroelectricity has consistently grown since 2002, adding an estimated 8,000 MW of installed capacity by the end of 2012. While most of the growth occurred in Quebec, British Columbia and Ontario, all provinces have increased their hydroelectricity installed capacity by some degree. According to the National Energy Board, Canadas total electricity generation in 2011 was 618 terawatt-hours (TWh), with Quebec and Ontario producing about 57% of the electricity generated in the country. While hydroelectric capacity has

grown quickly, wind and solar energy still remain the fastest growing sources of electricity in Canada. The average annual growth rate for both wind and solar has approached 40% over the past decade, although from a much smaller base. Hydroelectricity with reservoir storage plays an important role in enabling better integration of variable renewable electricity, such as wind power [3]. Over the last ten years, wind power has grown thirty-fold, reaching

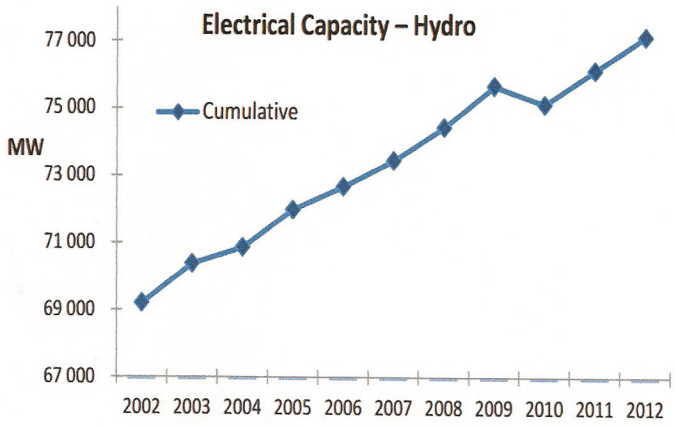

Figure 1.2: The growing electrical capacity of hydro energy [3]

6,201 MW in 2012. This is estimated to equal about 5% of total Canadian potential wind generation capacity, as shown in Figure 1.3. Currently, over 3,750 wind turbines generate electricity in 170 wind farms across the country. All provinces and two territories have wind power turbines in operation, and three provinces (Ontario, Alberta and Quebec) have surpassed the 1,000 MW threshold of installed capacity. This is in stark contrast to Canadas

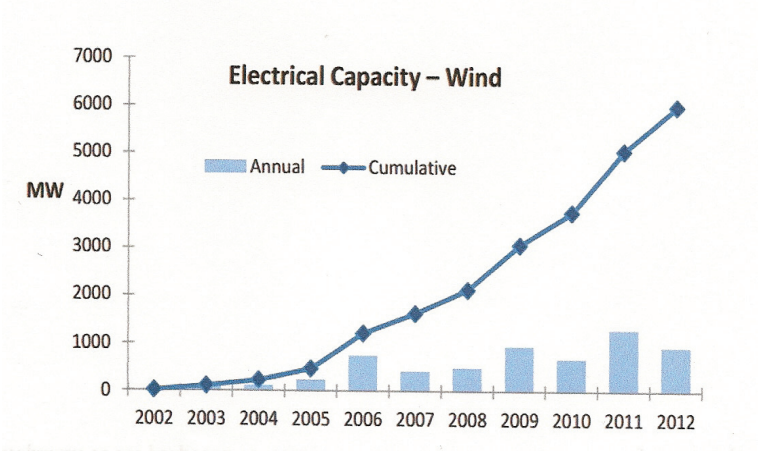

Figure 1.3: The growing electrical capacity of wind energy [3]

capacity in 2002, when just five provinces and one territory had a total of only 320 wind turbines in operation across 30 wind farms. In 2002, these wind farms amounted to only 231 MW in installed capacity. Similarly, solar photovoltaic (PV) has grown substantially, reaching 765 MW in 2012 from only 10 MW in 2002. The significant growth started in 2009 with the installation of 62 MW of solar PV capacity and continued with 186 MW in 2010, 216 MW in 2011, and 268 MW in 2012. The vast majority of these installations occurred in Ontario [3].

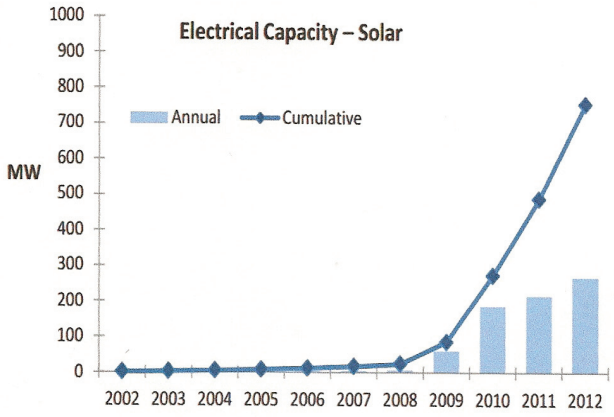

Figure 1.4: The growing electrical capacity of solar energy [3]

1.4 Wind energy for Nova Scotia

Wind energy makes good sense for Nova Scotia because each megawatt of wind power can reduce the provinces greenhouse gas emissions by enough clean energy to power 350,400 homes. Furthermore, wind energy creates local investment through land leases, municipal taxes, site preparation, construction, and operations and maintenance, and can also create a demand for local labor. To ensure a more diverse energy mix, Nova Scotia Power and the municipal electric utilities must have 40% renewable energy by 2020. Federal regulations establish a requirement for coal-fired units to meet specific emissions standards or shut down at the end of their useful life. As wind energy does not use up natural resources, capturing some of it to drive a turbine to transform the energy of wind into the energy of electricity makes no significant impact on the amount available, and thus wind can be described as infinitely renewable. The fuel for wind energy projects is free, and in Nova Scotia is subject to long-term fixed-price contracts or capital work orders resulting in renewable energy prices

that stay the same for decades [4].

Figure 1.5 shows the map of all large commercial wind farms either in operation or under development. The goal of 40% renewable electricity supplies by 2020 does not yet have the force of regulation. Despite the lack of regulation, the direction and pace the government wants to maintain in the quest for a secure sustainable energy supply is clear. To achieve

Location of all large commercial wind farms currently in Nova Scotia [4]

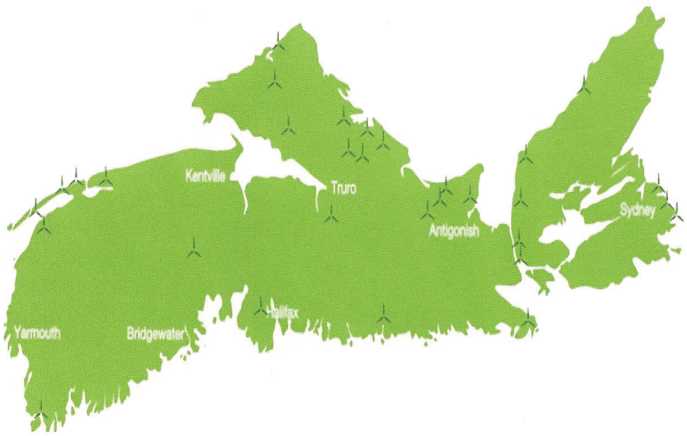

Figure 1.5: The map of all large commercial wind farms [4]

that goal, a further 1,800 GWh per year of renewable energy needs to be harnessed by 2020. Between 2009 and 2015, Nova Scotia more than doubled its renewable electricity supply, growing nearly 8 times faster than the period between 2001 and 2009. Table 1.1 shows Nova Scotias renewable electricity plan [1].

Table 1.1: Nova Scotia Renewable Electricity Plan [1]

Pre-2001	End-2009	2011	2013	2015	202
1100 GWh/yr	1300 GWh/yr	1700 GWh/yr	2300 GWh/yr	3000 GWh/yr	4800 GWh/yr
9%	11%	14%	19%	25%	%40

1.5 Types of wind turbine

Wind turbines are machines that generate electricity from the kinetic energy of wind. Historically, they were more frequently used as a mechanical device that turned machinery. Today, turbines can be used to generate large amounts of electrical energy in wind farms both onshore and offshore. There are, however, several problems that need to be taken into account when dealing with wind turbine farms.

1.5.1 Horizontal axis wind turbine

There are two kinds of wind turbine: the Horizontal Axis Wind Turbine (HAWT) and the Vertical Axis Wind Turbine (VAWT). Though many VAWTs are used nowadays to produce electricity, the HAWT still remains more practical and popular and is assumed as the focus of most wind turbine discussions. The horizontal axis wind turbine is a machine in which the axis of the rotor rotation is parallel to the wind stream and the ground. Most HAWTs today are two- or three-bladed, though some may have fewer or more blades. There are two kinds of HAWTs: the upwind wind turbine and the downwind wind turbine. HAWTs work when wind passes over both surfaces of the airfoil-shaped blade but passes more rapidly at the upper side of the blade, thus creating a lower-pressure area above the airfoil. The differences in the pressure at the top and bottom surfaces results in an aerodynamic lift. The blades of the wind turbine are constrained to move in a plane, with a hub at its center, so the lift force causes rotation about the hub. In addition to the lifting force, the drag force, which

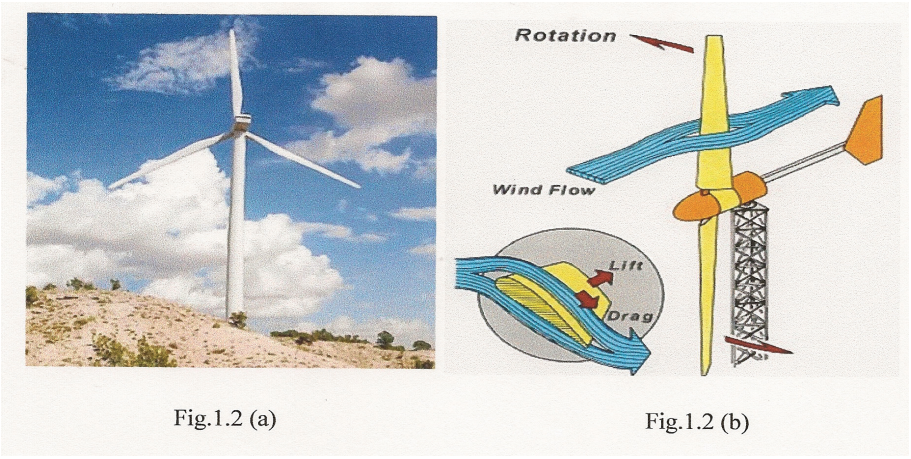

Figure 1.6: (a) Figure 1.6: (a) Photo of a horizontal axis wind turbine (HAWT); (b) diagram showing parts of a HAWT [5]

is perpendicular to the lift force, impedes rotor rotation.n.

1.5.2 Upwind turbine

The upwind turbine is a type of turbine in which the rotor faces the wind. The vast majority of wind turbines have this design. Its basic advantage is that it avoids the wind shade behind the tower. On the other hand, its main drawback is that the rotor needs to be inflexible and

placed some distance from the tower. In addition, this kind of HAWT also needs a yaw mechanism to keep the rotor facing the wind.

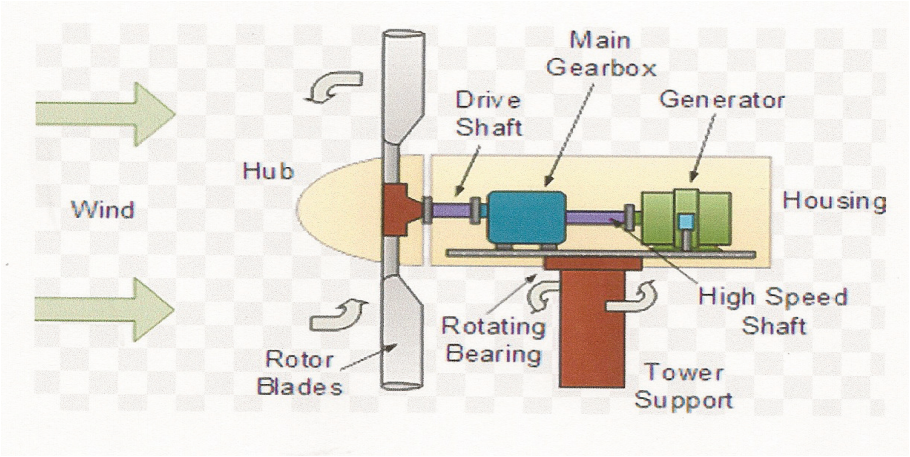

Figure 1.7: Upwind turbine design [5]

1.5.3 Downwind turbine

The downwind turbine is a turbine in which the rotor is on the downwind side (lee side) of the tower. It has the theoretical advantage that they may be built without a yaw mechanism, considering that their rotors and nacelles have a suitable design that makes the nacelle follow the wind passively. Another advantage is that the rotor may be made more flexible. Its main drawback however is the fluctuation in the wind power due to the rotor passing through the wind shade of the tower. Figure 1.8 illustrates a downwind wind turbine [5].

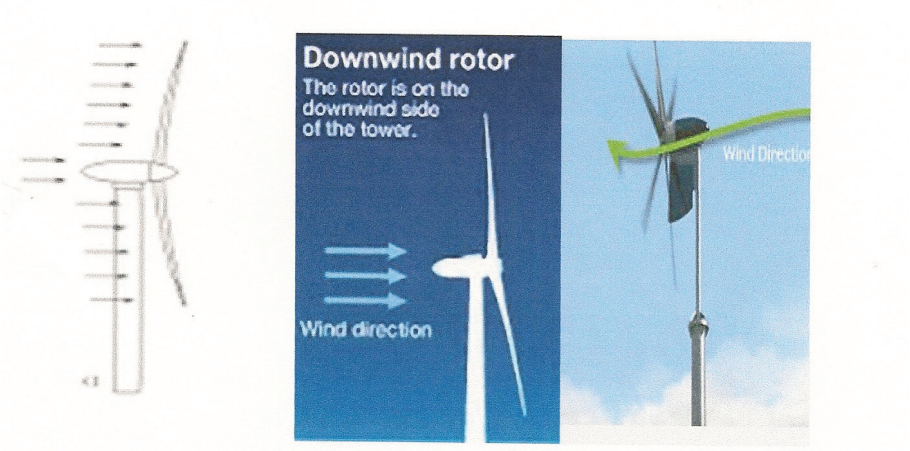

Figure 1.8: Downwind wind turbine [5]

1.6 Vertical axis wind turbines

The vertical axis wind turbine is an old technology that dates back almost 4,000 years. Unlike the HAWT, the rotor of the VAWT rotates vertically around its axis instead of horizontally. Although it is not as efficient as a HAWT, it does offer benefits in low wind situations in which HAWTs have a hard time operating. Moreover, VAWTs tend to be easier and safer to build, can be mounted close to the ground, and can handle turbulence better than HAWTs. However, because its maximum efficiency is only 30%, it is usually employed only for private use.

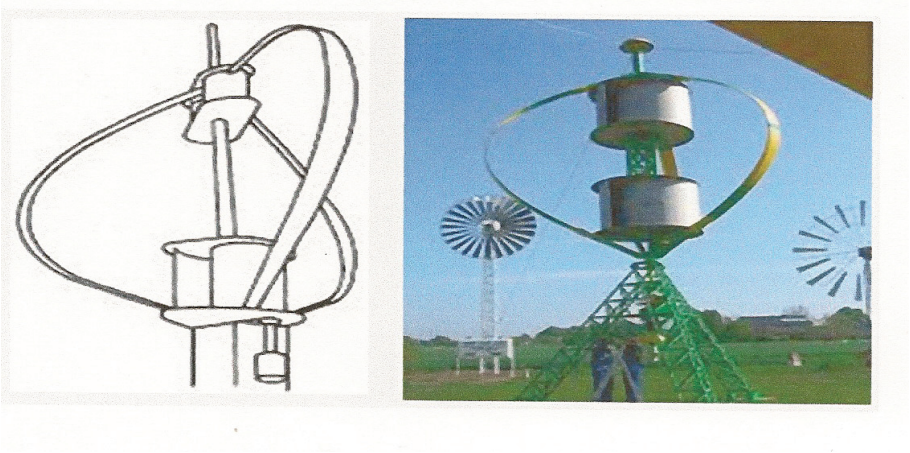

Figure 1.9: Vertical axis wind turbines [5]

1.6.1 Darrieus turbine

The Darrieus turbine is composed of a vertical rotor and several vertically oriented blades. A small powered motor is required to start its rotation, since it is not self-starting. When it achieves the necessary speed, the wind passing through the airfoils generates torque and the rotor is driven around by the wind. The Darrieus turbine is then powered by the lift forces produced by the airfoils. The blades allow the turbine to reach speeds that are higher than the actual speed of the wind, making them well-suited to electricity generation when there is a turbulent wind.

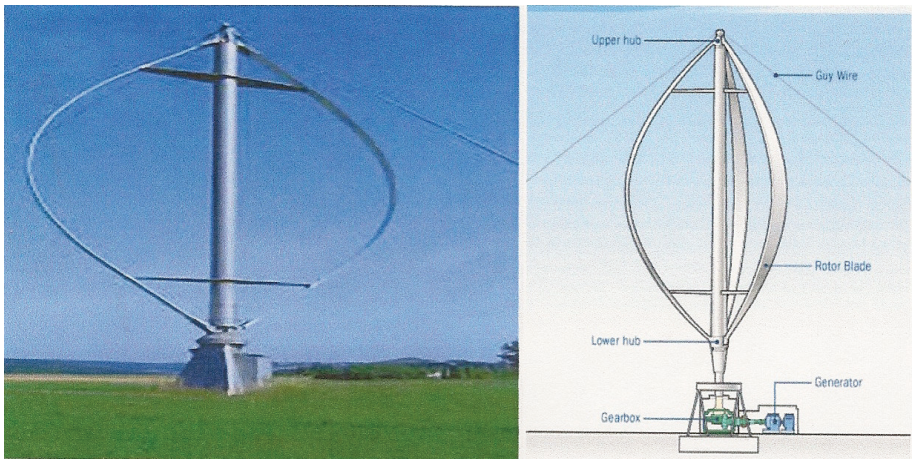

Figure 1.10: Darrieus turbine [5]

1.6.2 Savonius turbine

The Savonius wind turbine is one of the simplest turbines. It is a drag-type device that consists of two to three scoops. Because the scoop is curved, the drag when it is moving with the wind is more than when it is moving against the wind. This differential drag is what causes the Savonius turbine to spin. Because they are drag-type devices, this kind of turbine extracts much less than the wind power extracted by the previous types of turbines.

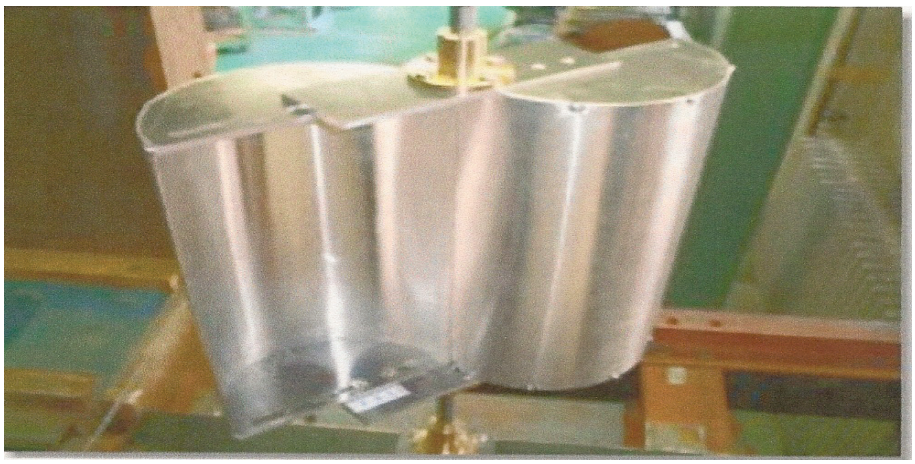

Figure 1.11: Savonius turbine [5]

1.7 Advantages and disadvantages of wind power

1.7.1 Advantages of wind power

1) Wind is free, and with modern technology can be captured efficiently.
2) Once the wind turbine is built, the energy it produces does not cause greenhouse gases or other pollutants.
3) Although wind turbines can be very tall, each takes up only a small plot of land. This means that the land below can still be used.
This is especially the case in agricultural areas, as farming can still continue.
4) Many people find wind farms an interesting feature of the landscape.
5) Remote areas that are not connected to the electricity power grid can use wind turbines to produce their own power supply.
6) Wind turbines have a role to play in both developed and developing countries.
7) Wind turbines are available in a range of sizes, which means a wide variety of people and businesses can use them.

1.7.2 Disadvantages of wind power

1) The strength of the wind is not constant and varies from zero to storm force. This means that wind turbines do not produce the same amount of electricity consistently, and that there will even be times when they produce no electricity at all.
2) Many people feel that rural areas should be left untouched and the landscape left in its natural form for everyone to enjoy, without these large structures obstructing the view.
3) Wind turbines are noisy. Each one can generate the same level of noise as a family car travailing at 70 mph 4) Many people see large wind turbines as unsightly structures that are neither pleasant nor interesting to look at. They see them as disfiguring the countryside.
5) When wind turbines are being manufactured, some pollution is produced. Therefore wind power does produce pollution.
6) Large wind farms are needed to provide entire communities with an adequate amount of electricity. For example, the largest single turbine available today can only provide enough electricity for 475 homes when running at full capacity.

1.8 Power in the wind

1.8.1 Aerodynamic principles of wind turbines

Figure 1.12(a) shows an airfoil, where the air moving at the top has a greater distance to pass before it can rejoin the air taking the shorter path under the foil. As a result, the air pressure on the top is lower than that under the airfoil. The air pressure difference creates the lifting force, which can hold up the airfoil. Wind turbine blades are more complicated than aircraft wings.

From Figure 1.12(b), we can conclude that a rotating turbine blade $feeds$ on air moving toward it not only from the wind itself, but also from the relative motion of the blade. The combination of the wind and blade motion is the resultant wind, which moves toward the blade at a certain angle. The angle between the airfoil and the wind is called the angle of attack, as shown in Figure 1.12. Increasing the angle of attack can improve the lift at the expense of increased drag. However, if we increase the angle of attack too much the wing will stall and the airflow will become turbulent and damage the turbine blades [6].

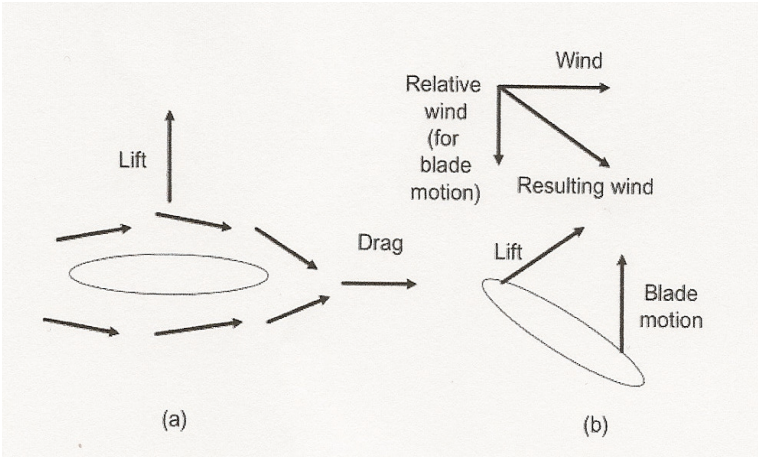

Figure 1.12: The lift in (a) is the result of faster air sliding over the top of the wind foil. In (b), the combination of actual wind and the relative wind due to blade motion creates a resultant that creates the blade lift [6]

1.8.2 Power available in the wind

The total power available in wind is equal to the product of the mass flow rate of wind $m_w, and\ V^2/2$. Assuming a constant area or ducted flow, the continuity equation states:

where ? is the density of air in kg/m3, A is the blades area in m2, and V is velocity in m/s. Thus, the total wind power, where ρ is the density of air in kg/m^3, A is the blades area in

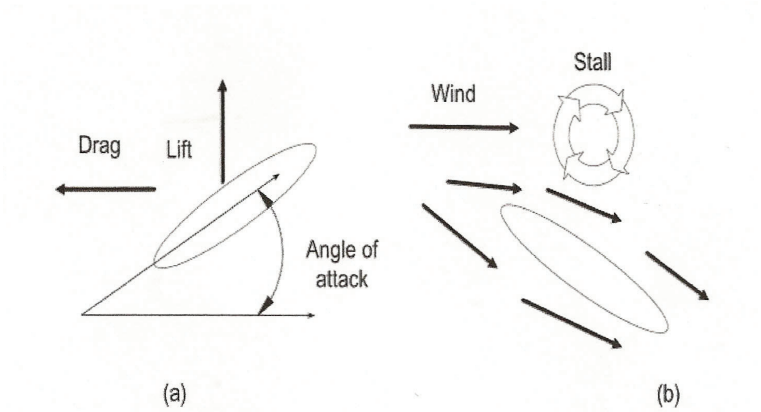

Figure 1.13: An increase in the angle of attack can cause a wing to stall [6]

m^2, and V is velocity in m/s.
Thus, the total wind power,

$$P_w = (m_w V^2)/2 = (\rho A V^3)/2 \tag{1.1}$$

1.8.3 Rotor efficiency

For a given wind speed, the rotor efficiency is a function of the rotor turning rate. If the rotor turns too slowly, the efficiency drops off because the blades are letting too much wind pass by unaffected. However, if the rotor turns too fast, the efficiency will reduce as the turbulence caused by one blade increasingly affects the blade that follows. The tip-speed ratio (TSR) is a function that illustrates rotor efficiency. The definition of the tip-speed-ratio is:

$$TSR = rotor/wind = \pi dN/60v \tag{1.2}$$

where N is rotor speed in rpm, d is the rotor diameter (m), and v is the wind speed (m/s) upwind of the turbine.

1.9 Statement of problem and thesis objectives

Among renewable energy technologies available today, wind power has emerged as one of the most promising. Wind turbine generator (WTG) output, similar to that of most other renewable energy sources, is naturally fluctuating. Therefore, it plays a different role in the power system compared to conventional power plants. If only single and small WTGs are installed in the power system, wind power does not significantly influence the operation of the power system and can easily be integrated. In contrast, as the integration of wind power into the power system increases and WTGs continue to complement conventional power plants, the impact of wind power on the power system becomes noticeable and must be taken into consideration [10].

With high wind power penetration, however, new challenges emerge to maintain the reliability and stability of the wind turbine operator. Therefore, new requirements have been established for WTGs, including taking the wind inflow angle into account. Thus the goal, is to optimize wind turbine energy capture.

1.10 Thesis objectives and contributions

This thesis presents new techniques, both practical and theoretical, within the field of controlling wind turbine energy capture. Applied mathematical and engineering control theory deals with the running of the systems to produce a desired output. The applied study deals with the wind turbine rotor (WTR) angle and wind direction. The wind turbines rotor angle and wind direction are controlled to optimize energy extraction from the wind.

In this thesis, the main focus is on the design of the controllers that optimally decrease the effect of the variability of the wind inflow angle. As showing in setup model the variability come with increase of the amount of energy capture. The angles of the wind turbine rotor and wind direction are used as the key control variables to achieve this goal. As we see in the result the compare between variability and invariability the decrease of variability come with a decease of the amount of energy capture. Approaches have been studied in which the wind turbine rotor angle and wind direction are controlled cooperatives and operate independently. The wind turbine rotor angle and wind direction have sequential and multidimensional variations with a natural surrounding wind inflow angle. Much of the thesis therefore deals with developed wind turbine models which can be used as experimental setup models for

controller design.

The theoretical study deals with rotor yaw angle models and rotor angular deflection models. The rotor yaw angle model is an optimal control method which is characterized by regulating the vertical rotor yaw angle, while the rotor angular deflection model is an optimal control method that is characterized by the use of regulating the horizontal rotor angular deflection. Rotor yaw angle models and rotor angular deflection models are new techniques used to track the wind inflow angle. Together they regulate the rotor inflow angle to keep it aligned with the wind turbine rotor. The universal market for the electrical power produced by the wind turbine generator has been increasing gradually, which makes wind technology into a more competitive field. Many customers who are environmentally aware now have the option of subscribing to clean energy such as wind energy from their power provider.

1.11 A wind turbine energy captures control

The essential purpose of a wind turbine controller is to improve the energy produced and to guarantee that this is completed without harming the wind turbine. To optimize the produced energy, the wind turbine direction and rotor angle should logically be orientated such that it is aligned with the wind direction and inflow angle. On the experimental setup wind turbine, this can be done passively if the turbine is fitted with a wind direction actuation and rotor inflow angle actuations Also on the experimental setup model, rotor actuation was used to redirect the rotor angle to tracking the wind inflow angle. At the same time, turbine direction actuation was used to redirect the wind turbine direction according to wind direction.

1.12 Problems to take into account when dealing with wind turbine farms

1.12.1 Complex flow

The wind industry defines complex flow as that which affects wind-turbine production or safety. Several parameters, such as wind shear, turbulence intensity and inflow angle, wind veer and wind speed, are useful to quantify flow complexity [2].

1.12.2 Wind shear (swinging around)

Wind shear is the variation of horizontal wind speed with height. Very large or very low wind shear implies high load on blades.

1) Increased fatigue loading

2) Reduced power output

3) Reduced availability

An average wind shear of 0.3 is usually considered acceptable by manufacturers.

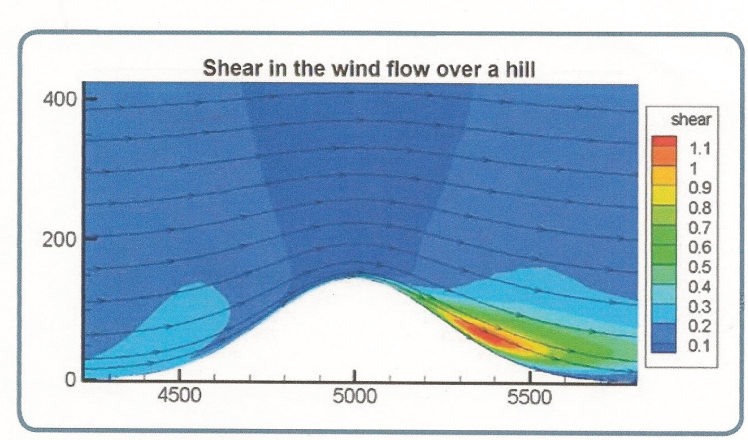

Figure 1.14: Wind shear flow over a smooth uniform hill changes on the approach and downwind side [2]

1.12.3 Turbulence intensity

Complex flow can be associated with large values of turbulence

1) Increased fatigue loading

2) Reduced power output

3) Reduced availability

1.12.4 Inflow angle

In flat terrain, wind typically reaches turbines perpendicular to the rotor. When the wind blows up a steep slope, it follows the slope close to the ground, usually reaching the rotor perpendicularly, not at an angle. This is called the inflow angle. The IEC $61400-11$ recommends that values of an inflow angle are within $\pm 8^{\circ}$ large values of the wind inflow angle effected.

1) Increased fatigue loading

2) Reduced power output

1.12.5 Summary

The IEC has developed sets of standardized wind conditions for which wind turbines are commonly designed. These conditions cover a range of mean and extreme wind speeds, a range of turbulence intensities, and a common set of conditions for wind shear and inflow angles, as shown in Table 1.2. The most arduous standard conditions are Class 1A, which is the number denoting the wind speed class and the letter denoting the turbulence class.

Table 1.2: Standardized wind conditions according to IEC 61400-1, 2005 [2]

Wind Speed Class	1	2	3
Turbulence Class	A-16%, B-14%, C-12 %	A/B/C	A/BC
Mean wind speed (m/s)	up to 10	up to 8.5	up to 7.5
Extreme 10 minute wind speed (m/s)	50	42.5	37.5
Extreme gust wind speed (m/s)	70	59.5	52.5
Mean Turbulence Intensity at 15 m/s (%)	16/14/12	16/14/12	16/14/12
Wind shear	0-0.2	0-0.2	0-0.2
Inflow angle	$\prec 8^{\circ}$	$\prec 8^{\circ}$	$\prec 8^{\circ}$

1.13 New research issues

The development, optimization and control of wind turbine energy capture must be done by ensuring that loads on the wind turbine are built with a particular increase for the lifetime of the wind turbine.That is mean when the lifetime of wind turbine increase the time of getting energy from wind turbine increase. Thus, a new adjustment in the design of wind turbines must be made. This thesis suggests a design that deals with multidimensional control. The main focus is on the design of the controllers that drive the rotor angle actuation and decrease the effect of the changeability in the wind speed inflow angle. The angles of the wind turbine rotor and wind direction have been used as the key control variables to achieve this goal.

Several approaches have been studied in which the wind turbine rotor angle and wind direction are controlled cooperatives and operate independently. This thesis deals with developed wind turbine models which can be used as experimental setup models for controller design. The theoretical study deals with rotor yaw angle models and rotor angular deflection models.

These types of models are new techniques used to track the wind inflow angle. Both regulate the rotor angle to keep it horizontal with the wind inflow angle.

1.14 Objectives

1) To develop an experimental setup model for a wind turbine rotor angle to drive the rotor angle based on a wind speed inflow angle, which augments the maximum energy capture.
2) To develop a mathematical model to introduce a strategy to control rotor speed with its output.
3) To enhance and optimize the operation and performance of wind turbine energy capture based on adding a new technique: a universal joint to control rotor angle according to wind inflow angle.
4) To introduce a strategy for adding the universal joint to the wind turbine rotor. The changeable nature of the wind inflow angle causes an increase in fatigue load on the wind turbine, which can impact on wind turbine life span.
5) To develop an enhanced control mechanism that enables a WTG to contribute to the changeability of the wind speed inflow angle, such that the stability of the WTG is maintained under different wind speed regimes.

1.15 Contributions

This thesis develops a new technique that will allow the wind turbine to have multidimensional variable rotor angle dynamics to control the wind speed inflow angle, allow the maximization of the wind turbine energy capture, and use wind direction and rotor angle to adjust the wind turbine speed. In addition, the thesis aims to reduce blade vibrations mainly in the in-plane direction. The main regulator will be developed using experimental setup models to achieve this goal, and two other models are implemented for comparison.

1.15.1 Using wind inflow angle measurements

To control the experimental setup the measurements of wind inflow angle are used to adjust the rotor angle allowing it to keep the rotor angle perpendicular to the actual wind inflow angle.

1.15.2 Wind turbine model

The wind turbine model can be combined with the rotor inflow angle model, as shown in Chapter 4. Moreover, with the model, we can determine the effects of rotor angle on wind turbine energy capture.

1.15.3 Model of multidimensional control of rotor angle turbine

The control system for the multidimensional wind turbine model can be dealt with using another models such as rotor yaw angle, rotor angular deflection, and wind direction control.

1.16 Thesis outline

This thesis consists of eight chapters. This chapter (Chapter 1) presents the research motivations, a brief description of wind turbine energy, and the thesis objectives and contributions. The second chapter provides a literature review of wind turbine energy capture and the control strategy of wind turbine-based energy capture. Chapter 3 discusses the development of the proposed mounted wind turbine rotor on a universal joint and also discusses the setup model. Chapter 4 addresses the development of the proposed experimental rotor angle setup model along with the proposed controllers for improving the stability of the wind turbine rotor angle. Chapter 5 addresses the design and development of the proposed experimental setup to achieve the goal of thesis. Chapter 6 discusses the results showing the impact of the modification adding the wind turbine rotor on energy capture. Finally, Chapters 7 and 8 provide concluding remarks about the thesis work and suggest the scope of future work.

Chapter 2

LITERATURE REVIEW

2.1 Control strategy statement of wind turbines

The essential approach to the design and operation of wind turbines is based on a first-principles methodology using conservation of mass and energy in a wind stream. To develop wind turbine energy capture capabilities, it is essential to optimize variables related to wind speed so that the wind turbine can operate close to the point of optimum power output. Improvements to energy capture through variable-speed operation can be obtained by enhancing the tracking of wind direction (WD) and predictive wind inflow angles [11, 12]. Apart from this progress, there have been many changes during the last two decades, such as the redesign of wind turbine rotor blades, shape, and individual control mechanisms. In addition, advances in energy storage technologies like storage batteries, flywheel energy storage and super-conducting magnetic energy storage equipment have led to an increase in investment in the use of wind turbines as viable sources of electrical energy [13, 14].

Modeling allows the improvement of complete control algorithms and assistance in the optimal operation of a wind turbine. The wind turbine speed model is important for the understanding of the performance of the wind turbine control system over its region of operation. Optimizing manufacturing costs leads to a decrease in the cost of wind energy, making it economically feasible as an alternative source of energy [15, 16].

. The micro-controller-based supervisor, conventional controller, self-tuning controller, and adaptive controller designs have been explored. The main new progress in controller de- development in this area is the application of artificial intelligence techniques such as neural networks, fuzzy logic and genetic algorithms to solve problems related to the design of controllers with nonlinear models or those lacking knowledge about the system. The aerodynamic pitch angle control showed a continuous improvement in energy production [17, 18, 19, 20].

While the details of the control systems used in wind turbines may vary considerably from one installation to another, they all have common elements which are considered in the design of any controller. This is illustrated using a simple wind turbine model that permits the display of the intervening turbine components and the review of ordinary basic functional elements that are used to build the controllers. A wind turbine can be typically modeled to a first approximation as a rigid mass-less shaft linked to the rotor inertia at one side and to the drive train inertia on the other side, as shown in Figure 2.1. The captured aerodynamic torque acts on the rotor and the generator electrical torque acts on the drive train [7].

Neglecting elastic and aero-elastic effects, the dynamics of the wind turbine rotor can be

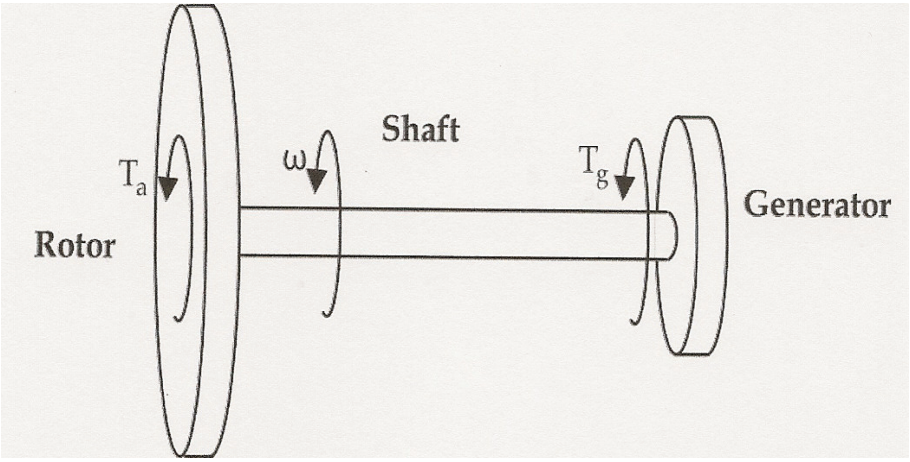

Figure 2.1: Simplified model of a wind turbine [7]

described by a one degree-of-freedom rigid body model as:

$$J\dot{\omega} + D\omega = T_a - T_g \tag{2.1}$$

where ω is the rotor speed, J the equivalent inertia of power train, D the equivalent damping coefficient, T_g the applied generator torque as seen from the rotor, and a T_a the aerodynamic torque. The wind turbine power coefficient is denoted by $C_p(\beta, \lambda)$ and is a function of the pitch angle and the tip-speed ratio λ . The aerodynamic torque acting on the rotor is therefore written as:

$$T_a = \frac{1}{2}\lambda\pi R^3 v^2 \times \frac{C_p\,(\beta, \lambda)}{\lambda} \tag{2.2}$$

where ρ is the air density, R the rotor radius, and v the effective wind speed. The tip-speed ratio is defined by $\lambda = \omega R$. Due to the speed amplification resulting from the gear box, the high-speed shaft rotates with the rate $\omega_g = n\omega$, where n is the gear box amplification factor. The effective wind speed appearing in Equation 2.2 is not the average wind speed that acts on the rotor plane but some hypothetical wind speed that has to be identified. This can be evaluated, for instance, if the pitch angle and the rotor speed are fixed, and then the aerodynamic torque is measured and the nonlinear Equation 2.2 is solved to compute the effective wind speed, v. Using a reference wind speed in Equation 2.2 instead of the unknown effective wind speed will result in an error in wind speed and consequently in aerodynamic torque. These two errors are not directly correlated because in aerodynamic torque, air density and the rotor blades aerodynamic coefficients may also vary as functions of the ambient conditions or because of wear affecting the blades. The surface that defines $C_p(\beta, \lambda)$ depends on the geometric configuration of the wind turbine blades and the aero-foils composing them. This surface admits a unique maximum denoted $C_{p,opt}$, which is obtained for $\beta = \beta_{opt}$ and $\lambda = \lambda_{opt}$. As the extracted power is given by $T_g = \frac{1}{2}\rho\pi R^2 v^3 \times C_p(\beta, \lambda)$, the energy extraction from the kinetic energy of wind is optimal for $C_p(\beta, \lambda)$ = C_{p-opt}. The control strategy is usually defined by indicating the desired variations of wind turbine velocity and torque in the plane. Among the common strategies used in practice, one finds one depicted in Figure 2.2.

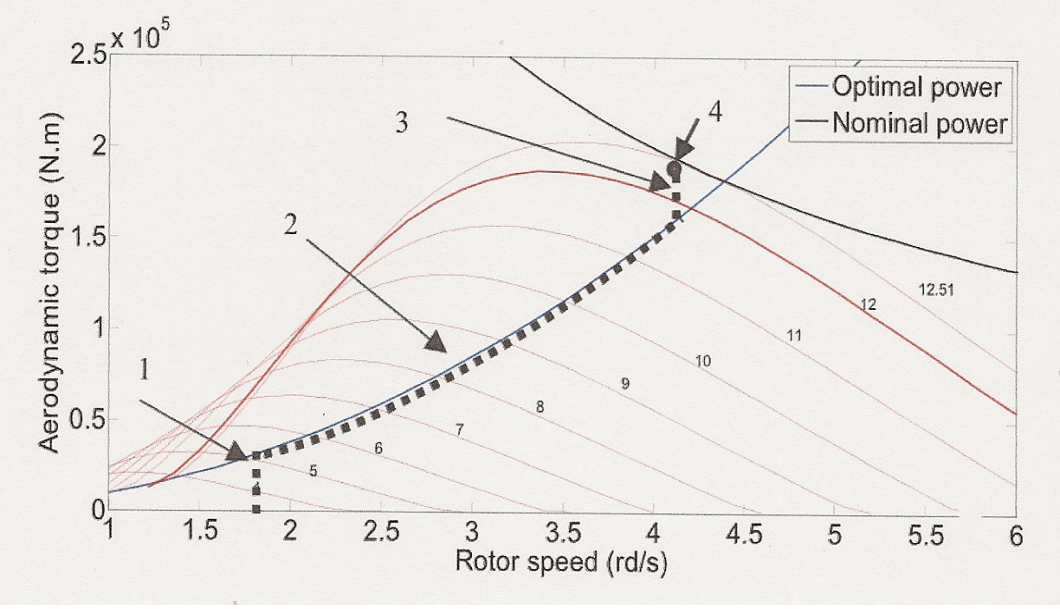

Figure 2.2: Strategy of control illustrated in the (ω, T_a) plane as the dashed curve [7]

In the (ω, T_a) plane, the red curves are obtained for different wind speeds by imposing the constant pitch angle $\beta = \beta_{opt}$ [7].

2.1.1 Schemes of pitching control

The concept of wind turbine rotor pitching control for regulator designs of the energy capture of power systems was well established in other applications. The control performance of pitch angle can greatly influence the quality of power regulation for variable-speed adjustable-pitch wind turbines.

Zhang [21] and Xia [22] used fuzzy logic pitch angle controller rather than conventional pitch angle control strategies. Compensating for non-linear sensitivity and wind turbulence using fuzzy logic controller is shown to achieve better control performance than conventional pitch angle control strategies, namely lower fatigue loads, lower power peak and lower torque peak,

Xiyun and Xinran [23] proposed a sliding mode control with adaptive fuzzy characteristic for the pitch system. Using a combination of feedback linearization theory and adaptive fuzzy scheme, a sliding mode controller was designed that can achieve control performance effectively with an uncertain model. The simulation also demonstrates that the control system has high smoothness and can eliminate wind speed disturbance. The results show that the adaptive fuzzy scheme guarantees good stability and dynamic behavior of a system.

Zhang, Cheng and Wang [21] implemented an independent variable pitch control technique based on the traditional variable pitch control. The outcome shows that the wind power generation system can reduce the loads on the blades and extend the service life of wind turbines, as long as the output power is kept stable.

Putrus, Ghanim and Chen [24, 25] demonstrated the possibility of using variable speed on variable and fixed-pitch wind turbines without any major difficulties. Therefore it is possible to control the output power and to operate the rotor at high as well as at low tip-speed ratios. The most difficult operating region is when the rotor is operating with a speed above the stall speed. They used the performance of a Fuzzy Logic to Maximum Power Point Tracking

(MPPT) controller to examine the applications on variable-speed fixed-pitch small- scale wind turbines.

Zhang [26] described a pitch control method, which uses the equivalent input disturbance (EID) approach for the control of the pitch angle of a constant-speed wind turbine. The study demonstrated that the EID compensator plays an important role in improving the control performance of the whole system. They also show that the equivalent input disturbance, which has the same effect on the produced power as the wind disturbance, can be estimated by an EID estimator used to eliminate the effect of the wind disturbance.

Mirzaei [27] dealt with the problem of individual pitch control of a variable- speed variable pitch wind turbine in the full load region. Model predictive control (MPC) is used to solve the problem, which linearizes the nonlinear model for different operating points. They show that the operating point is a direct function of rotor rotational speed, pitch angle and wind speed, with wind speed estimation being used to find the operating point.

2.1.2 Wind turbine optimal control techniques

Research using optimal control and conventional control methods has shown that applying optimal control leads to increased power capture and reduced load fatigue more than conventional control methods [28, 29]. Moreover, the wind turbine models which are used to represent the optimization of wind turbine control show improved results in the enhancement of power production. The optimal control regulator strategy techniques using modern optimal control theory enable power engineers to design an optimal control system with respect to given performance principles [30, 31].The main objective of optimizing the aerodynamic performance of wind turbine rotors is to reduce fatigue loads while mitigating the effects of extreme loads.

Tutty [32] employed a simple computational fluid dynamics model to represent the flow past an airfoil and undertook a detailed investigation into the level of control possible by combining iterative learning control with classical control action, with an emphasis on how the performance improvements can be effectively measured.

Van Zwieten [33] reported on the adaptation of a numerical simulation algorithm for predicting ocean current turbines with performance prediction to wind turbine control. The numerical algorithm used an unsteady blade element momentum rotor model (BEM) to calculate the rotor forces and seven degree-of-freedom (DOF) equations of motion to represent the coupling effects between the rotor and the main body. The results show that the maximum rotor power coefficient of the turbine of 0.45 and that the vertical current gradient will only minimally affect the system performance.

2.2 Approaches to wind turbine control

Historically, the problem of wind turbine power generation control systems was dealt with using control schemes based on integrated control. Xie [34] discussed control schemes to enhance the ability of reactive power support of a doubly fed induction generator (DFIG)-based wind turbine during serious voltage dips. The study proposed an advanced low voltage ride through (LVRT) control scheme, with which a portion of the captured wind energy during grid faults is stored temporarily in the rotors inertia energy and the remaining energy is available to the grid, while the (DC)-link voltage and rotor current are kept below dangerous levels. Various optimal control studies made on multilevel control and variable aerodynamic construction model strategies have been reported in literature.

Muyeen [35] introduced a simple fuzzy logic controlled inverter system for the control of a grid side inverter system. The approach suits a variable speed wind turbine (VSWT) and a permanent magnet synchronous generator (PMSG) operation in a wide operating range. In most of the optimal control studies, the wind inflow angle is constant and assumed not to affect power generation therefore is not used as one of the aerodynamic parameters.

Eisenhut [36] considered a wind turbine model for energy capture and switching simulation at lull wind conditions that included aerodynamics and wind inflow direction and angle; as well as the controller part. The scheme was based on the idea that control parameters can optimize energy capture and turbine profits near cut-in wind speed.

Colin [37] considered a technique known as aerodynamic moment control to limit transient gust loading on horizontal-axis wind turbine rotors. The method was implemented

by enclosing a patchable section of the blade in an active control loop, using the external aerodynamic load as feedback variable.

Sikandar [38] discussed dynamic analysis and pitch control of horizontal axis wind turbines. Simulation techniques and an experimental setup were developed. The results show that by introducing the pitch control, the power output was successfully controlled in high and low speed conditions. Overloading and outage of the wind turbine was prevented.

Schreck [39] made an effort to identify how the blade aerodynamic forces responsible for power production must be augmented to maximize energy capture; while, at the same time, adverse aerodynamic loads that fatigue turbine components need to be mitigated to extend machine service life.

Min [40] proposed a control scheme of individual pitch control based on inflow angle prediction. By analyzing the reason why blades vibrate in flap-wise and the extrinsic excitation, a control strategy based on inflow angle prediction was suggested for the design of individual pitch control and the corresponding mechanism. Min reported that the individual pitch control based on the inflow angle prediction can effectively reduce the axial aerodynamic periodic changes caused by wind speed and uneven distribution along height and reduce the aerodynamic fatigued load of blades. It is also concluded that power control of the individual pitch control based on inflow angle prediction is stable.

2.3 Model of multidimensional control of turbine rotor angle

The most accurate method employs the dynamic inflow model (blade element momentum method) plus a dynamic equation for the induction factor. Knudsen [41] used the suggested model and showed that the models behavior, which is demonstrated using simulated data and real full-scale turbine data, indicated the use fullness of the extended Kalman filtering.

Lixun [21] included the aerodynamic coefficients of blades using the simulation and experiments, along with a prototype of a variable-pitch vertical axis wind turbine (VAWT).

A mathematical model and dynamic model were built to compute the optimal pitch angle of VAWT. The results show that aerodynamic performances have been greatly improved and the tangential force coefficient is twice as large as that of a fixed-pitch VAWT.

A study conducted by Zhang [42] found that certain improvements in the wind turbine aerodynamic performance were obtained by contrasting P-V curves and rotational speed model with original twisted wind turbine blades.

2.4 Conclusion

The review of literature in this chapter concentrated largely on empirical observations of the performance of wind turbines at nominal turbine speeds, control strategies, and optimization of wind turbine operation. Research on wind turbine design determined that some studies improved wind turbine operation relating to speed, control strategy, optimization and energy capture. The major concern in optimizing the wind turbine performance is to increase energy capture and reduce fatigue load. The increase in energy capture with reduced fatigue load leads to the increased lifespan of the wind turbine and reduced cost of power energy. A number of studies look at the performance of wind turbines to achieve this goal. With regard to speed, pitch angle performance has been considered in terms of state variables such as adjusting pitch angle and redesign of plate shape. In addition, an increase of energy capture and reduction in fatigue load has been considered in terms of wind turbine aerodynamics. Certain important concepts, such as model and experimental setup, have been presented and used to explain the performance of wind turbine operation behavior. To determine wind turbine behavior, it is necessary to develop a theory for the process, which may be a complex mechanical model. The study concluded that an automatic design environment and aerodynamic simulation are combined to obtain an improved windmill blade. During this review, it was determined that the techniques used for wind turbine optimization and behavior enhancements require more practical observation. The proposed design can be used as a solution for the problem of the relocation of wind turbines due to weather changes, which will change the wind inflow angle and make it either larger or smaller than the designed boundaries. Hence, it will save the cost of relocating the wind turbine and ensure that the performance of the turbine always remains in the acceptable region. It also increases the lifetime of the wind turbine by decreasing the fatigue load. This chapter provides a basis

for Chapter 3, in which the development of wind turbine optimization theories is outlined and various design equations are critically analyzed [43].

Chapter 3

DYNAMIC MODELING OF WIND TURBINE WITH ROTOR ANGLE AND WIND DIRECTION

3.1 Introduction

The identification of a wind turbine (WT) as a source of clean, non-polluting and renewable energy has motivated researchers to look at the optimum design of the system and the control strategies of the different possible parameters that can operate efficiently under extreme variations in wind conditions [44]. The general goal of this thesis is to increase the wind turbine energy capture and reduce wind turbine fatigue load. The power coefficient is achieved at a particular tip speed ratio(λ), which is specific to the design of the turbine. The wind turbine model consists of new post-modifications, which allow the wind turbine rotor to change its angle. The energy capture of the wind turbine can be varied by changing the wind inflow angle conditions at the rotor scheme. Variable rotor angle turbines are used to control rotor speed, which leads to increased energy capture. Rotor angle and wind direction controls are also used to control the output power above their rated wind speed. Moreover, variable speed wind turbines use the rotor angle to control and optimize energy capture. This thesis deals with the performance of the wind turbine for the energy capture of a horizontal axis wind turbine (HAWT) through incoming variable wind speeds. The overall objective has been to study variable wind turbine rotor angles according to the wind inflow angle for fixed-pitch angle and variable wind direction turbines, especially in cases where the wind inflow angle changes. The variable rotor inflow angle has been presented to optimize and increase the energy capture and reduce fatigue load, which affects wind turbine lifespan. As we know, the wind turbine performance is sensitive to the following parameters: 1) Wind speed

2) Air density

3) Wind shear

4) Wind veer

5) Turbulence intensity

6) Wind directional variation

7) Wind inflow angle

3.2 Wind inflow angle

Our concern and formulation problem in this study is inflow angle. It is the off-horizontal angle, a required position at which the mean flow comes into the rotor. The inflow angle affects both the turbine loading and the aerodynamic efficiency of the rotor [11] and should be perpendicular to the wind turbine rotor. Figure 3.1 represents the relation of the wind

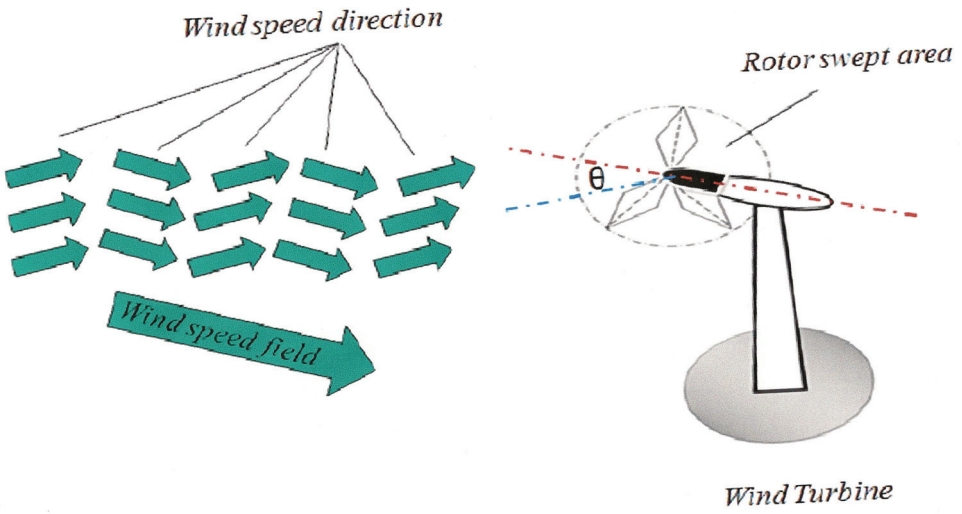

Figure 3.1: Relationship of wind turbine to wind inflow angle

turbine to the wind inflow angle. Wind turbines are certified for inflow angles usually within ± 8, as required by the IEC 61400-1 standard.

3.2.1 Inflow angle causes

Steep slopes force the flow at the ground to a given direction in the vertical plane. Equation (3.1) gives the value of wind inflow angle:

$$Wind\,inflow\,angle = tan^{-1}\frac{Vertical\,wind\,speed}{Horizontal\,wind\,speed} \tag{3.1}$$

Equation (3.1) is known as the wind inflow angle equation. This relationship holds for components of wind inflow angle, so if the wind speed in the vertical direction increases, the wind inflow angle also increases. If the wind speed in the horizontal direction is increased, the wind inflow angle decreases.

3.2.2 Wind turbine rotor angle

Through the study of proposed variable turbine rotor angle designs, it is expected that the turbine rotor angle tracking the changes in wind inflow angle will be discovered. This eliminates the need to model the rotor angle tracking system, as the wind turbine rotor is modeled by adding elements to the wind turbine dynamic model. In this model the rotor angle, which is represented by horizontal and vertical angles, is divided into a multi-directional of divisions called rotor inflow angle. In these, the horizontal angle is considered as the direction of the rotor in the x-axis, and the vertical angle is considered as the direction of the rotor in the y-axis. Hence, both directions give the rotor angle. Figure 3.2 shows the mechanism of rotor angle direction.

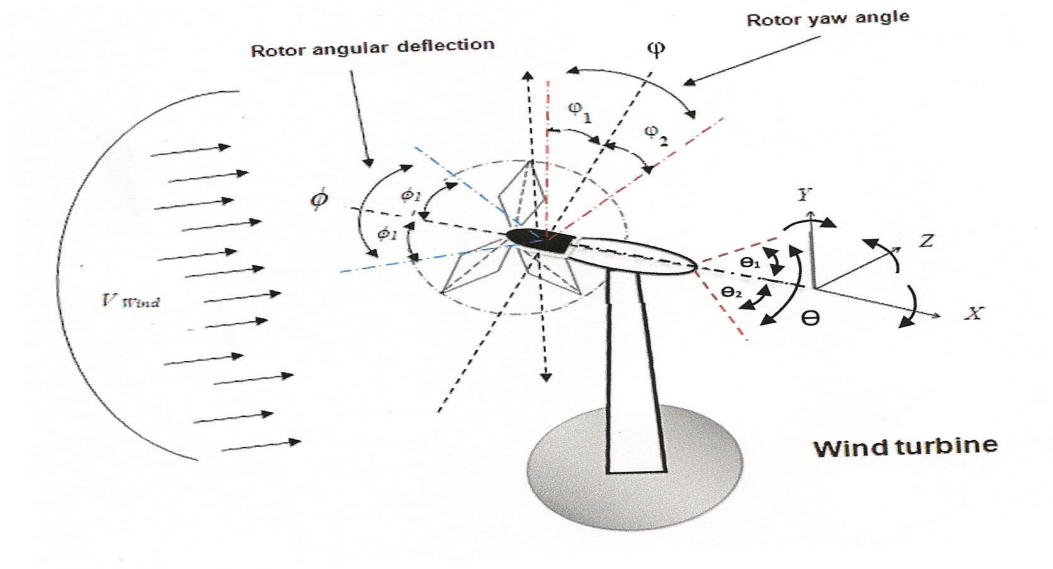

Figure 3.2: Rotor angle direction function

3.3 Structure and control of wind turbines

The variable rotor angle can help in providing additional control of the wind turbine generator. The design of the variable rotor angle requires measuring wind inflow angle variations at different positions and adjusting the rotor angle according to the wind inflow angle. This structure of performance measurements uses sensors for measuring the wind inflow angle in real time and for adjusting the rotor angle to track the wind inflow angle.

3.3.1 Problem description

The problem in tracking the wind inflow angle is to keep the rotor angle perpendicular to the wind inflow angle. Furthermore, the tracking control uses a closed loop feedback control system and rotor angle control efforts to keep the energy capture at rated power and rated rotor speed. As such, the rotor angle can increase or decrease the rotor speeds while providing increased safety in merging and reducing damage effects on the wind turbine themselves. The actuation of this system can be achieved using the position sensor for rotor angle in both vertical and horizontal environments.

3.4 Control system strategy of proposed model

This study focused on the interaction between wind direction and rotor angle control systems, as well as the strategy and the impact on wind turbine performance. The way in which multiple aspects of control systems can be combined in a variety of ways to enhance the performance of wind turbine for energy capture was also considered.

a) Wind direction

As shown in Figure 3.3, the first step in this strategy measures the wind turbine direction angle θ_m and compares it with the reference angle θ_{ref}. If there is any deviation, the turbine direction actuation will regulate the deviation.

b) Rotor yaw angle

The second step measures the rotor yaw angle φ_m and compares it with the reference angle φ_{ref}. If there are any deviations the rotor yaw actuation will regulate the deviation.

c) Rotor angular deflection

The third step measures the rotor angular deflection angle ϕ_m and compares it with the reference angle ϕ_{ref}. The rotor angular deflection (RAD) actuation will regulate any existing

deviations. Figure 3.3 shows the starting strategy flow chart of the wind rotor angle turbine and wind direction control.

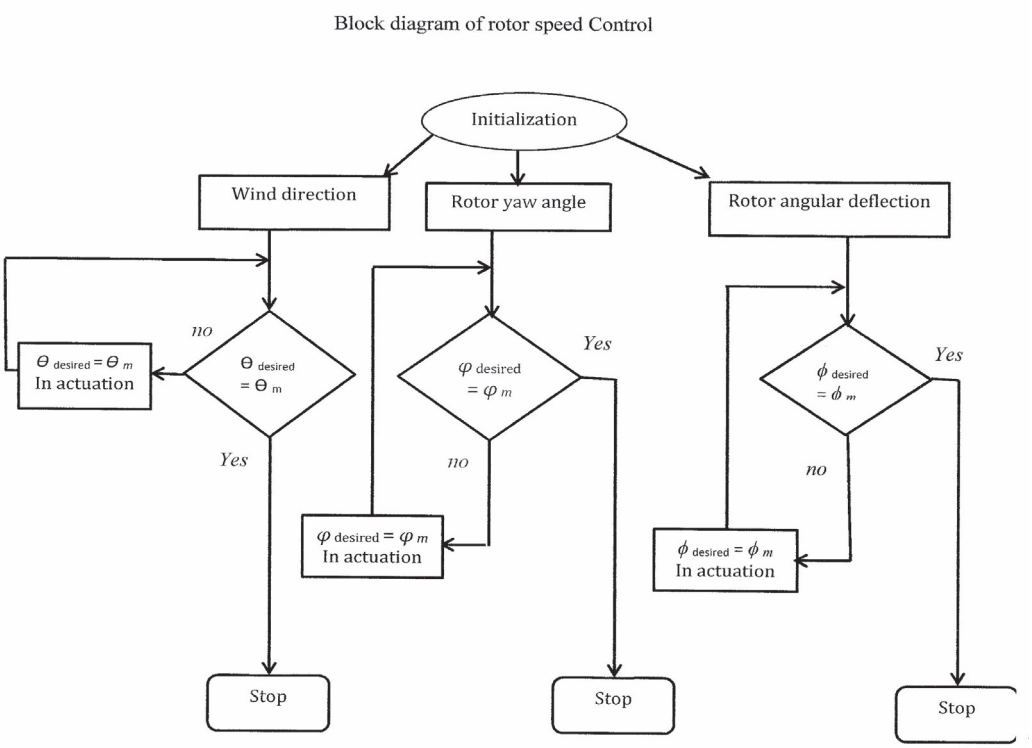

Figure 3.3: Control system strategy of proposed model

3.4.1 Control problem formulations

To convert the kinetic energy of wind into electrical energy, the wind turbine is prepared with a control system that draws the operation for all stages of the wind turbine together. A wind turbine is always designed for specifically rated conditions. By rated conditions, we mean here rated wind speed, rated rotor speed, and rated power. A wind turbine is designed to generate rated power, which is the maximum power that the generator is designed to deliver.

3.5 Universal joint motions

In this section, we explain the type, application and mechanics of a universal joint to provide an understanding of how universal joints work. Universal joints usually transmit torque and motion between shafts with misalignment [45].

3.6 Typical applications of universal joint

Following is a partial list of usages for universal joints: agitators, balancing machines, blowers and fans, compressors, conveyors, cooling tower, fans, crushers, farming equipment, generators, glass manufacturing, mining equipment, oil and gas, packaging, and mixers [8]. Figure 3.4 shows several types of a universal joints, which are used for different purposes.

Figure 3.4: Different kinds of universal joints

3.6.1 Kinematics and motion characteristics of universal joints

While a universal joint works at an angle (β), a non-uniform motion is established. With the driving yoke of the joint operating at a uniform rotational velocity to ω_1, the driven yoke rotates non-uniformly with respect to angular displacement, velocity ω_2, and acceleration. Figure 3.5 shows the kinematics and motion of a universal joint. With a constant angular velocity (ω_1) of the driving yoke, the driven yoke has a maximum difference of output angular velocity (β) with respect to the driving yoke when the driving yoke lies in the plane of the joint angle and also when the driving yoke is normal or perpendicular to this plane. The driven yoke has the same angular velocity as the driving yoke at approximately $45°$ from the joint angular plane for small angles [8].

$$\omega_2 = \left(\frac{cos\beta \times \omega_1}{1 - sin^2\alpha_1 \times \sin^2 \beta} \right) \tag{3.2}$$

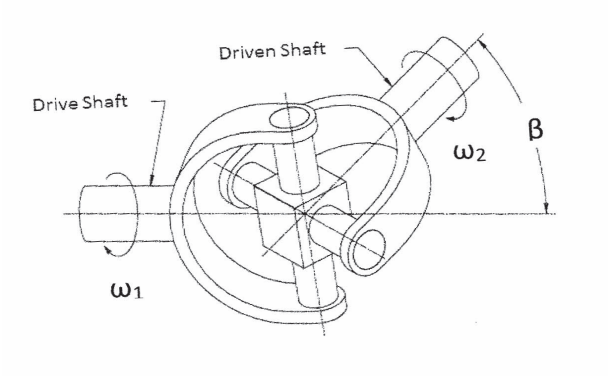

Figure 3.5: Kinematics and motion of universal joint [8]

3.6.2 The dynamic rotation of a universal joint

For dynamic rotation, the angular velocity of the driven yoke ω_2 can be determined for a given angular displacement α_1, with the formula. During one revolution of the drive yoke, the driven yoke will reach a maximum angular velocity twice at $\alpha = 0° \; and \; 180°$. Figure 3.6 shows the maximum angular velocity, which here will be: The maximum angular

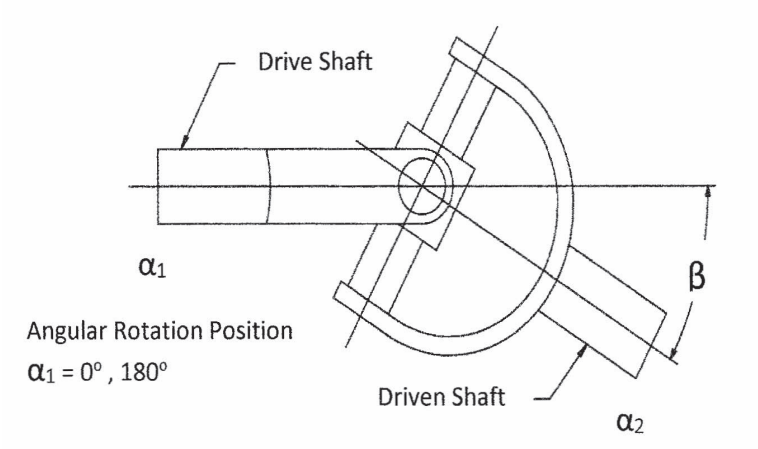

Figure 3.6: Maximum angular velocity [8]

velocity will be:

$$\omega_2 max = (\frac{\omega_1}{cos\beta}) \tag{3.3}$$

The driven yoke will also reach a minimum angular velocity twice during one revolution at $\alpha = 90° \; and \; 270°$. Figure 3.7 shows the minimum angular velocity, while Equation (3.4) represents the minimum angular speed.

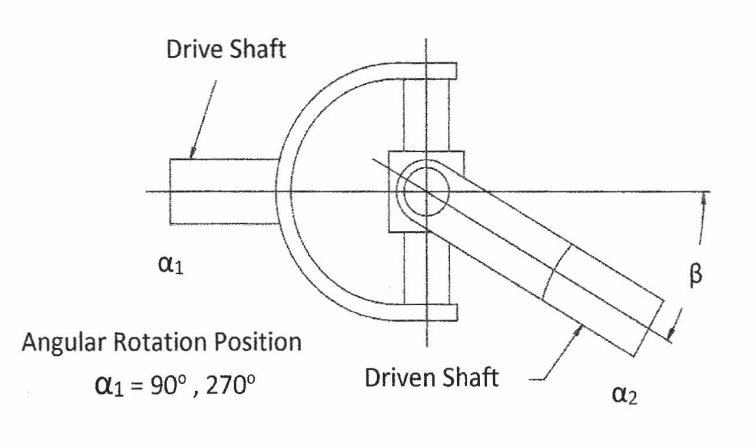

Figure 3.7: Minimum angular velocity [8]

$$\omega_2 min = cos\beta\omega_1 \tag{3.4}$$

3.6.3 Model of rotor mounted on a universal joint

Figure 3.8 shows how the rotor is mounted on a universal joint, which allows multidimensional movement. The rotor angle can be adjusted to match the predicted wind inflow angle, and the universal joint will be attached to the wind turbine rotor. As shown in Figure 3.8, one side is connected to the rotor blades and the other to the low-speed shaft.

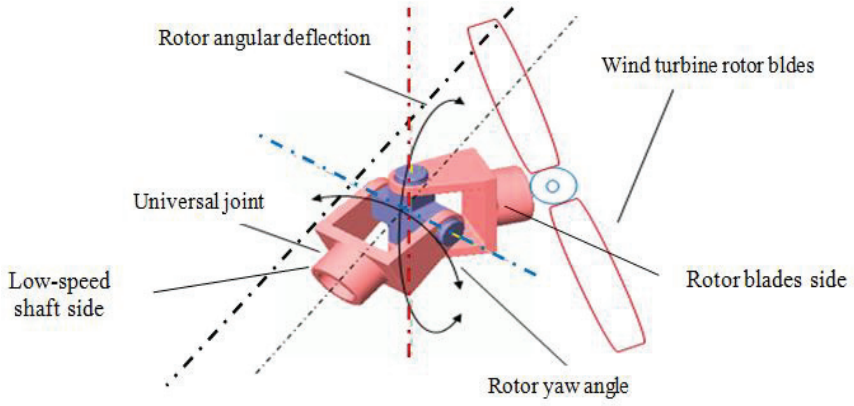

Figure 3.8: Rotor attached with universal joint

3.6.4 Rotor angle adjustment

To adjust the rotor angle, the U-Joint is driven by two actuators: one for the rotor yaw angle (RYA), and the other for the rotor angular deflection (RAD). The main function of the actuators is to enable the U-Joint to move in two directions horizontal and vertical so that the blades will be continually facing the wind inflow angle. Figure 3.9 the shows direction and movement of turbine rotor angles in RYA and RAD. This research focuses on

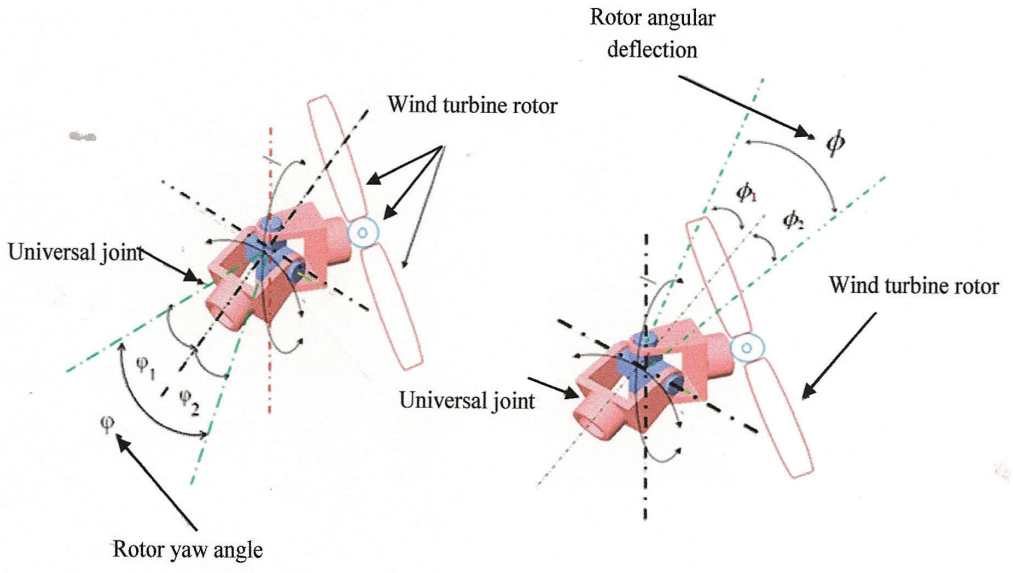

Figure 3.9: Rotor yaw angle and rotor angular deflection

the inflow angle-controlled wind turbine rotor, and examines the use of rotor angles to obtain the maximum power output capture of a wind turbine. The technique uses regulation of the vertical and horizontal angle of the rotor to guarantee how much power must be sacrificed to achieve a specified level of fatigue load drop. The function of the rotors direction is shown in Figure 3.2. Electrical, pneumatic or hydraulic actuators can be used to drive the WD, RYA and RAD. In this particular experimental setup, an electrical actuator was utilized. Thus, this part of the main goal to achieve wind turbine energy will maintain the continuity of the rotor motion facing the wind inflow in order to obtain more energy.

3.7 Model of wind turbine rotor angle control

Energy capture from the wind turbine can be optimized or limited by adjusting the rotor angles of the wind turbine. The wind turbine model is highly nonlinear, so a smart controller should be designed to adjust the rotor angles of the wind turbine. In this thesis, the pole placement and a linear quadratic controller have been used to control the rotor angle according to the incoming wind inflow angle. Simulation results show that the proposed controller is highly effective for adjusting the rotor angles. the maximum power tracking achieved at inflow angle become perpendicular to the rotor angle which approximately 4-6% of fixed wind turbine rotor angle. The maximum power tracking achieved in this research by tracking the rotor angle the wind inflow angle. Pole-placement technique is used to determine a proper weighting matrix for the linear quadratic controller such that satisfactory damping characteristics can be achieved for the closed-loop system. Effects of various system disturbances on the dynamic performance , and the results reveal that the proposed controller is effective in regulating the transient operation of the turbine

3.7.1 Model of rotor yaw angle control

The control system illustrated in Figure 3.10 shows a mechanism that physically turns the rotor yaw angle in a horizontal direction. This assists the rotor angular deflection in matching the wind inflow angle for the purpose of increasing or decreasing the energy capture. The adjustment of the rotor yaw angleφ can be easily improved by adjusting the rotor yaw actuator. This control design can be used with variable rotor angles in order to obtain safe high or low rotor speeds. The rotor yaw control mechanism starts mechanically when the wind inflow angle changes to keep the energy capture at a stable value. The rotor yaw angle and the rotor angular deflection controls are dependent on each other to turn the rotor angle physically, but in different directions (i.e., the rotor angular deflection in a vertical direction, and the rotor yaw angle in a horizontal direction). The object of this control is to determine the rotor angle for wind inflow angle predictions. This technique will help the wind turbine rotor to track the wind inflow angle.

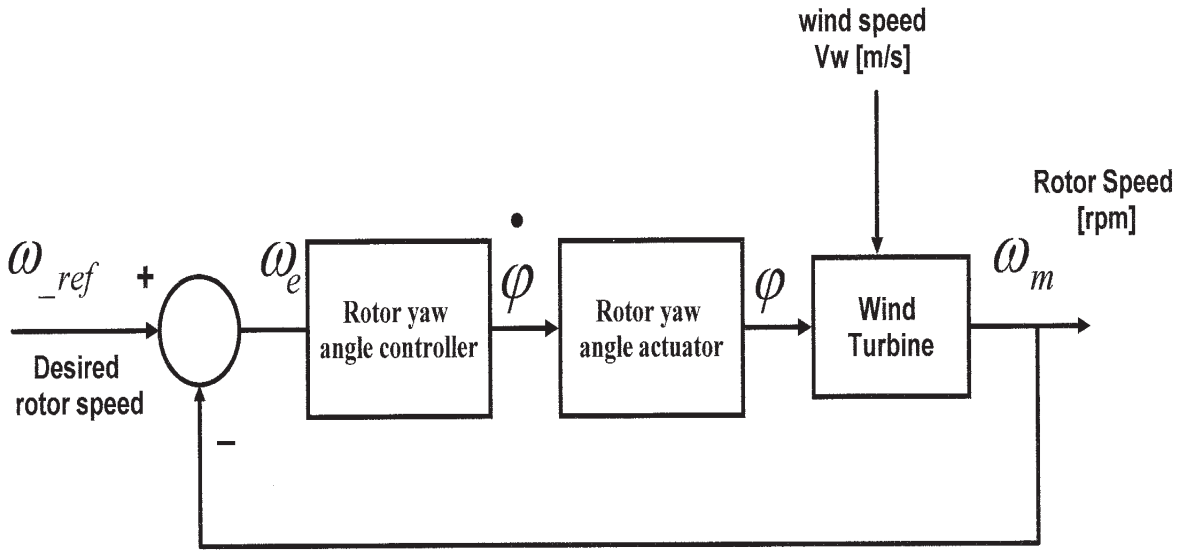

Figure 3.10: Rotor yaw angle control

3.7.2 Model of rotor angular deflection

The control system demonstrated in Figure 3.12 shows rotor angular deflection control, which physically turns the rotor angular deflection in a vertical direction. The adjustment of the rotor angular deflection ϕ can be easily made by adjusting the rotor angular deflection actuator. By adjusting both the rotor angular deflection actuator and the rotor yaw angle actuator, the rotor angle changes according to the wind inflow angle. The objective of this control is to adjust the rotor angle in a vertical direction in a stable way.

3.7.3 Model of wind turbine direction control

The wind turbine direction control system is illustrated in Figure 3.11. It shows the mechanism which physically drives the wind turbine direction to face the wind speed direction. This helps the wind turbine to capture more energy. The greater exposure the rotor blades have to the direction of the wind, the faster the optimum power rate is achieved. The wind turbine direction angle θcan be adjusted by the wind turbine direction actuator. This design of wind direction control can be used with variable wind speed directions to keep wind turbine directions tracking the wind speed direction.

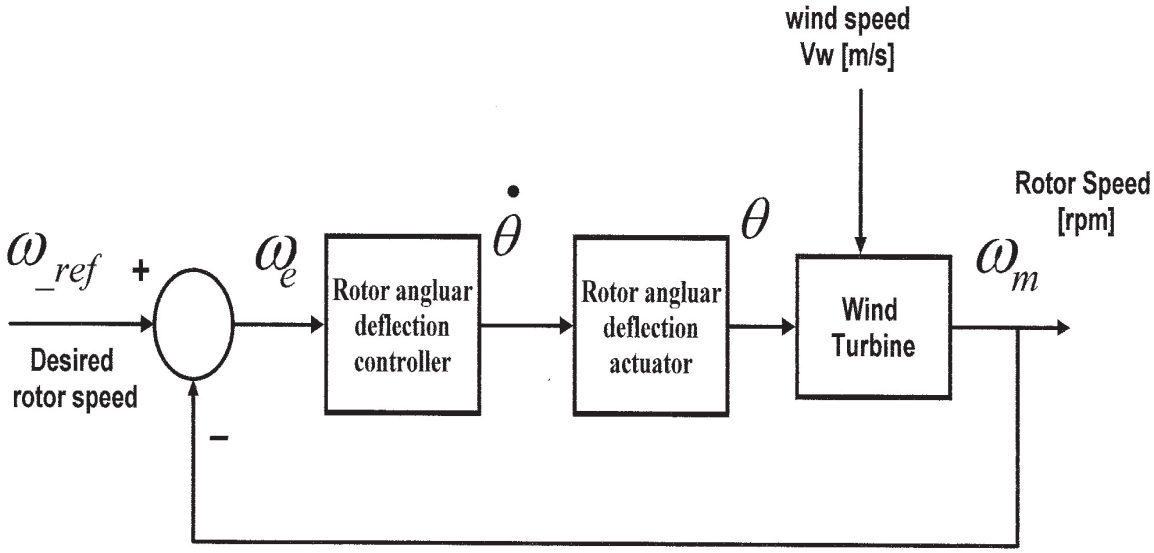

Figure 3.11: Wind turbine direction control

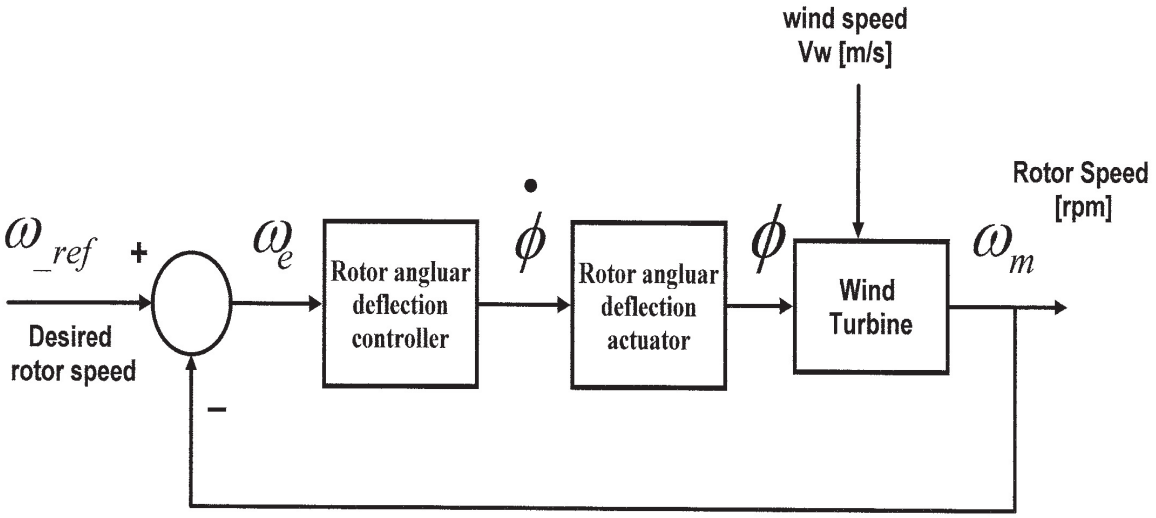

Figure 3.12: Rotor angular deflection control

3.7.4 Motivation of rotor angle technique

The motivation for adding rotor angle control to the wind turbine model will have the following impacts:

a) The rotor angle within the high or low wind speeds will also help to maximize the energy extracted from the wind speed.

b) The rotor angle technique will minimize the wind turbine fatigue load.

c) The rotor angle adjustment at high or low wind speeds can help to minimize or maximize rotor speed to its rated speed value. As shown in the results the objectives is achievable simultaneously. One of the reason for fatigue load increase the wind inflow angle not perpendicular to the rotor blades but by this technique the rotor blades most of the time perpendicular to the wind inflow angle which minimized fatigue load.

3.8 The proposed model of aerodynamic for new modifications

Figure 3.13 shows the aerodynamic wind turbine control model after it is combined with the wind direction control system and the rotor angle control system (as described in sections 3.7.1, 3.7.2 and 3.7.3) to give a multi-control system with a multi-controller, meaning each control system has its own controller.

A complex and highly uncertain system with a multi-control system and a multi-controller can provide satisfactory performance. The multi-control system consists of three controllers: two for rotor angles, and a third for wind turbine direction. All control systems with

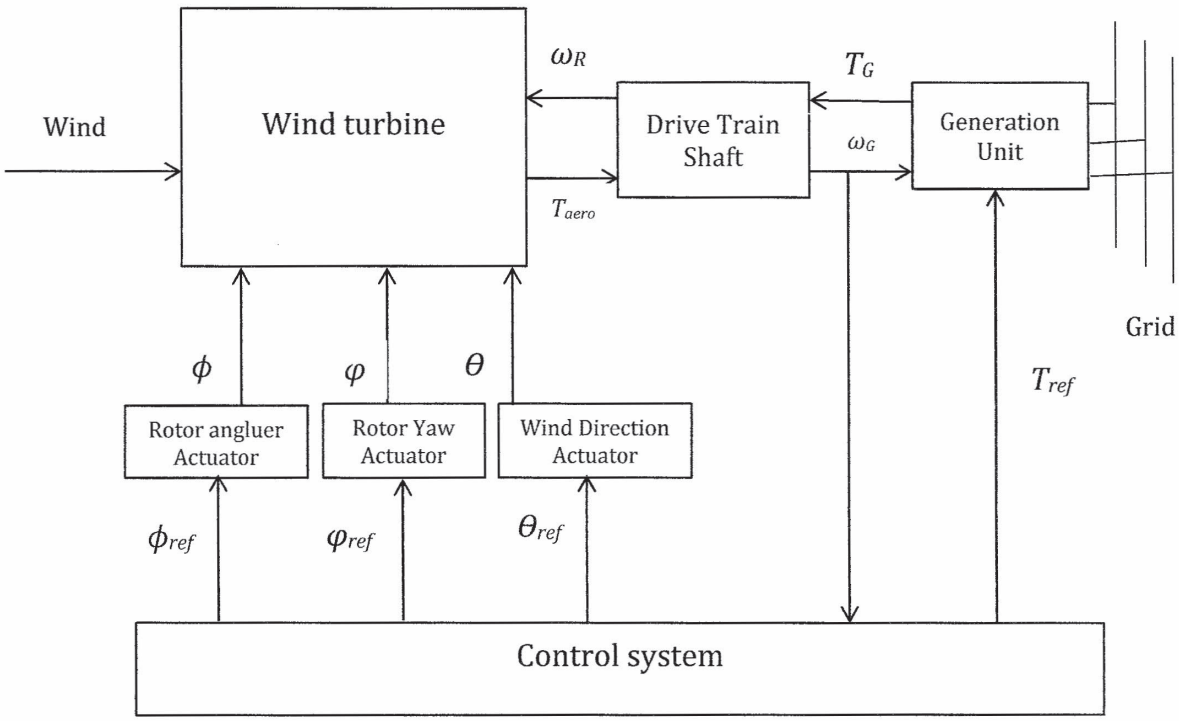

Figure 3.13: Aerodynamic wind turbine model

controllers are designed and implemented with the wind turbine model. The accepted control schemes are chosen by considering the stability of the wind turbine direction and turbine rotor angle and how much the variations are expected to affect the turbine rotor speed.

3.9 Turbine rotor angle energy capture control

According to the aerodynamic wind turbine model in Figure 3.13, the aerodynamic efficiency of a wind turbine is maximized at a specified tip-speed ratio and controlled so that it operates at that specific tip-speed ratio. The tracking characteristic is represented by the power curve shown in Figure 3.14. The rotor angle control can be used to help achieve this condition by adjusting the rotor angle to increase or decrease the energy capture. This curve represent the relationship of wind turbine speed and the outcome power the part under the power rate give the under rate power. The rotor angle correspond to this curve under the rate power. The actual speed of the wind turbine rotor ω_r measured at a rated speed and the

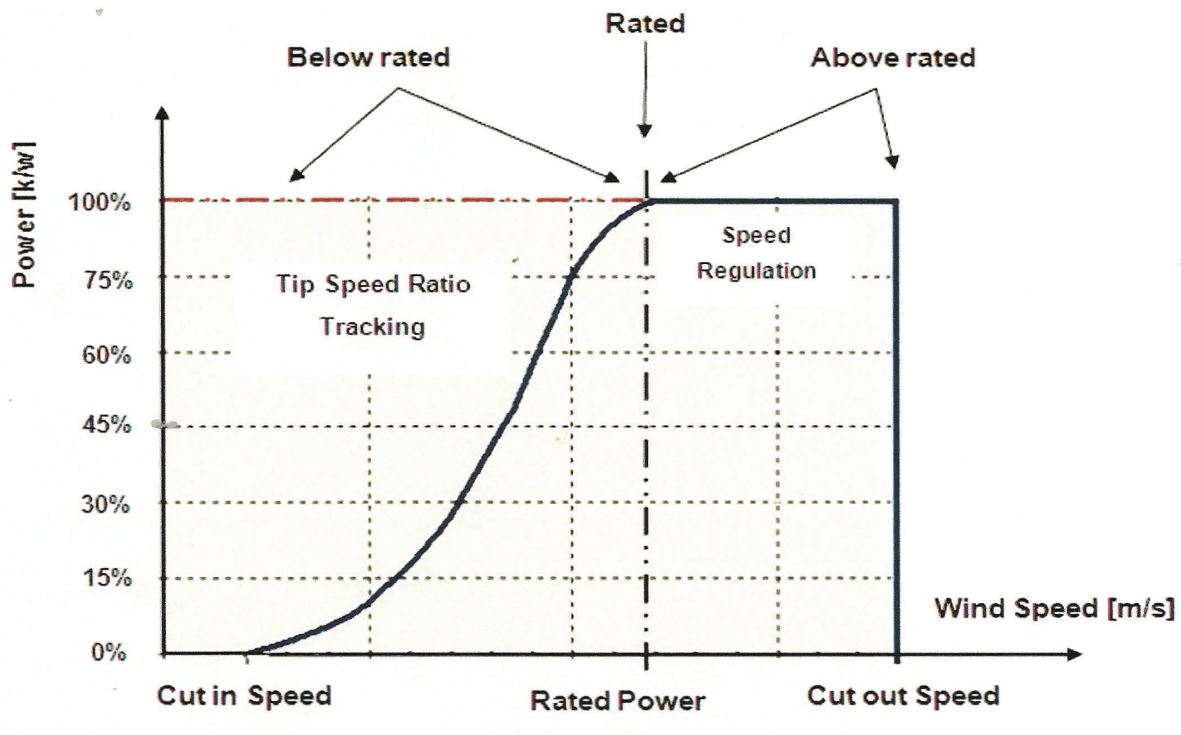

Figure 3.14: Power/speed characteristic and tracking characteristic

corresponding mechanical power of the tracking characteristic is used as the reference

power for the power control loop. The tracking characteristic curve shows the maximize power output as measured by the area between cut in speed and rated power (tip speed ratio tracking).

Chapter 4

DESIGN AND IMPLEMENTATION

4.1 Overall study aim

The inflow angle is the angle off the horizontal at which the mean flow comes into the rotor, and we want to keep this as close to the horizontal as possible. It affects both the turbine loading and the aerodynamic efficiency of the rotor (i.e., the power curve). The main point of this thesis is to find the influence of the wind inflow angle on wind turbine energy capture and to solve this problem.

4.1.1 Energy capture loss due to inflow angle

This [53] research studies energy capture loss due to inflow angle without solving this problem, but the researchers do figure out the effect of the inflow angle in energy capture. Figure 4.1 shows the relation between inflow angle and energy loss at 15 sites and 270 turbines. In Figure 4.1(A), the horizontal axis presents the inflow angle [deg], while the vertical axis shows the relative frequency [%]. The graph indicates the calculated average inflow angle (3.5 deg). In Figure 4.1(B), the horizontal axis presents the energy loss due to inflow angle [%] and the vertical axis shows the relative frequency [%]. The graph indicates that at a 0 degree rotor tilt, there is an average loss of 0.5%. In Figure 4.1(C), the horizontal axis presents the energy loss due to the inflow angle [%] and the vertical axis shows the relative frequency [%]. The graph indicates that at a 4 degree rotor tilt, the average loss is 1.8%. In Figure 4.1(D), the horizontal axis presents the energy loss due to the inflow angle [%] and the vertical axis shows the relative frequency [%]. The graph indicates that at a 6 degree rotor tilt, the average loss is 2.8%. This research motivated me to solve the inflow angle problem by letting the rotor change its angle.

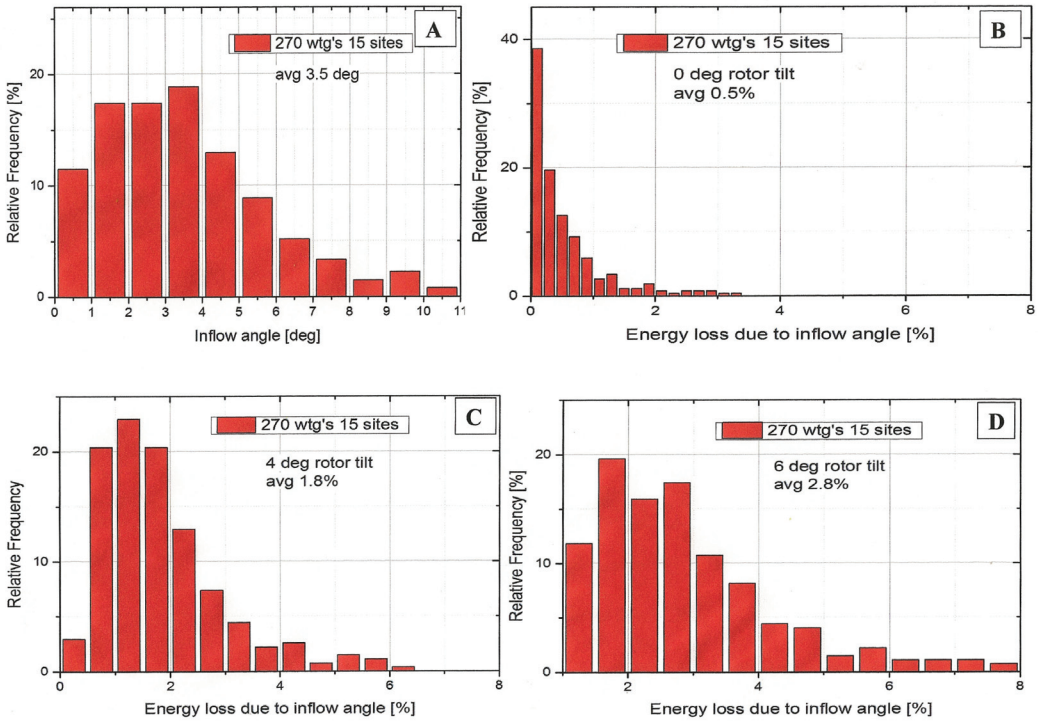

Figure 4.1: Energy loss due to inflow angle [53]

4.1.2 Summary of this study

This study evaluates the leveled loss of energy due to the inflow angle for 15 recent sites and 270 turbines. The results show that the inflow angle can have a significant influence on energy production. If the rated power of the turbine is $100\ /kWh$, the total power for 270 turbines is $27000\ KWh$. As seen in Table 4.2, if we calculate the power loss for one site with 270 turbines, the cost of power loss in North America at a rate of $0.07\ to\ 0.11/kWh$ is $0.09\ /kwh$.

Table 4.1: Calculation of the cost of power loss

Rotor angle	Avr. energy lost	Total power	Loss power	Loss power	$/d Loss cost
Rotor tilt 0 deg.	0.5%	27000[KWh]	135[KWh]	3240[KWd]	291.6
Rotor tilt 4 deg.	1.8%	27000[KWh]	486[KWh]	11664[KWd]	1049.76
Rotor tilt 6 deg.	2.8%	27000[KWh]	756[KWh]	18144[KWd]	1632.96

4.2 Wind turbine performance

Wind turbine performance is sensitive to the following parameters: wind speed, air density, wind shear, wind veer, turbulence intensity, wind direction and wind inflow angle. Moreover, variable wind speed causes variable power generation. To overcome this difficulty, a number of controlling techniques are proposed in literature. Generally, the pitch control technique is used in variable speed turbines to reduce power fluctuations caused by changing wind speeds, especially above the cut-off speed [48]. Most wind turbine manufacturers prefer to present the performance of their turbines in terms of the energy produced by a turbine over a period of time (usually one year). As the output power of a wind turbine depends on the availability of the energy source (i.e., the wind speed and the power-wind characteristics of the wind turbine generator), the capacity factor could be a proper indicator for measuring the operating performance of a wind turbine [49]. The horizontal axis wind turbine is used in this work because it is easier to add the suggested modification of the universal joint to rotor.

4.3 Modeling

In this chapter, the process of deriving a model that describes the physical components of the system will be examined. The first section of this chapter gives an overview of the components that are to be modeled. The general structure (Figure 4.2) shows the overall feedback diagram. The figure also illustrates the entire control loop with all the feedback paths drawn. This diagram is divided into smaller subsystems which will be explained further in this chapter. Finally, the model is verified using the MATLAB package.

4.3.1 Model Testing

The model testing stage is important for evaluating a models capabilities. This phase has three main objectives:

1- To prove that the desired inflow angle is achieved.

2- To demonstrate the impact of the rotor angle on energy capture.

3- To demonstrate rotor angle controller action.

4.3.2 Proposed model for wind turbine, wind turbine direction and rotor angle

The control systems designed for stability and height control are based on the same control theory, with a negative feedback control loop, as explained in sections 3.7.1, 3.7.2 and 3.7.3. As seen in Figure 4.2, there are three control loops shown.

1) Wind turbine direction control is a negative feedback control loop which uses sensors to gauge the wind directions measured value compared with the required value. The objective of this control loop is to maintain wind turbine tracking of wind direction.

2) Rotor yaw angle control is a negative feedback control loop which uses wind inflow angle sensors to measure the x-axis direction of the wind inflow angle of a HAWT. This value is compared to the desired value. The purpose of this control loop is to keep track of x-axis wind inflow angles.

3) Rotor angular deflection control is a negative feedback control loop which uses wind inflow angle sensors to measure the y-axis direction of the wind inflow angle of a HAWT. This value is compared to the desired value. The purpose of this control loop is to keep track of the y-axis direction of wind inflow angles. Moreover, the main purpose of both the rotor yaw angle and the rotor angular deflection control is to keep the rotor angle perpendicular to the wind inflow angle.

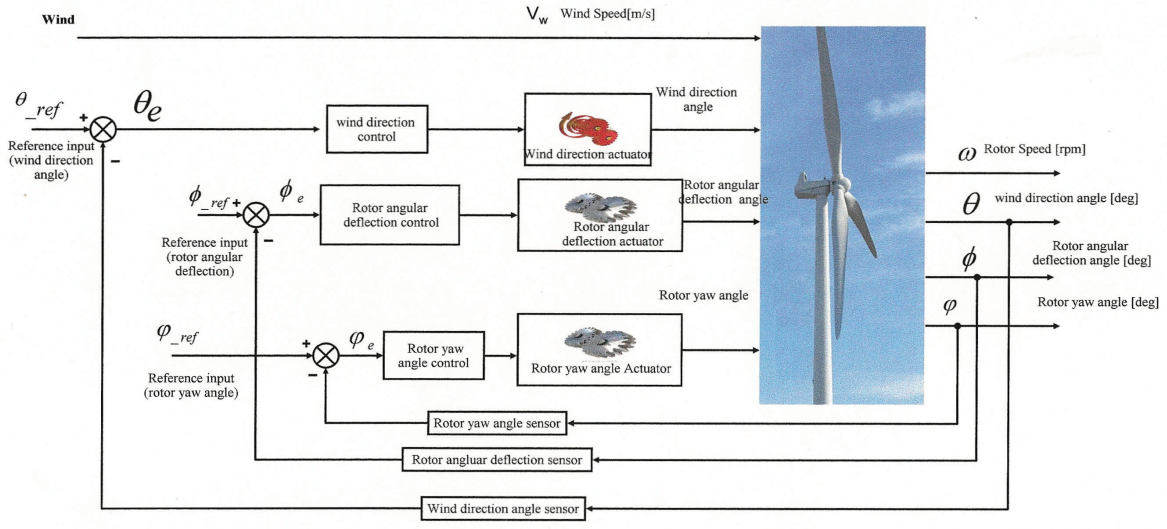

Figure 4.2: Rotor angle and wind direction proposed model

4.4 Rotor angle control

This thesis examines the impact of the relationship between wind inflow angle and rotor angle for wind turbines on energy capture. Due to quick variations in the receiving wind speed, wind direction and wind inflow angle, the value of energy capture becomes a control technique problem. Many optimization control techniques are presented in wind turbines in order to become a continuous output rated power. This work has focused on dynamic analysis control of wind turbine direction and rotor angle of horizontal axis wind turbines (HAWTs). Variable rotor angle is designed to increase the value of the wind speed passing through the rotor blades, leading to increased energy capture.

4.5 Wind turbine model

Using aerodynamics, a simplified mathematical model can be created for the wind turbine based on the aerodynamic power and torque as shown in Equations (4.1) and (4.2):

$$P_w = \frac{1}{2}\rho\pi C_p\left(\beta,\lambda\right)R^2V^3 \tag{4.1}$$

$$T_w = \frac{1}{2}\rho\pi R^3V^2\frac{C_p\left(\beta,\lambda\right)}{\lambda} \tag{4.2}$$

where P_w is the wind turbine output power (W), T_w is the rotor aerodynamic torque (Nm), ρ is the air density (kg/m^3), R is the rotor radius (m), β is the blade pitch angle (deg.), λ is the tip-speed ratio, $C_p(\beta,\lambda)$ is the rotor power coefficient, and ω_r is the rotor angular speed (rad/s).

$$\lambda = \frac{\omega_r R}{V} \tag{4.3}$$

The relationship between P_w and T_w is as follows:

$$P_w = T_w\omega_r \tag{4.4}$$

$$P_w\left(\beta,\theta,\varphi,\phi\right) = T_w\left(\beta,\theta,\varphi,\phi\right)\omega_r\left(\beta,\theta,\varphi,\phi\right) \tag{4.5}$$

$$T_d = T_d \omega_d \tag{4.6}$$

where P_d is the wind turbine power deviation, T_d is the total aerodynamic torque deviation, and ω_d is the rotor speed deviation.

In this study β is pitch angle, is constant:

θ the yaw rotor is variable

φ the yaw rotor angle variable

ϕ the rotor angular deflection, is variable

4.6 Model of wind turbine base on variable rotor angle and yaw direction

The proposed model for a wind turbine with variable rotor angle uses simulation tools that are able to assist in the test of the interaction design between the mechanical structure and energy capture of wind turbine during various operation modes. The wind turbine system, rotor angle and turbine direction are represented by transfer functions, as shown in Figure 4.3.

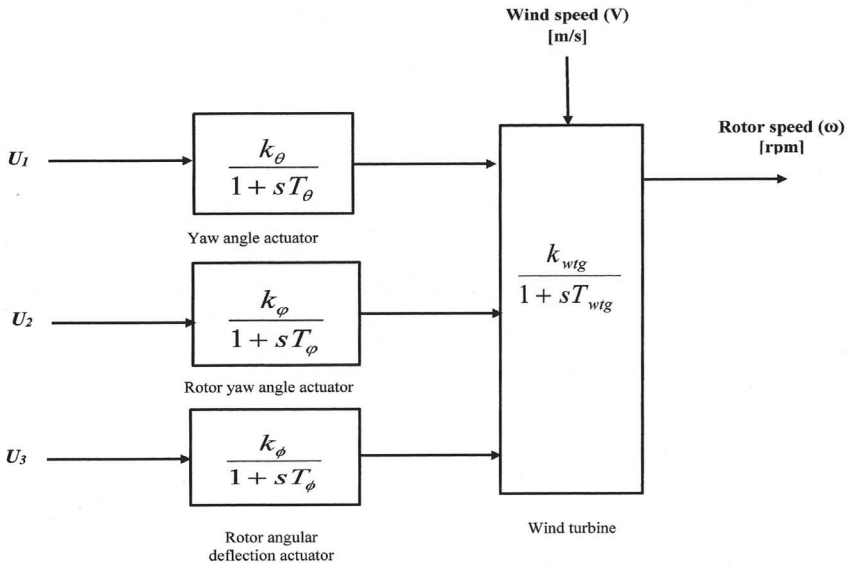

Figure 4.3: Three area controls interconnected model of WT

1- Wind turbine

The wind turbine is represented by the first-order transfer function:

$$\frac{k_{wtg}}{1 + sT_{wtg}} \tag{4.7}$$

2- Yaw actuator

The yaw of wind turbine direction is changed by an electrical/DC motor actuator. A simplified model of the dynamics is presented by the following transfer function model:

$$\frac{k_{\theta}}{1 + sT_{\theta}} \tag{4.8}$$

3- Rotor yaw angle actuator

The rotor yaw angle actuator of a rotor yaw moves in the x-axis direction and is changed by an electrical/DC motor actuator. A simplified model of the dynamics is presented by the following transfer function first-order model:

$$\frac{k_{\varphi}}{1 + sT_{\varphi}} \tag{4.9}$$

4- Rotor angular deflection actuator

The rotor angular deflection actuator of a rotor angular deflection moves in the y-axis direction and is changed by an electrical/DC motor actuator. A simplified model of the dynamics is presented by the following transfer function first-order model:

$$\frac{k_{\phi}}{1 + sT_{\phi}} \tag{4.10}$$

4.7 Wind power formulation

From Figure 4.3, we can figure out the power output equations. The output power without change of wind direction and inflow angle is:

$$P_w(out) = \frac{k_{wtg}}{1 + sT_{wtg}} \times rotorspeed = T_w \times \omega_r \tag{4.11}$$

The output power with change of wind direction only is:

$$P_w(out1) = \frac{k_\theta}{1 + sT_\theta} \times T_w \times \omega_r \tag{4.12}$$

The output power with change of rotor yaw angle only is:

$$P_w(out2) = \frac{k_\varphi}{1 + sT_\varphi} \times T_w \times \omega_r \tag{4.13}$$

The output power with change of rotor angular deflection only is:

$$P_w(out3) = \frac{k_\phi}{1 + sT_\phi} \times T_w \times \omega_r \tag{4.14}$$

The total power output:

$$P_w(total) = P_w(out1) + P_w(out2) + P_w(out3)$$

Than:

$$P_w(total) = (\frac{k_\theta}{1 + sT_\theta} + \frac{k_\varphi}{1 + sT_\varphi} + \frac{k_\phi}{1 + sT_\phi}) \times T_w \times \omega_r \tag{4.15}$$

4.8 Power deviation due to wind yaw direction and rotor angle

4.8.1 Case study one

In this case study, we consider the power deviation of a wind turbine for yaw direction and rotor angle on energy capture through the following equation:

$$P_w(out) = (yaw\ \ angle + rotor\ \ angle)(T_w \times \omega_r) \tag{4.16}$$

$$Yaw\ angle = (\theta + \Delta\theta[Yaw\ \ angle\ \ actuator(Transfer\ \ function)]) \tag{4.17}$$

$$Rotor\ \ angle = (\xi + \Delta\xi[rotor\ \ angle\ \ actuator(transfer\ \ function)]) \tag{4.18}$$

Where ξ=θ + ϕ

$$p_{out} = (\left(\theta + \Delta\theta \frac{k_\theta}{1+sT_\theta}\right) + (\xi + \Delta\xi \begin{pmatrix} rsin(\varphi)\frac{k_\varphi}{1+sT_\varphi} \\ rcon(\phi)\frac{k_\phi}{1+sT_\phi} \end{pmatrix})) \times T_w \times \omega_r \tag{4.19}$$

Than power deviation equation is:

$$p_1 = ((1 - yaw\ \ direction\ \ losses) + yaw\ \ direction\ \ losses \times TF_\theta) \tag{4.20}$$

$$p_2 = \left(1 - rotor\ \ angle\ \ losses) + rotor\ \ angle\ \ losses \begin{pmatrix} rsin(\varphi)FT_\varphi \\ rcos(\phi)FT_\phi \end{pmatrix}\right. \tag{4.21}$$

$$P_{deviation} = p_1 + p_2 \times T_w \times \omega_r \tag{4.22}$$

For example:

1-Wind yaw direction: First, if we assume that the initial condition of the yaw direction is 85% and the deviation of it is (Δ yaw direction 7%)).

2- Rotor angle: Second, if we assume that the initial condition of the rotor angle is 6% and the deviation of it is (Δ rotor angle 7%)).

Then the power deviation equation is:

$$P_{deviation} = (0.85 + 0.07 \times TF_\theta) + \left(0.06 + 0.02 \begin{pmatrix} rsin(\varphi)FT_\varphi \\ rcos(\phi)FT_\phi \end{pmatrix}\right. \times T_w \times \omega_r$$

4.8.2 Energy loss due to inflow angle

According to the data in Table 4.2 , we can see the graph of the rotor angle vs average energy lost x=[0.5 1.8 2.8];

y=[0 4 6];

plot(y,x)

xlabel('Rotor angle')

ylabel('Average energy lost %')

title('Energy loss due to inflow angle')

grid

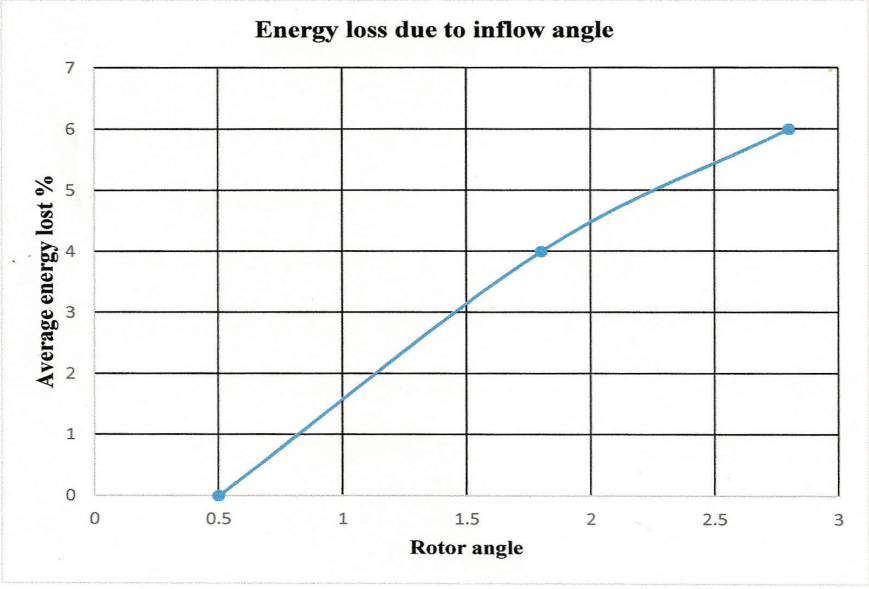

Figure 4.4: Energy loss due to inflow angle

4.8.3 Linear model graph of energy loss due to inflow angle

For our case study, we use Equation 4.21 to linearize the energy loss due to the inflow angle.

x1=[0.5 0.6114 0.7375 0.8781 1.0333 1.2031 1.3874 1.5864 1.7999 2.0280 2.2708 2.5280 2.799];
y1=[0 0.5 1 1.5 2 2.5 3 3.5 4 4.5 5 5.5 6];
plot(y1,x1,'r')
xlabel('Rotor angle')
ylabel('Avrage energy lost % ')
title('Energy loss due to inflow angle')
grid

4.8.4 Case one

We consider the power deviation caused by yaw direction and rotor angle according to the data in Table 4.2 regarding calculation of power loss costs. At wind inflow angle = 4 degrees, Equation 4.21 gives us the value of rotor angle losses which we used to find the

Table 4.2: Energy loss due to inflow angle

Rotor angle [deg.]	Average energy lost %
0	0.5
0.5	0.6114
1	0.7375
1.5	0.8781
2	1.0333
2.5	1.2031
3	1.3874
3.5	1.5864
4	1.7999
4.5	2.0280
5	2.2708
5.5	2.5280
6	2.7999

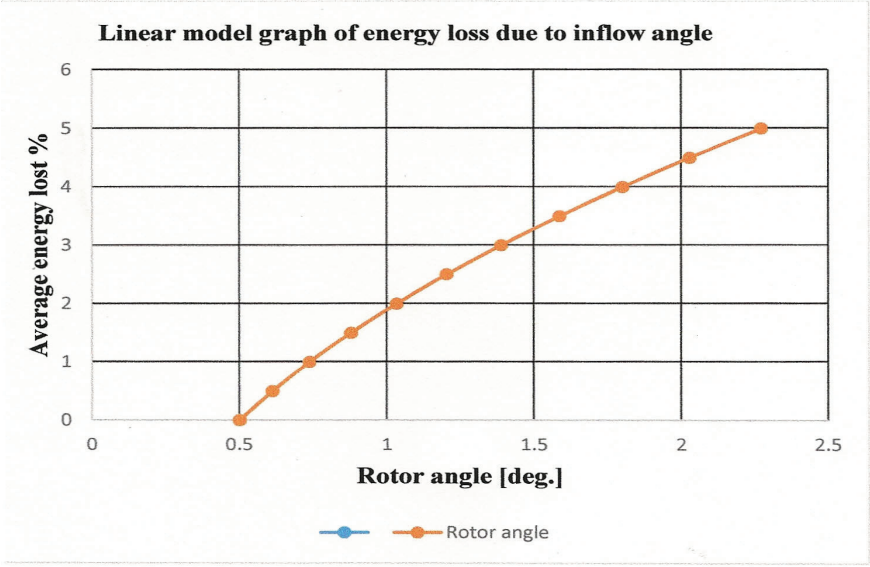

Figure 4.5: Linear model graph of energy loss due to inflow angle

power deviation. The average energy mean the energy per day.

MATLAB code for case one

clear all

close all

clc

degree =4

Coefficients:

p1 = 0.02917

p2 = 0.2083

p3 = 0.5

Linear model Poly2:

losses = p1*degree$^2 + p2 * degree + p3$

$$roter - angle - losses = (p1 * degree^2 + p2 * degree + p3)/100 \quad (4.23)$$

$Equation 4.23 used to find rotor deviation at know degree.$

4.8.5 Efficiency 100% with no deviation

In case one, we consider if there is no deviation on yaw direction and rotor angle on wind turbine power production.

Wind-Speed=10

s = tf('s');

Kwtg=21.655

t1=0.811

Wind-Turbine=Kwtg/(1+ s*t1)

Energy-Capture-without-losses=Wind-Speed*Wind-Turbine

step(Energy-Capture-without-losses)

xlabel('time')

ylabel('Power output [kW]')

In Figure 4.6, we see that there is no deviation in power output due to there being no deviation in yaw direction or rotor angle, which means no deviation in output power.

4.8.6 Case two

Efficiency 85%

In case two, we consider the effect of the power output deviation when the rotor angle deviation is at 4 degrees with a +7% yaw direction deviation.

In figure 4.6 this graph generated when the rotor angle deviation is at 4 degrees with a +7% yaw direction deviation. The MATLAB code for case two is:

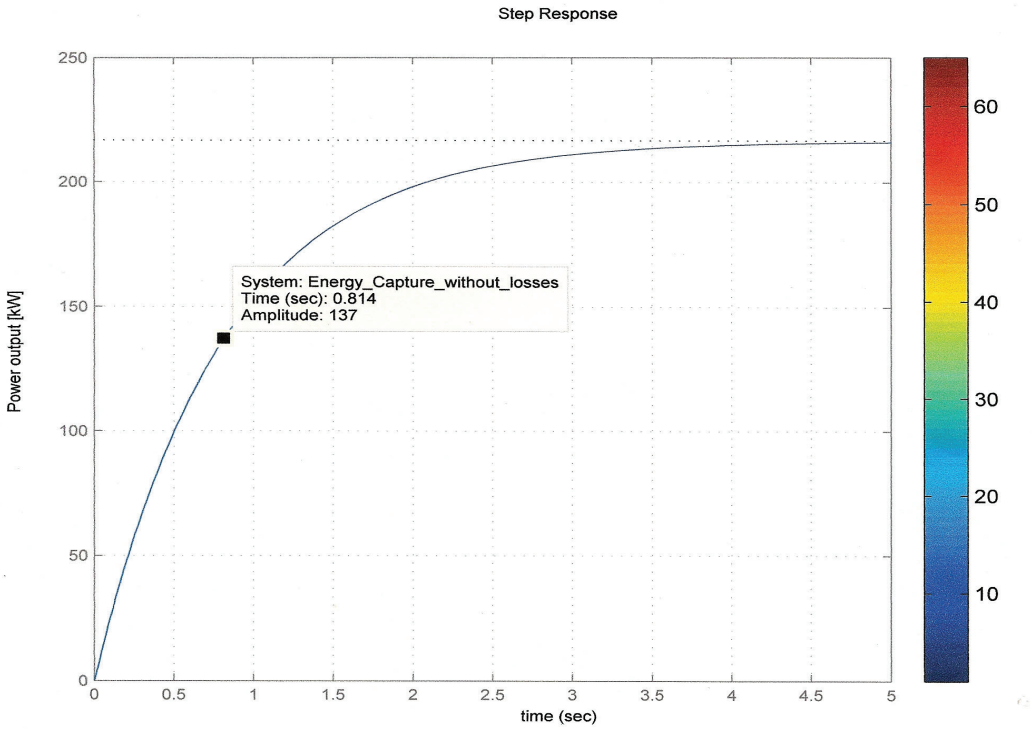

Figure 4.6: The power output without deviation

roter-angle-losses-Initial=8/100

roter-angle-Initial-efficiency= roter-angle-losses-Initial- roter-angle-losses

wind-direction-losses=7/100

wind-direction-Initial-efficiency= 92/100 - wind-direction-losses

Overall-Efficiency= roter-angle-Initial-efficiency + wind-direction-Initial-efficiency

Energy-Capture-with-losses=Overall-Efficiency*Wind-Speed*Wind-Turbine

step(Energy-Capture-without-losses,Energy-Capture-with-losses)

xlabel('time')

ylabel('Power output [Kw]')

Figure 4.7 shows that the power output deviation increased due to the effects of rotor angle loss and yaw direction loss on energy capture.

4.8.7 Case three

In case three, we consider power output deviation when the efficiency is 85% at rotor angle losses of 4 degrees and +0% yaw direction losses.

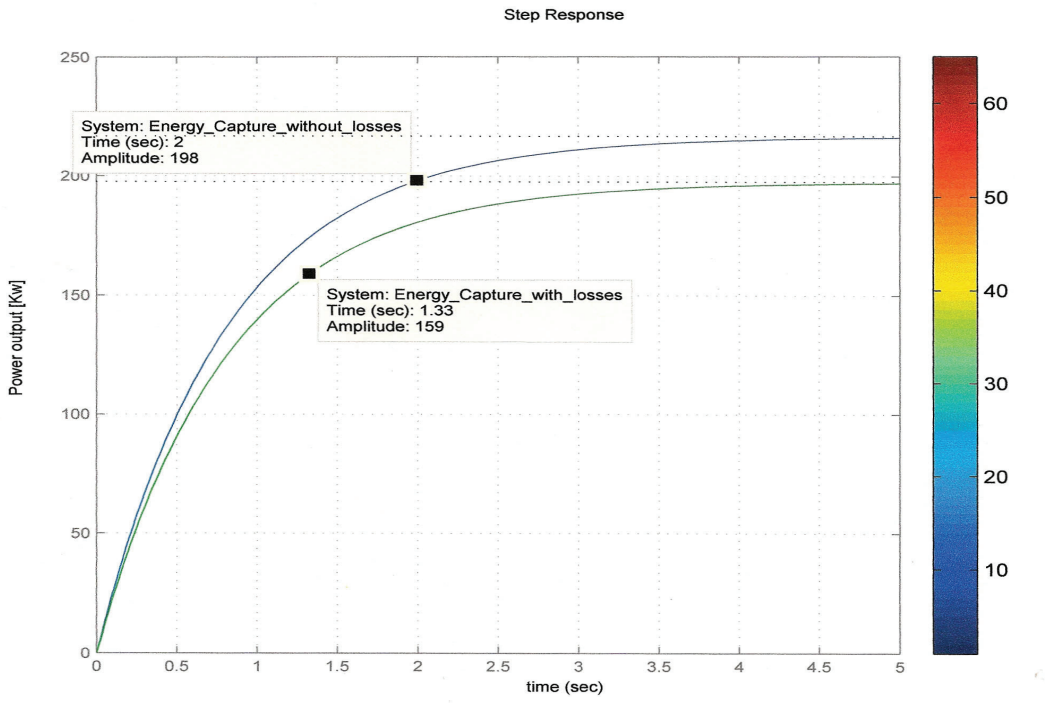

Figure 4.7: Power output at 85% efficiency and rotor angle losses at 4 degrees +7% yaw direction losses

MATLAB code for case three:

roter-angle-losses-Initial=8/100

roter-angle-Initial-efficincy= roter-angle-losses-Initial- roter-angle-losses

wind-direction-losses=0/100

s = tf('s');

P-motor = 0.07/(1+5*s);

step(P-otor)

wind-direction-losses=P-motor

wind-direction-Initial-efficincy= 92/100 - wind-direction-losses

Overall-Efficincy= roter-angle-Initial-efficincy + wind-irection-Initial-efficincy

Energy-Capture-with-Direction-losses=Overall-fficincy*Wind-Speed*Wind-Turbine

step(Energy-Capture-without-losses,Energy-Capture-with-losses,Energy-Capture-with-Direction-losses)

xlabel('time')

ylabel('Power output [Kw]')

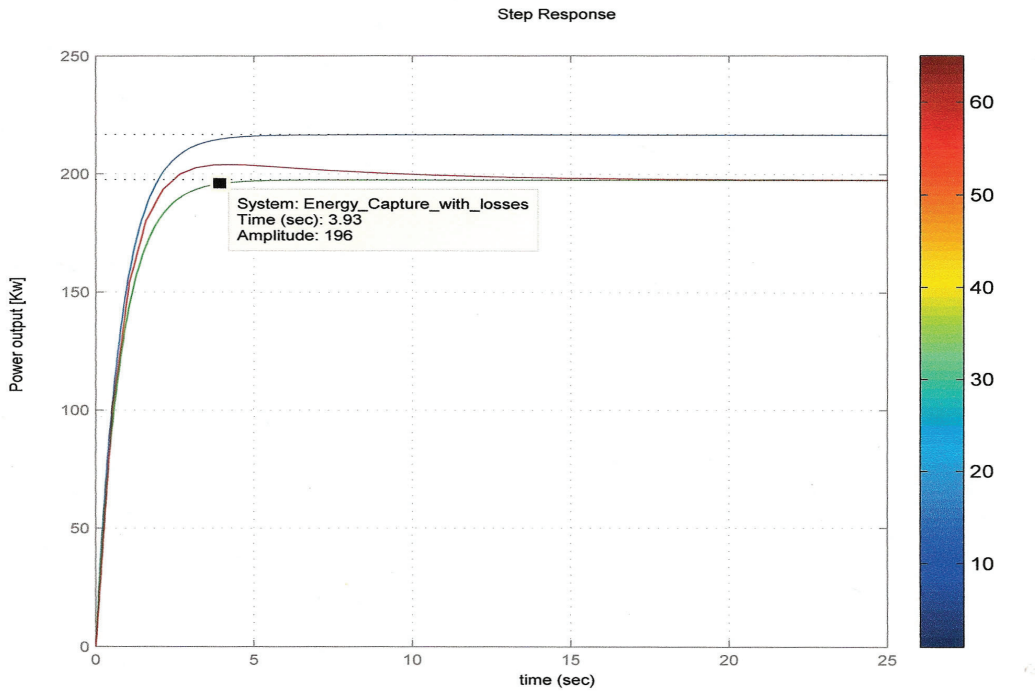

Figure 4.8: Power output deviation at 8% rotor angle loss and +7% wind direction loss

Figure 4.8 shows that the power output deviation increased more due to the rotor angle and yaw direction loss increases.

Case four

In case four, we consider the effect of 8% rotor angle loss and +7% wind direction loss on power output deviation.

The MATLAB code for case four is:

s = tf('s');

P-otor = 0.07/(1+5*s);

step(P-motor)

roter-angle-losses=P-motor

roter-angle-Initial-efficincy= roter-angle-losses-Initial- roter-angle-losses

P-motor = 0.07/(1+5*s);

step(P-motor)

wind-direction-losses=P-motor

wind-direction-Initial-efficincy= 92/100 - wind-direction-losses

Overall-Efficincy= roter-angle-Initial-efficincy + wind-direction-Initial-efficincy

Energy-Capture-with-Direction-and-Rotor-Angle-losses=Overall-Efficincy*Wind-Speed*Wind-Turbine

step(Energy-Capture-without-losses,Energy-Capture-with-losses,Energy-Capture-with-Direction-losses,Energy-Capture-with-Direction-and-Rotor-Angle-losses)

xlabel('time')

ylabel('Power output [Kw]')

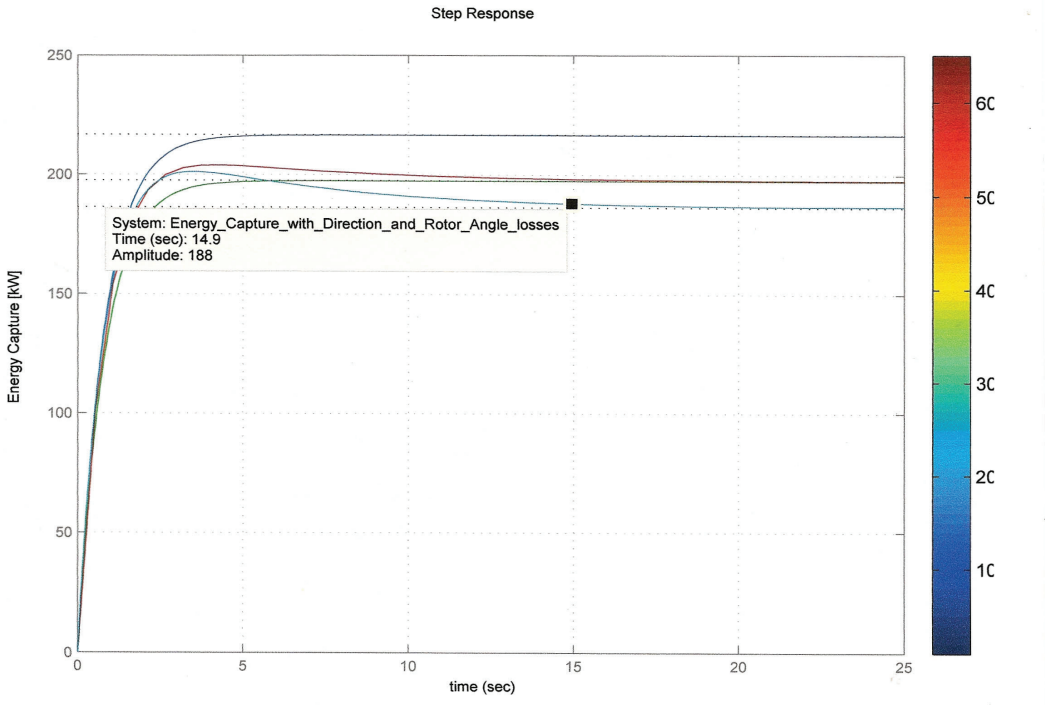

Figure 4.9: Power output at 85% efficiency with 1% rotor angle loss and +7% yaw direction loss

4.9 Case study 2

4.9.1 Wind turbine system and controller

Figure 4.10 shows a block diagram of wind turbine system dynamics and control. The change of inflow angle problem can be controlled by altering the rotor yaw angle (φ) and rotor angular deflection (ϕ) signals to keep the inflow angle perpendicular to the rotor blades. The control senses the deviation between the inflow angle and rotor angle in order to reduce the error between them. The optimal control system is used to optimize the control of rotor angle system loop of wind turbine. The practical implication of the turbine control is that when the inflow angle changes, the rotor angle control tracks it.

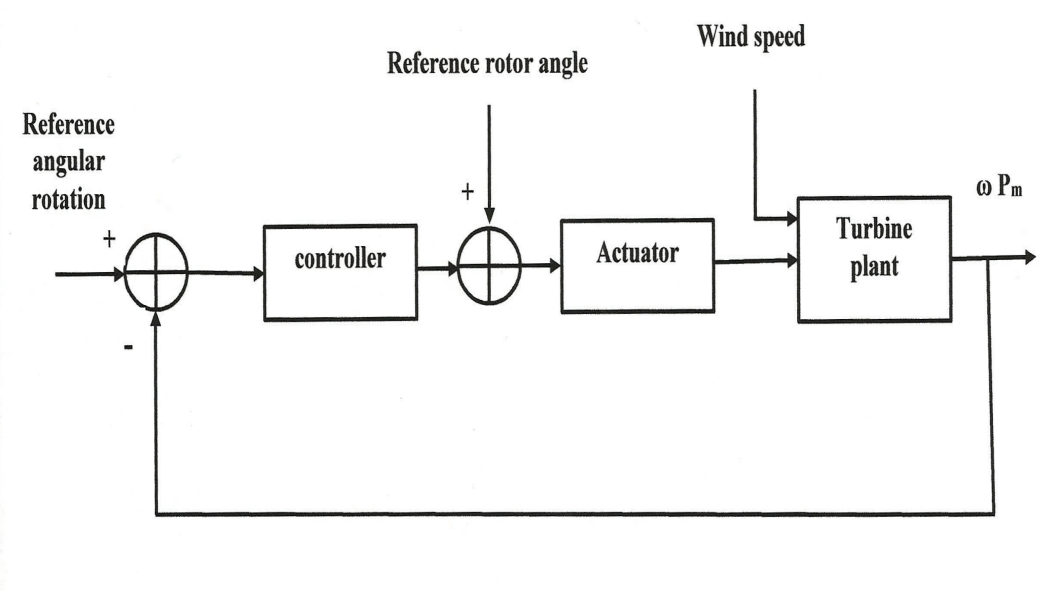

Figure 4.10: Block diagram of wind turbine system dynamic and control

4.9.2 Wind turbine transfer function

The transfer function for wind turbine Equation 4.21 is found in [54]. Used together with the values in Table 4.2, this gives the final transfer function for the wind turbine:

$$G(s) = \frac{\frac{K_G}{R_G}}{s.J_{tot} + B_G + \frac{K_G^2}{R_G}} \tag{4.23}$$

Table 4.3: Motor and gear parameters from data sheet [54]

Property	Symbol	Value	Unit
Torque constant	K	38.2 $\times 10^{-3}$	N_{m}/A
Terminal resistance	R_G	7.19	Ω
Terminal inductance	L_G	1.04$\times 10^{-3}$	H
Gear ratio	N	1:11	-
Generator inertia	J_G	4.4$\times 10^{-6}$	Kg$\times m^2$
Inertia of generator and gears	J_{GG}	12.6$\times 10^{-6}$	Kg$\times m^2$
Inertia of blades	J_r	186$\times 10^{-6}$	Kg$\times m^2$
Total inertia of system	J_{tot}	199$\times 10^{-6}$	Kg$\times m^2$
Viscous friction coefficient	B	42.4$\times 10^{-6}$	Nm/(rad/s)

$$G(s) = \frac{21.655}{0.811s + 1}$$

where:

G(s) is the plant in the frequency domain [-]

K_G is the generator constant [Nm/A]

J_{tot} is the inertia for the generator and rotor [kg*m$_2$]

B_G is the friction in the generator and rotor [Nm/(rad/s)]

R_G is the generator resistance [W]

4.9.3 Combined model (plant and rotor actuator transfer function)

Figures 4.11 and 4.12 represent the control and combined model of the wind turbine transfer function and the rotor yaw actuator transfer function. In order to derive a state space model for the rotor yaw actuator and the wind turbine, the states to be controlled must be identified, together with the input and output of the system.

where:

States: The angular velocity of rotor, ω_r and the rotor yaw angle in x- axis, φ .

Input: The angular velocity ω_{ref}.

Output: The angular velocity ω_r and rotor yaw angle φ

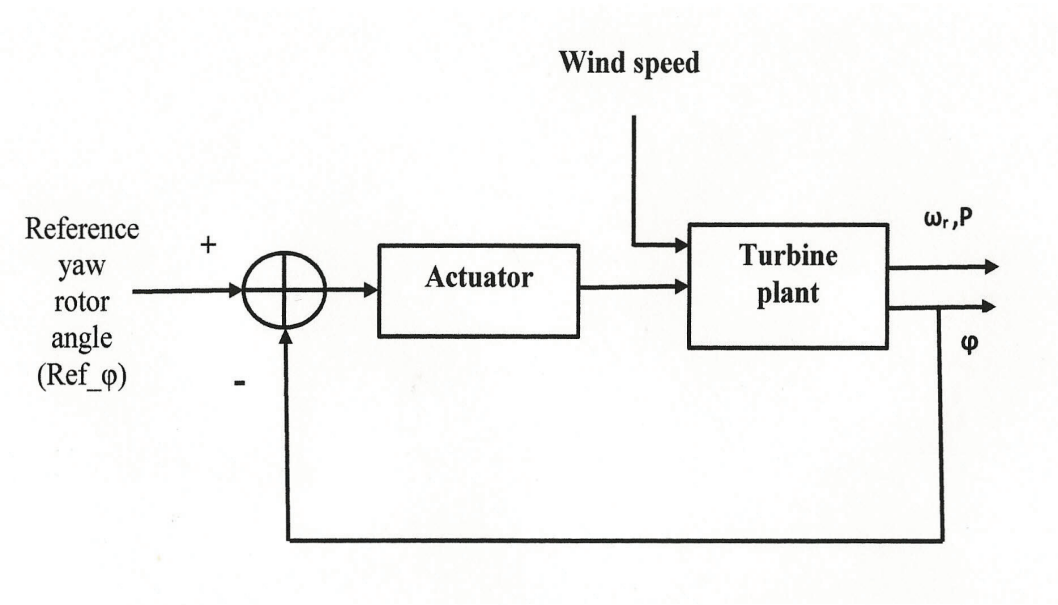

Figure 4.11: Yaw actuator and wind turbine control loop

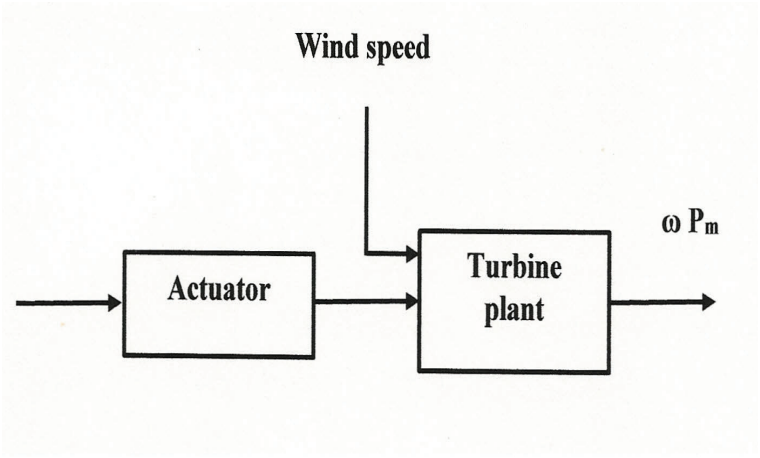

Figure 4.12: Combined wind turbine with rotor yaw actuator

4.9.4 Feedback control design

From the state space representation of the model, it is now possible to design a state space controller for the combined model. Before a controller is designed, however, it is important to ensure that the modeled system is controllable. This statement can be expressed with the model matrices, which can be seen in Equations 4.22 and 4.23. The system is controllable if and only if the rank of the controllability matrix equals the number of states in the system shown in Figure 4.12.

The system will be uncontrollable if the link between control input and system dynamics is lost.

$$\dot{x} = Ax + Bu \tag{4.24}$$

$$y = Cx + Du \tag{4.25}$$

MATLAB has been used to determine the combined system which is described by the derived matrices A, B, C and D.

num1=$\begin{bmatrix} 21.655 \end{bmatrix}$

den1=$\begin{bmatrix} 0.811 & 1 \end{bmatrix}$

g1 = tf(num1,den1)

The transfer function of the wind turbine:

$$g1 = \frac{21.66}{0.811s + 1}$$

The transfer function of the rotor yaw actuator:

num2=$\begin{bmatrix} 1 \end{bmatrix}$

den2=$\begin{bmatrix} 0.28 & 1 \end{bmatrix}$

g1 = tf(num21,den2)

$$g2 = \frac{1}{0.28s + 1}$$

The combined transfer function of the wind turbine and rotor yaw actuator:

num = conv(num1,num2)

den = conv(den1,den2)

g = tf(num,den)

The combined transfer function:

$$g = \frac{21.66s + 1}{0.2271s^2 + 1.091s + 1}$$

System state space:

$\begin{bmatrix} A, & B, & C, & D \end{bmatrix}$=tf2ss(num,den)

A = $\begin{bmatrix} -4.8045 & -4.4037 \\ 1 & 0 \end{bmatrix}$, B = $\begin{bmatrix} 1 \\ 0 \end{bmatrix}$, C = $\begin{bmatrix} 95.3629 & 4.4037 \end{bmatrix}$, D =0

Theorem

Assuming that the pair (A, B) is controllable, there exists a feedback matrix F such that the closed-loop system eigenvalues can be placed in arbitrary locations.

4.9.5 Controllability

For the combined system, the rank of the controllability matrix 4.26 is 2, which equals the number of states in the system, and thus the system is controllable. MATLAB has been used to determine the rank of the controllability matrix using the following command: rank (CO).

$$CO = \begin{bmatrix} B & AB & . & . & . & A^{n-1}B \end{bmatrix} \tag{4.26}$$

where:

CO is the controllability matrix [-]

n is the number of states in the system

$$CO = \begin{bmatrix} -4.8045 & -4.4037 \\ 1.0000 & 00.00 \end{bmatrix}$$

rank(CO) = n = 2

4.9.6 Observability

In order to ensure that an observer can be designed, the system should be checked for observability, which means calculating whether it is possible to estimate the unknown states

from those available. One way to test this is by creating the observability matrix, as seen in matrix 4.27. Observability is then given if the rank of the OB-matrix is equal to the dimension of A.

$$OB = \begin{bmatrix} C \\ CA \\ . \\ . \\ . \\ CA^{n-1} \end{bmatrix} \tag{4.27}$$

$$rank(OB) = rank\left(\begin{bmatrix} 95.3629 & 4.4037 \\ -453.7647 & -419.952 \end{bmatrix}\right) = 2$$

Therefore, the model describing the combined system is observable.

Chapter 5

DESIGN AND DEVELOPMENT

5.1 Introduction

The essential philosophy of the design and operation of wind turbines is derived based on a first-principles methodology using conservation of mass and conservation of energy in a wind stream. To develop the wind turbine energy capture capabilities, it is essential to optimize variables related to wind speed, which is required for the wind turbine to operate close to the point of optimum productivity. Developments in energy capture through variable-speed processes can be obtained by improved tracking of the wind direction and predictive wind inflow angle. Under varying wind situations, there is potential to use the rotor angle turbine to improve energy capture by forcing the rotor to operate close to the maximum energy capture point. Apart from progress in optimization ideas as well as control and operation concepts of wind turbine, there have been many changes lately, such as the redesign of turbine rotor blades, shape, and individual control. Moreover, the power manufacturing of energy storage such as storage batteries, flywheel energy storage and super-conducting magnetic energy storage has led to an increase of optimization and control in the use of wind turbines and photo-voltaic cells as other sources of electrical energy.

5.2 Design procedure

The main design consideration was building and developing a successful design model whose goal is to increase the energy capture of the wind turbine. Furthermore, the mechanical equipment and control scheme must connect to improve the variable turbine rotor, which can be tracked by the wind inflow angle. It was decided that the most effective method for achieving the desired outcome is to use the experimental setup model to test the target in real time and get data from it to analyze the results. This was implemented in the mechanical model by creating a wind turbine with its own control system.

5.3 Experimental setup model goals

1. Increase energy capture from the wind.
2. Protect the wind turbine lifespan by adapting wind speed to the turbine capacity.
4. Prevent wind speed disturbances.
5. Use wind inflow angles to improve wind turbine performance.
6. Gain the required accuracy by modifying the rotor angles to face the wind inflow angle.
7. Compare the energy capture of fixed rotor angle turbines and variable rotor angle turbines.

5.3.1 Experimental setup mechanical model

In this section, a model for the wind turbine discussed in the case study is described. The wind turbine components are a shaft, two ball bearings, a rotor, pulley and tower. The wind turbine model will be used to analyze multidimensional optimal control. Figure 5.1 shows the experimental setup model. The models for the wind turbines are created according to two different approaches: The first one is modeling the wind power based on a fixed rotor angle turbine, and the other is based on modification of the multidimensional control variable rotor angle turbine. There are two main types of wind turbines: fixed rotor angle turbines and variable rotor angle turbines.

5.3.2 Achieving the goals

The following extra parts will be added to the mechanical model:

1. Universal Joint (U-joint)
2. Actuators
3. Ball bearing
4. Ball joint
5. Measuring position sensors
6. A speed monitoring sensors
7. Micro-controller
8. Auxiliary relays

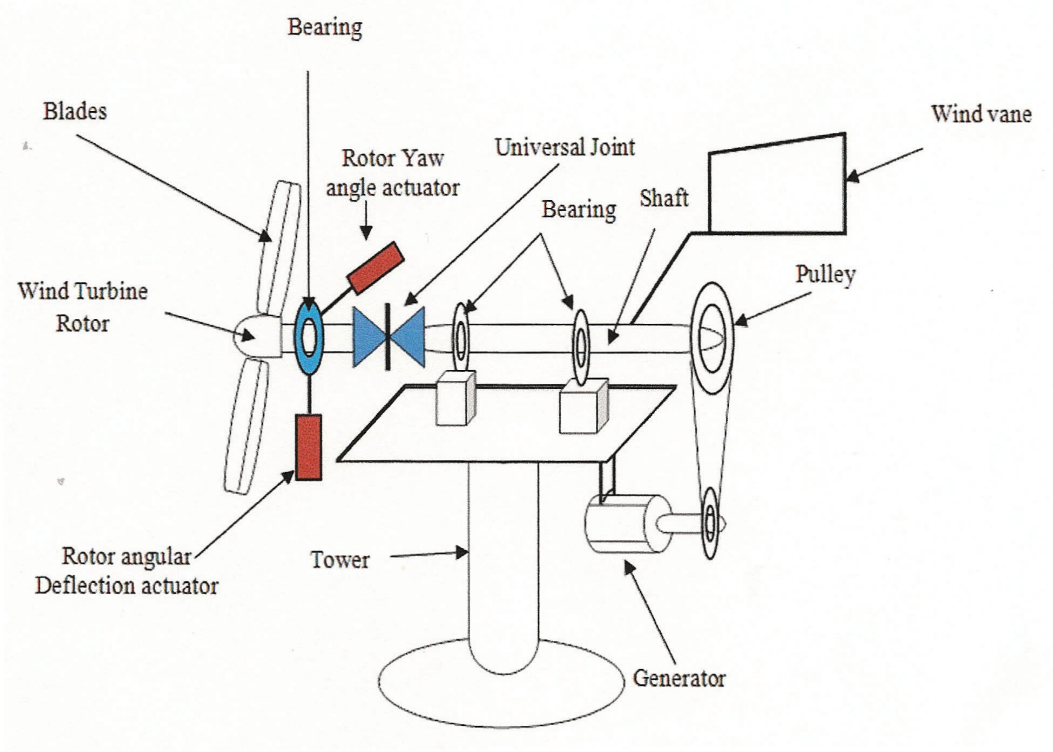

Figure 5.1: Wind turbine experimental setup mechanical model

5.3.3 Ball joint

The ball joint or spherical joint is the coupling between two rod tubes. It consists of a spherical part fitted into a spherical socket, allowing free movement within a specific conical volume called a multi-axial joint [46]. Figure 5.2 shows the ball joint movement in all directions.

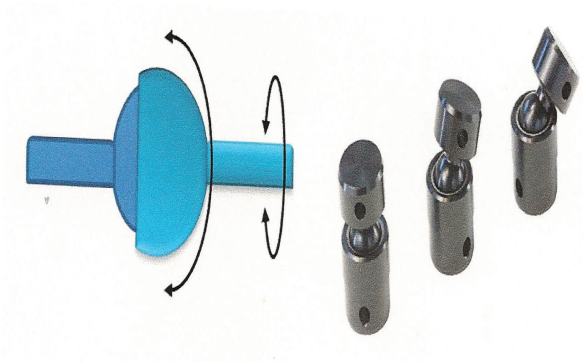

Figure 5.2: Ball joint movement in all directions

5.3.4 Ball joint or spherical joint connections

The ball joint is linked with the drive actuator, rotor yaw actuator and rotor angular deflection actuator. The function of the ball joint on the experimental model is to help determine if the rotor is at the proper angle. Moreover, actuators interchange freely without resistance in order to rotate in the direction-finding path of the rotor inflow angle.

5.4 Actuators

Actuators are transducers that convert an electrical, hydraulic or pneumatic signal to a required movement amount [47]. Actuators are used to drive the universal joint to move the rotor to the right inflow angle. Figure 5.3 shows different types of actuators. Electrically

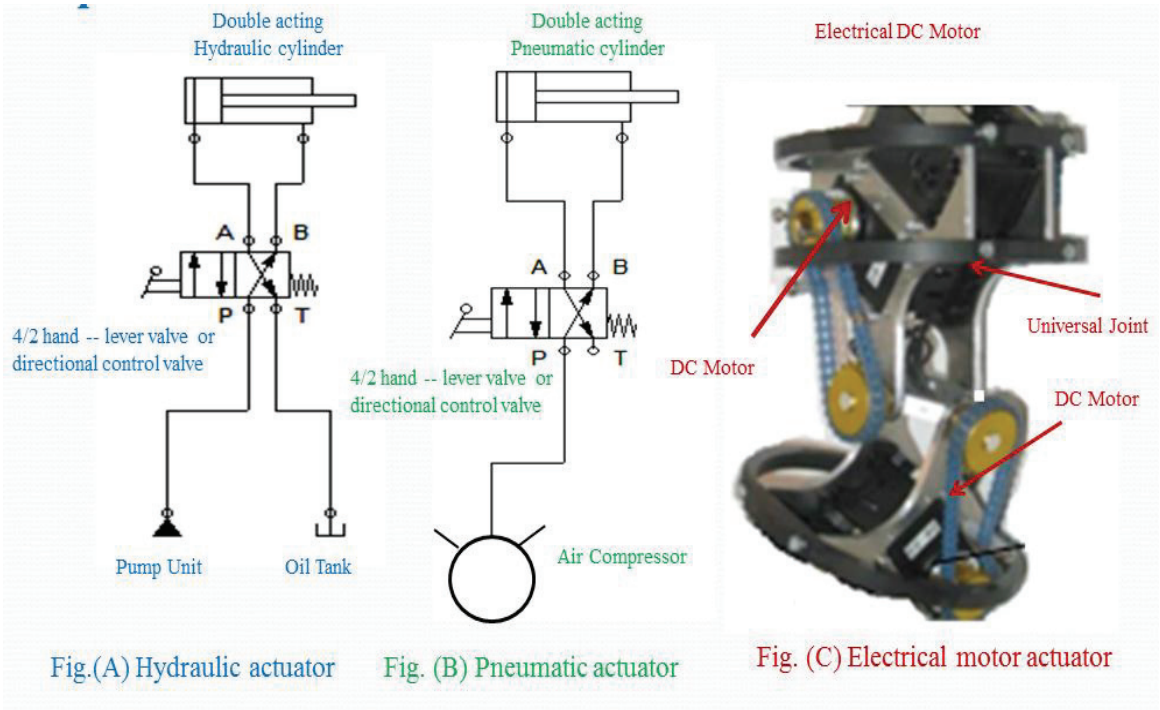

Figure 5.3: Different types of actuators

actuated systems are very widely used in control systems, because they are easy to interface with the control systems, which are also electric, and because electricity is easily available, unlike fluid power which requires pumps and compressors [48]. Electrically actuated systems are widely used in control systems because they are easy to interface with the

control systems, which are also electric, and because electricity is easily available, unlike fluid power which requires pumps and compressors [48]. Due to the advantages of electrical systems, DC motors were used with the actuators.

Advantages of electrical systems:

1. Electricity is easily routed to the actuators
2. Electricity is easily controlled by electronic units
3. Electricity is clean
4. Electrical faults are often easier to diagnose.

5.5 Implementation of new technique

The wind turbine seen in Figure 5.4 shows the model was made for the purpose of determining the impact of variable rotor angles on wind turbine energy capture. The model was made in the mechanical workshop of the Electrical and Computer Engineering Department at Dalhousie University, Halifax, Canada. The equipment used was assembled in collaboration with the mechanical workshop.

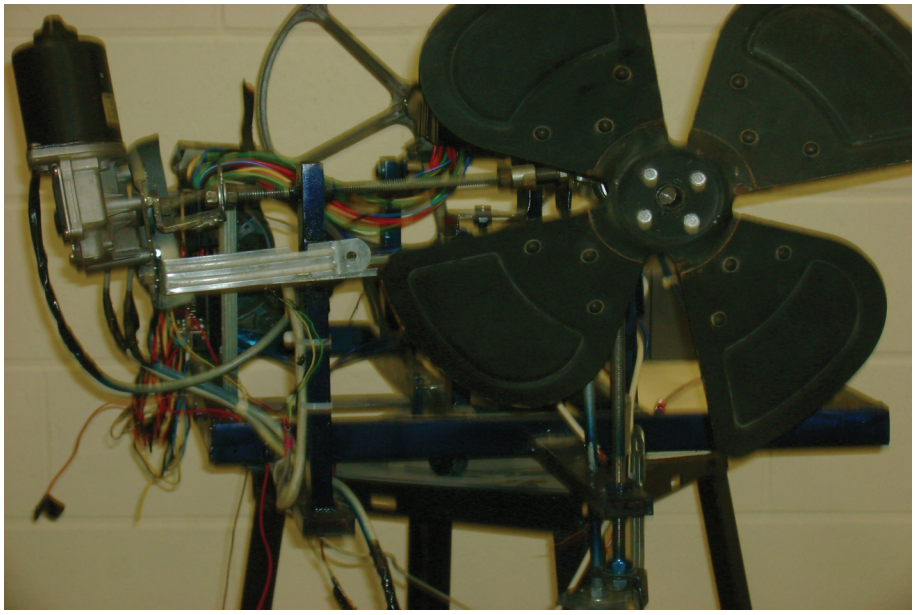

Figure 5.4: Wind turbine model

5.5.1 Modification of wind turbine

The data listed in Table 5.1 for the modification of the wind turbine were used to improve wind turbine energy capture. As can be seen, column one describes the elements name, column two gives its value, and column three shows the units used for each element.

Table 5.1: Data of modification wind turbine

description	Value	Unit
Blade number	4	–
Generator power	DC	Voltage
Gear ratio	1:3.45	Revolution
Pitch mode	Fixed actuator	–
Variable rotor angle	Horizontal actuator	φ°
Variable rotor angle	Vertical actuator	ϕ°
Wind direction	Yaw actuator	θ°

5.6 Blade design

The core of conversion of kinetic energy of wind to rotary-mechanical energy is the blade. The angle of the blades also greatly impacts how much lift is generated. On large wind turbines, the blade angle is constantly adjusted to give the blades the optimal angle into the apparent wind. The angle of the blade relative to the plane of rotation is known as the pitch angle. The angle of the blade relative to the apparent wind is called the angle of attack [49]. In this thesis, we used four blades at a fixed pitch angle. The blades are 0.36 m in diameter with typical blade design, as shown in Figure 5.5, and are mounted to the fixed pitch assembly.

5.6.1 Wind turbine blade design related

The design of the wind turbine depends on the blade, blade size, number and angle of blades, blade material, airfoil shapes, and twisted pitch blades.

5.7 Generator and gears

Wind turbines generate electricity by harnessing the power of the wind. The energy in the wind speed turns the blades around a rotor connected to the main shaft, which is the

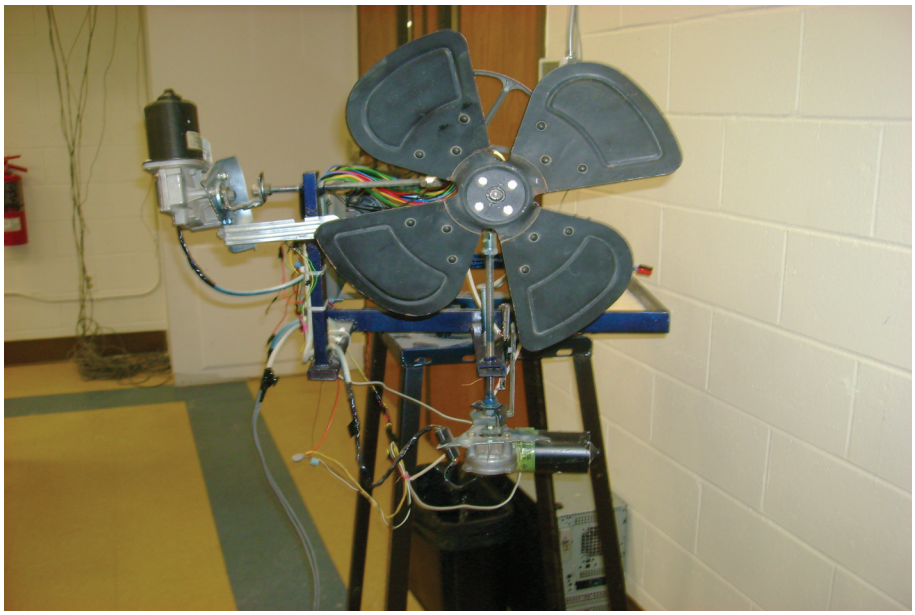

Figure 5.5: Blade design model

low-speed shaft. The drive train (including the gears) increases the rotational speed. The high-speed shaft is connected to a generator which creates electricity. The rotor is connected to the main shaft, which ends in a large diameter pulley. The high-speed shaft with pulley is connected to a DC generator by a belt, which then creates electricity. In this study, the generator was connected to the rotor blades through a gear with a ratio of 1/3.45, meaning one revolution of the rotor blades gives 3.45 revolutions of the generator. The motor used was an A-max 12V DC-motor, as shown in Figure 5.6.

5.8 Rotor angle turbine

By modifying the rotor angle by mounting it on a universal joint, as shown in Figure 5.10, we were able to construct a horizontal axis wind turbine (HAWT) that could be dynamically controlled while in the wind stream. We investigated the relationship between the energy capture of the wind turbine relative to the rotor of its angles and the speed at which the turbine was rotating. The rotor angle utilizes two (one for each rotor direction) independent electric motors and controllers to provide adjustment of the x-axis and y-axis rotor angle during operation. The rotor angle is adjusted by an electric drive mounted near the rotor hub and is coupled to the mechanical gear to increase the driver torque. The rotor angle controller enables the wind turbine rotor to regulate its angle according to the wind inflow

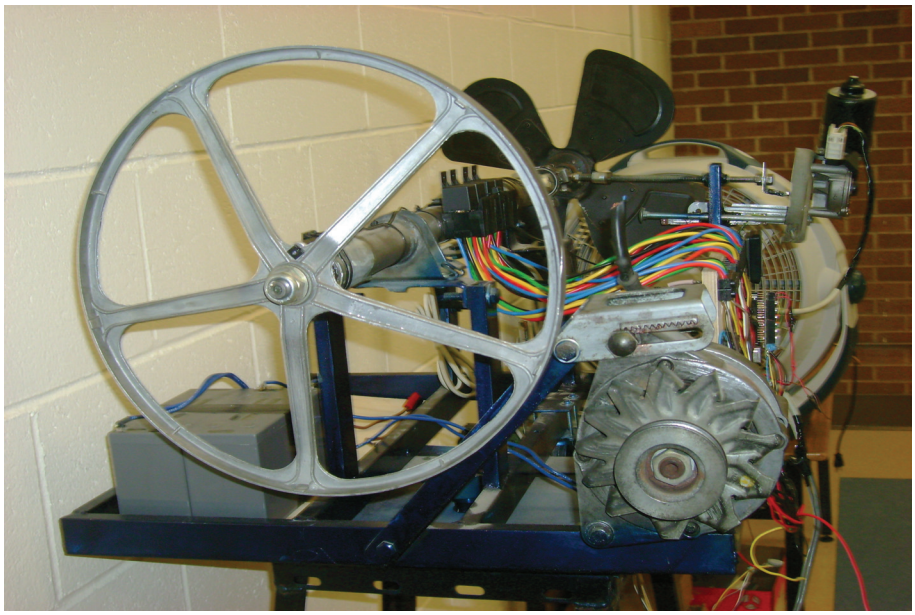

Figure 5.6: Generator and gears

angle. Moreover, the electric driver can adjust its angle to regulate the energy capture by increasing or decreasing the rotor speed. To be able to control the rotor angle of the wind turbine generator, a rotor angle model was designed. The rotor angle was adjusted according to the wind inflow angle (through the two actuators), as shown in Figure 5.7.

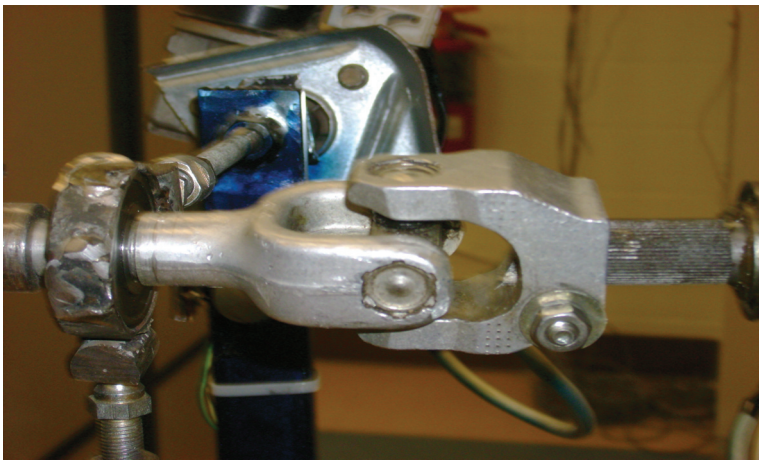

Figure 5.7: Rotor angle turbine

5.9 Wind speed source

Because our experimental setup did not fit inside the Dalhousie wind tunnel, we used a fan as the wind source with variable speed and variable wind inflow angle (see Figure 5.8). It is worth nothing that had we used the wind tunnel, the results would have been more precise.

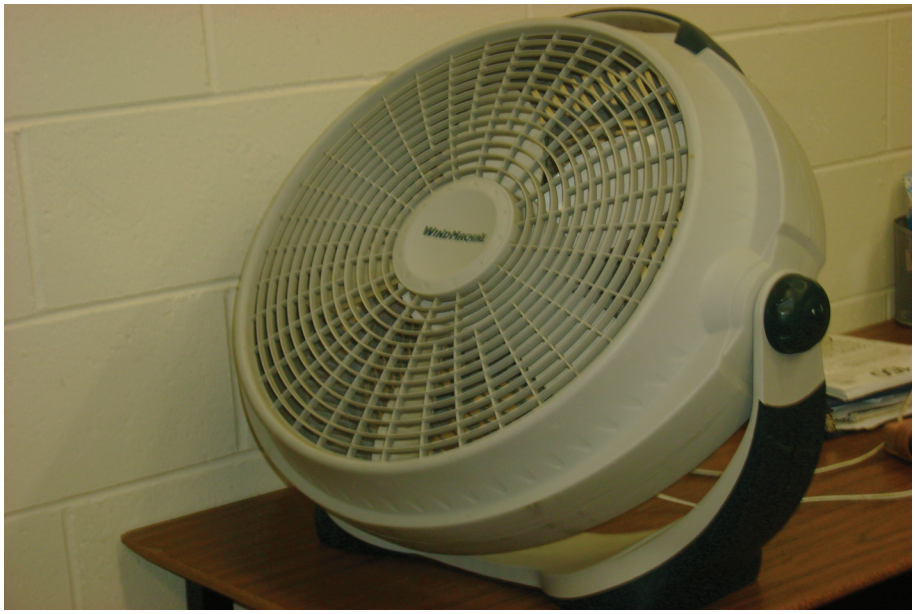

Figure 5.8: Wind speed source

5.10 Wind turbine control panel

The control system of wind turbine machines is usually controlled automatically or manually from either an interface located inside the nacelle or from a control box at the bottom of the tower. For a rotor angle system, however, a control panel is needed that will typically include power supply, micro-controller, DC motor driver, speed monitor, wire terminal, and axillary relays. Figure 5.9 shows the control panel used to operate a wind turbine with variable rotor angle. All data sheets and specifications of the DC driver are in Appendix C

5.10.1 The micro-controller

The micro-controller is used to collect and process all the data, check the feed-in, and communicate with the control equipment. All data sheets and specifications for the micro-controller can be found in Appendices A and B. After the different components of the model

are combined, a program code is used to operate the micro-controller for experimental setup (see Appendix E). This program code provides some of the data values in the model.

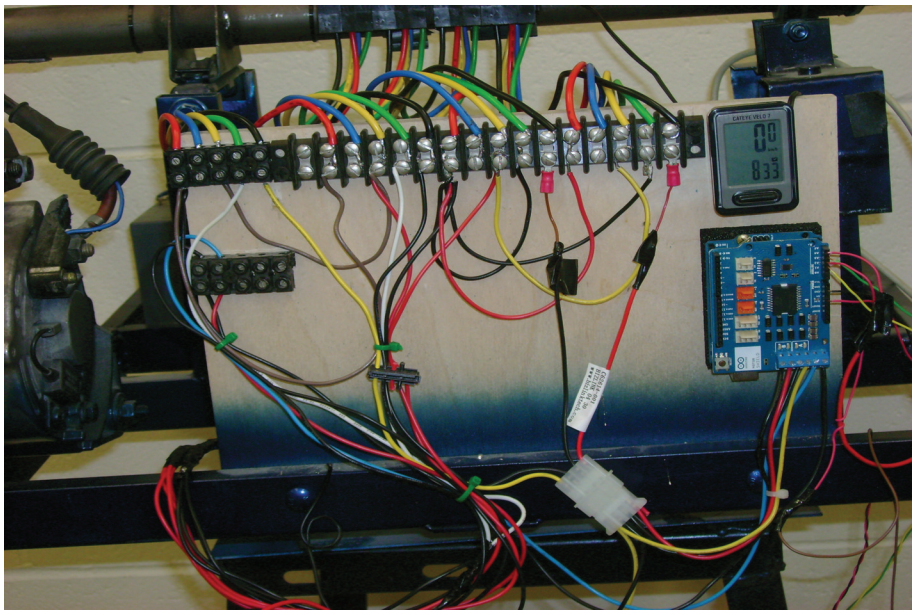

Figure 5.9: Wind turbine control panel

5.11 Wind turbine sensors

In a wind turbine system, sensors play a critical role. At the same time, the measurement system is important both in optimizing and defending the turbine by controlling the rotor angle and yaw to maximize the amount of power generated under varying wind conditions while protecting the wind turbine from damage.

5.11.1 Sensors and control systems

The main role of sensors is to detect data in the environment around the wind turbine model. The data are then passed to a micro-controller inside the device, which analyses them and decides what action to take. The micro-computer sends instructions to the device telling it what to do, and the device carries out the instructions. Several different sensors are used in this model. Position sensors are used to give the position of the rotor in relation to the x-axis and y-axis directions, wind turbine direction sensors are used to give wind turbine direction, speed sensors are used to measure the rotor speed, and wind inflow sensor are used to give the inflow angle.

Chapter 6

RESULT AND DISCUSSION

6.1 Experimental setup model

This section will show which components and parameters have impacted the WTG energy output and thus demonstrate how the output from the wind turbine can be optimized. The aerodynamic parts of a conventional wind turbine (fixed turbine rotor angle) are affected by the pitch angle, but in this study three other mechanical controls were used to achieve the rotor inflow angle, which increased the wind turbine rotor speed.

The focus of this work is to achieve power optimization. Generally, small turbines are assumed to be designed with a variable rotor inflow angle. The turbine will track the maximum power point. This was performed by using a fixed pitch angle, wind direction, variable rotor yaw angle and variable rotor angular deflection. The research work began with the construction of an experimental setup of a wind turbine model with a fixed pitch angle and a variable rotor inflow angle. The wind speed source (air fan) had variable speeds, directions and inflow angles. The experimental setup used for achieving a changing rotor inflow angle is shown in Figure 6.1.

6.1.1 Wind turbine energy capture

The experiment was designed to show the effects of wind inflow angles on the energy capture outcome of a wind turbine and to study the influence of challenging wind inflow angle setup experiments needed to measure the impact of wind inflow angles on the performance of a wind turbine. The setup model shown in Figure 6.1 uses an Arduino UNO micro-controller to deal with the input and output signals to keep the rotor angle tracking the inflow angle. The program code used to operate the system is listed in Appendix A5 while, the micro-controller used to control all inputs and outputs is listed in Appendices A1-A4. The following signals are the inputs and outputs of the micro-controller:

1. Measuring wind inflow angle as inputs

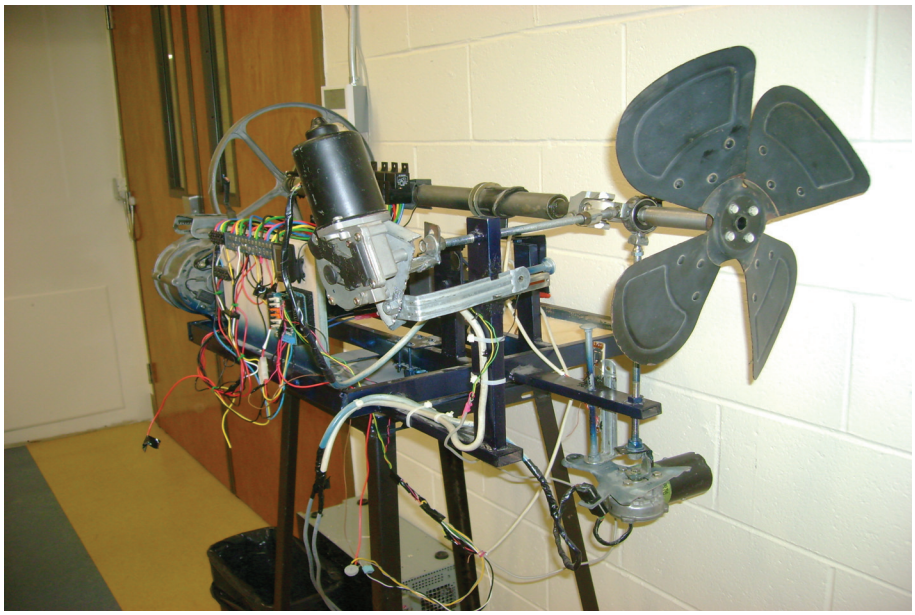

Figure 6.1: Experimental setup model

2. Motor drive as outputs
3. Actuation position as inputs
4. Draw out the inflow angle as output

6.2 Testing and results analysis

The testing and results analysis is divided into three parts: tracking the wind inflow angle, energy capture, and the flexibility of wind turbine operation. The results gained from the experimental setup of the wind turbine test model were fairly hopeful. The results of rotor angle adjustments in the X- and Y-axis direction tests were as expected.

The practical knowledge was gained in building the prototype:

- learn practical skills for real-life project development
- Estimate impact of proposed design on energy capture
- Deploy and user-test preliminary prototypes and the final design product
- Gather knowledge and insight from developing working prototypes, being both building components and industrial products

The rotor angle of the X- and Y-axis direction output only varied when the wind inflow angle changed and the output power of the wind turbine model varied only when the input of wind inflow angles and wind direction changed. Further analysis could also be carried out on

these results to confirm that the wind direction and wind inflow angle are tracked. The wind direction sensor measures the angle of wind direction and the wind inflow angle sensors sense the X- and Y-axis of the wind inflow angle. Thus, if we know the wind direction and wind inflow angle representing the input data of the wind turbine, the sensors can be controlled to face the appropriate wind direction and wind inflow angle. The results show that the energy captures of the wind turbine increase when the wind turbine is adjusted according to wind direction and wind inflow angle. If we compare the results between the variable turbine rotor angle and the fixed turbine rotor angle, we see that the output power of the variable rotor angle is better than the fixed rotor angle. Tables 6.1 and 6.2 show that the variable turbine rotor improves output voltage.

6.3 Results of increasing the flexibility of wind turbine operation

Adding a universal joint to the wind turbine generator will increase the need for wind energy capture flexibility. This means that the ability for wind generation increases or decreases in response to changes in rotor speed according to load. In addition, long startup and shutdown times should be avoided, as they will affect the wind turbine life span and load effect. The operational flexibility of a wind turbine is more significant during times of minimum wind speed and can be achieved by adding flexible wind turbine rotor angles. Figure 6.5 is giving the compare between Figure 6.3 and 6.4 the results of fixed and variable. We note that the output of the modified turbine show approximately 4-6% better results than the fixed turbine rotor angle. The output voltage measured to shows the output of generator during the rotor rotating. Its shown when more wind speed passing through the blades giving more output which represent more energy capture.

6.4 Results of rotor angle tracking wind inflow angle

Table 6.1 lists the wind turbine parts to be adjusted and regulated according to inflow angle and wind direction. The rotor angle is adjusted to face the inflow angle, and the turbine direction to face the wind. All of the adjustments and regulations are dependent on actuation responses to measurement input signals. Based on the information obtained from the sensors, we can see that a signal represents the wind inflow angle both vertically and horizontally according to the rotor angle position. However, the information regarding the wind inflow

Table 6.1: Possible design of wind turbine adjustable types

Adjustable type	Design adjustable	Requirement
Rotor angle	Adding Universal Joint	Rotor yaw angle Rotor angular deflection
Wind direction	Wind turbine yaw direction	Actuation
Regulation	Rotor rotational speed	Output power
	Rotor angle	Facing wind inflow angle
	Turbine direction	Facing wind direction

angles changed to rotor actuation with the set point to allow for rotor actuation changes, indicating that the rotor actuation of these output variations is quite controlled. Thus, if the measured values of wind inflow changes, the rotor angle also changes. The results of this test for the X- and Y-axis of wind inflow angles are tracked by the X- and Y-axis of the rotor angle. As can be seen in Figure 6.2, the outputs varied in a linear mode, making them suitable for use in the control system.

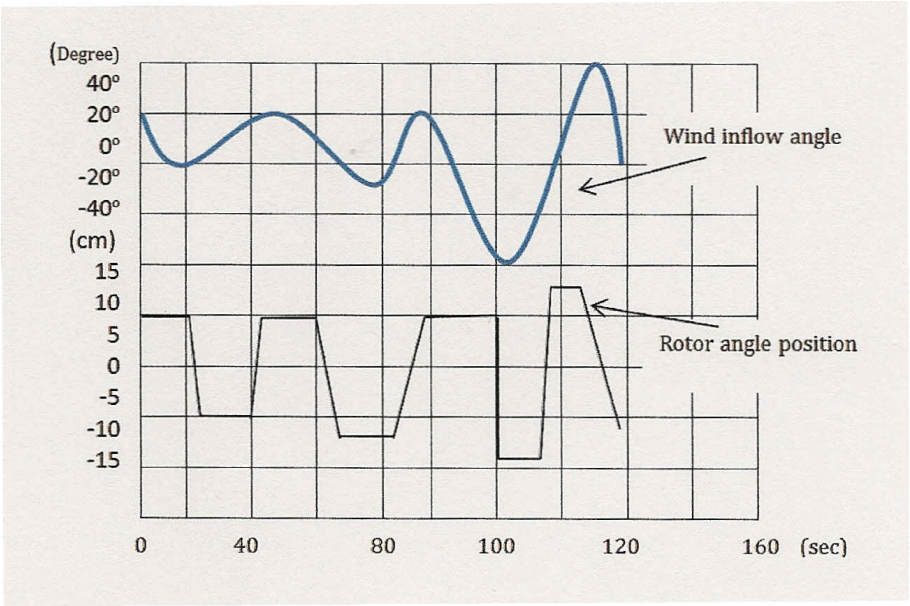

Figure 6.2: Inflow angle tracking

6.5 Energy capture result

In order to see what effect the modification of the wind turbine had on energy capture, we used the model as a fixed rotor angle once, and then used it as a variable rotor angle. For

the test, all inputs and outputs were recorded, including the predicted inflow angle. The analysis and application of the experimental setup shows that the output voltage, which represents the energy capture, improves the outcome. Thus, we can see from the success of the proposed model that we achieved our goal. The results shown in the following figures and table provide details on the impact of the proposed modification.

6.5.1 Fixed turbine rotor angle results

We consider the effect of inflow angle in wind turbine energy capture by using an experimental model with a variable rotor angle. Table 6.2 shows the results of an experimental model using a fixed rotor angle, fixed wind direction, variable wind speed and variable inflow angle. As indicated in the table, the increase in wind speed corresponded to the increase in output voltage. The inflow angle, whose effects on power outcome we are hoping to prove, is not used in these results. Figure 6.3 shows the output voltage of a fixed turbine rotor angle.

Table 6.2: Fixed turbine rotor angle result

Wind direction (θ)	Rotor speed (m/s)	output voltage(V)
15	2.38	0.0022
15	4.76	0.022
15	7.42	0.076
15	9.53	0.180
15	11.94	0.352
15	14.28	0.608
15	16.66	0.966
15	19.04	1.442
15	21.42	2.053
15	23.8	2.816
15	26.18	3.749
15	28.56	4.867

The x-axis represents wind speed [m/s] and the y-axis represents the output voltage [V]. The graph shows the speed of wind speed from $5\ to\ 27\ [m/s]$ and the output from $0 - 5V$ as a result of various wind speeds. It can clearly be seen that the increase in wind speed increases the output voltage.

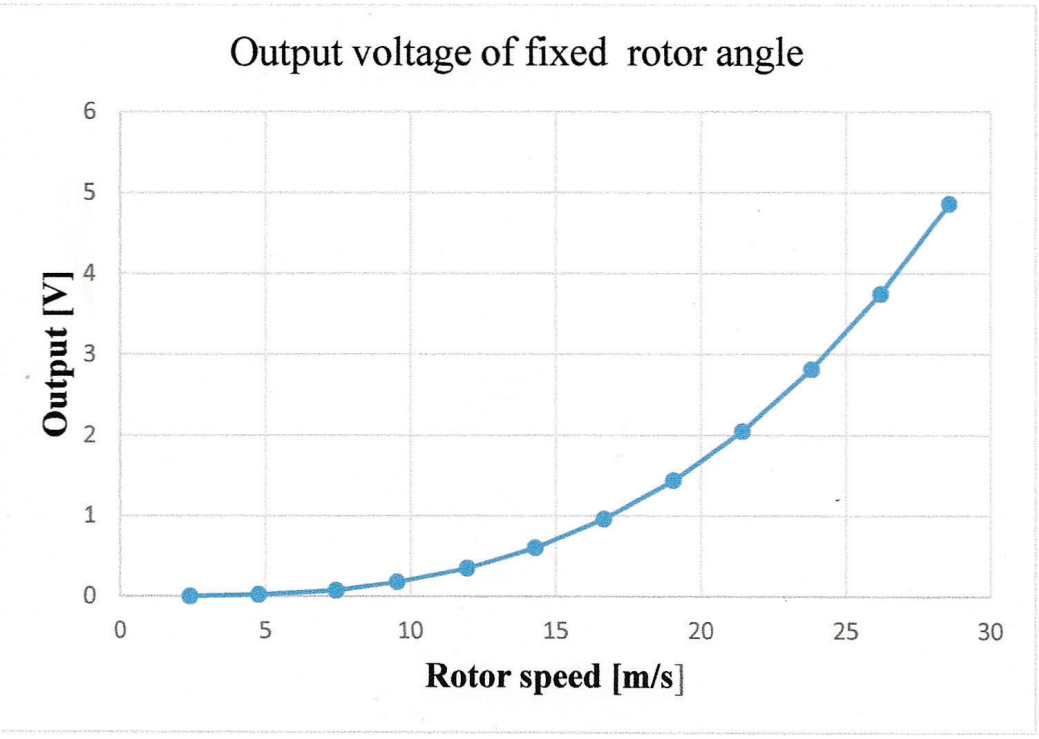

Figure 6.3: Output voltage of fixed rotor angle

6.5.2 Variable turbine rotor angle result

We consider the impact of inflow angle in wind turbine energy capture by using an experimental model that can adjust its rotor angle to keep the inflow angle perpendicular to the rotor blades. Table 6.3 lists the wind turbine parts which should be adjusted to achieve the target. Table 6.3 also shows the results of wind speed and output voltage when the wind direction is constant but the rotor angle varies. It can clearly be seen that the increase in wind speed gives more output voltage than a fixed rotor angle.

6.5.3 Result of fixed and variable turbine rotor angle

We compare the results of fixed and variable turbine rotor angles, as can be seen in Figure 6.5. The output of the DC generator (output voltage) shows the output of the fixed turbine rotor angle and the variable turbine rotor angle (modified wind turbine). We note that the output of the modified turbine show approximately 4-6% better results than the fixed turbine rotor angle.

Table 6.3: Variable turbine rotor angle (fan with inflow angle (+15, +15)) $\beta = constant$; $\rho = 1.225kg/m \wedge 3$; $R = 0.36m$

WD (θ)	RYA (φ)	RAD (ϕ)	Rotor speed (m/s)	Output voltage (V)
constant	+25	+25	27.56	5.1574
=	+20	+20	25.23	3.9884
=	+15	+15	23.83	2.9796
=	+10	+10	20.77	2.1778
=	+5	+5	18.40	1.5282
=	0	0	16.66	1.0182
=	-5	-5	13.80	0.6448
=	-10	-10	12.00	0.3726
=	-15	-15	9.53	0.1904
=	-20	-20	5.86	0.0803
=	-25	-25	4.30	0.0233
=	-30	-30	2.25	0.0023

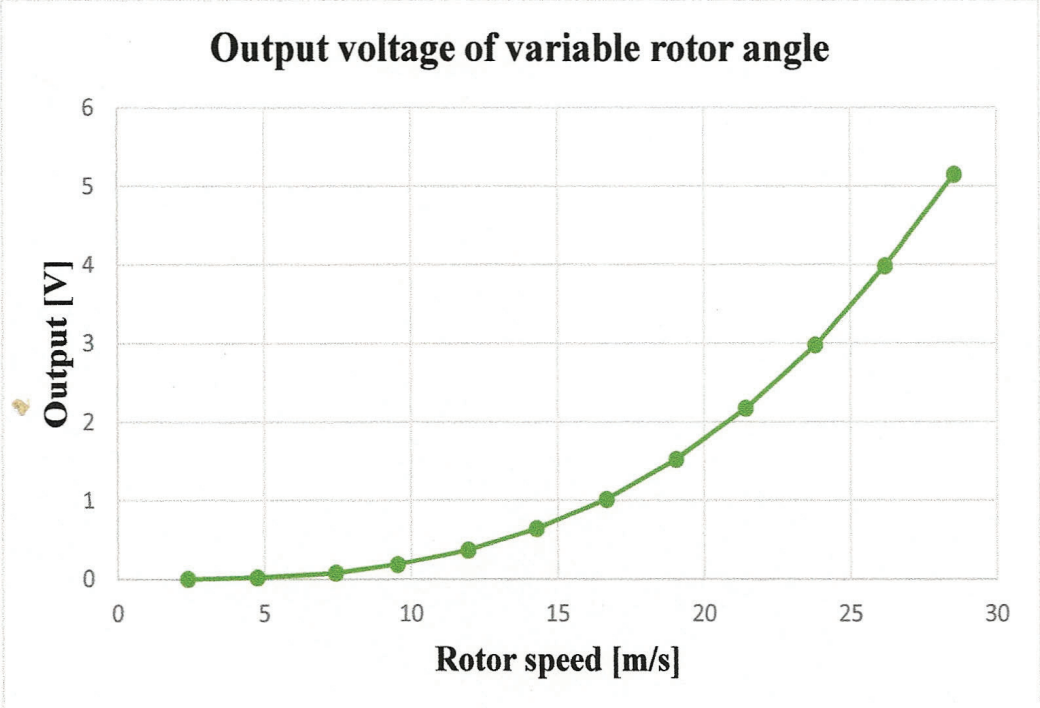

Figure 6.4: Output voltage of variable turbine rotor angle

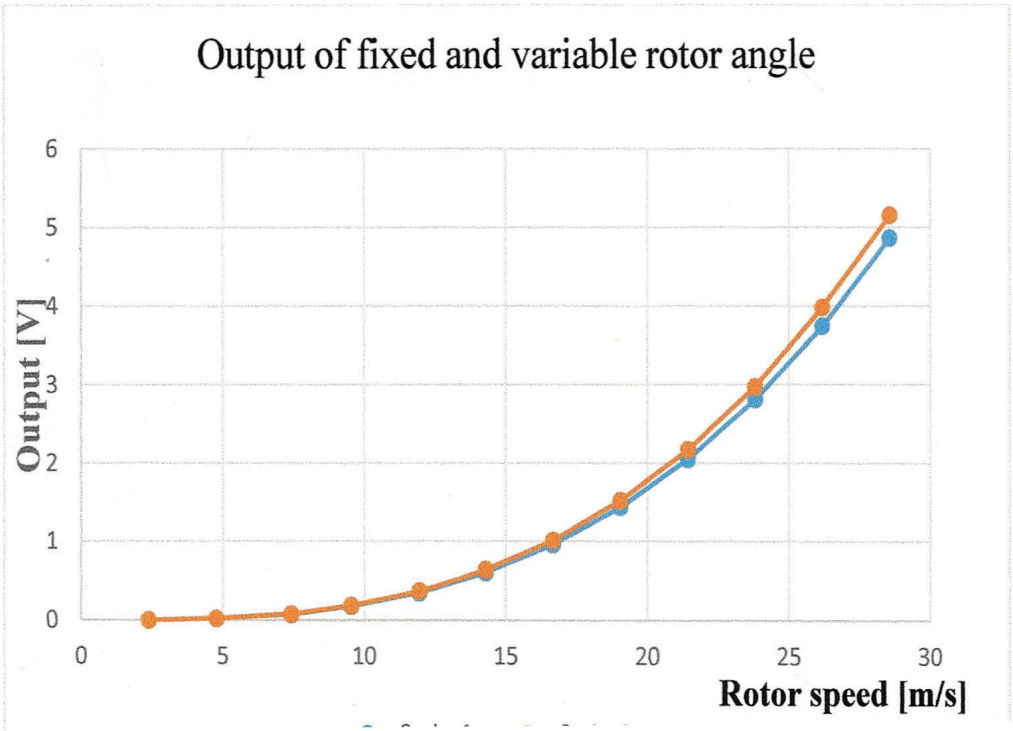

Figure 6.5: Power output of fixed and variable turbine rotor angle

6.5.4 Energy capture deviation

The summary of the experimental model (setup) can be seen in Figure 4.6, showing the energy gained and lost due to inflow angle. We can also see how the modified technique reduced the energy capture loss. The figure of the wind vector, which is the component that generates energy and corresponds to the rotor angle, show a positive result indicating that the fixed rotor angle gives less energy than the rotor with variable rotor angle. The reason for this is because the variable rotor angle is constantly tracking the inflow angle, leading to more wind crossing the rotor blades.

6.5.5 Results of wind turbines in relation to location

We now consider the effect of wind turbine location in relation to inflow angle and wind direction. As shown in Figure 6.7, the goals of this technique are to appropriately locate wind farms due according to inflow angle and wind direction and to adjust the rotor angle according to changes in wind inflow angle and wind direction. After combining all the results in Table 6.4, we can see that there is a large difference in the operation performance

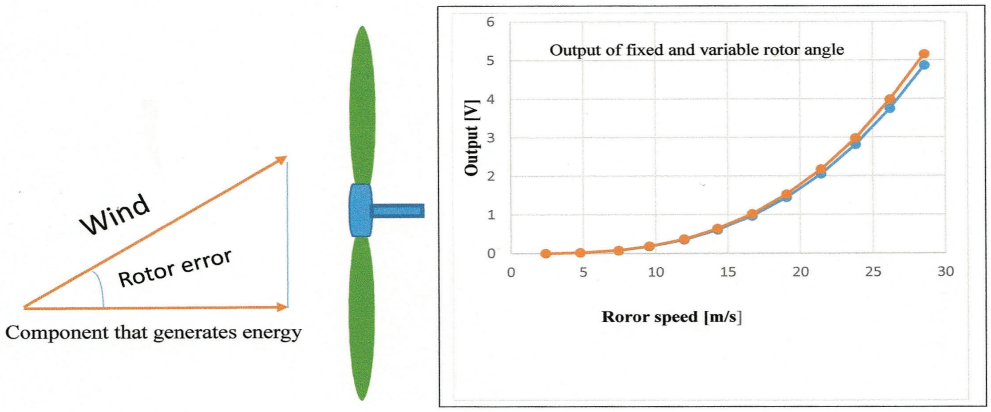

Wind speed (m/s)	Fixed rotor angle output voltage (V)	Variable rotor angle output voltage (V)	V increase [%]
2.38	0.0022	0.0023	4.545 %
4.76	0.022	0.0233	5.579 %
7.42	0.076	0.0803	5.658 %
9.53	0.180	0.1904	5.777 %
11.94	0.352	0.3726	5.852 %
14.28	0.608	0.6448	6.053 %
16.66	0.966	1.0182	5.403 %
19.04	1.442	1.5282	5.978 %
21.42	2.053	2.1778	6.079 %
23.8	2.816	2.9796	5.809 %
26.18	3.749	3.9884	6.386 %
28.56	4.867	5.1574	5.967 %

Figure 6.6: Energy capture deviation

of variable turbine rotor angles compared to fixed turbine rotor angles. However, weather is constantly changing on wind farms. So, if the angle of the wind inflow angle changes by + or 8 degrees, we may need to reposition the turbine so that it can be optimized within + or 8 degrees in relation to the wind inflow angle. For example, in looking at Figure 6.7, we can see it is possible to locate the wind turbine on the side of a hill to optimize its features.

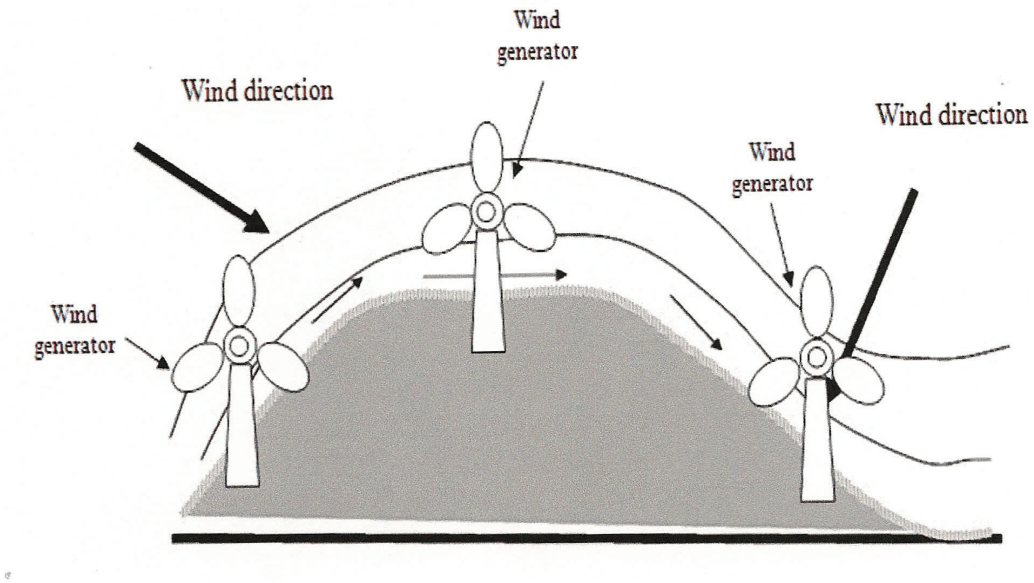

Figure 6.7: The benefit of modification

Table 6.4: Comparing between fixed rotor angle and variable rotor angle turbine

Description	Fixed rotor angle	Variable rotor angle
Inflow angle	$\pm 8_{\circ}$ only	variable
Location at high wind inflow angle	relocate	fixed
Energy capture	less	more 4-6%
Operation performance	less than variable rotor angle	more better
Fatigue load	more fatigue load	less fatigue load
Lifetime	20 year lifetime	more than 20 year lifetime

Chapter 7

OVERVIEW OF OPTIMAL CONTROLS AND CONTRIBUTIONS

7.1 Design and control outline

Figure 7.1 illustrates the systematic and organized problem of predicated inflow angle and the proposed solution. The figure illustrates the impact and solution of the angle.

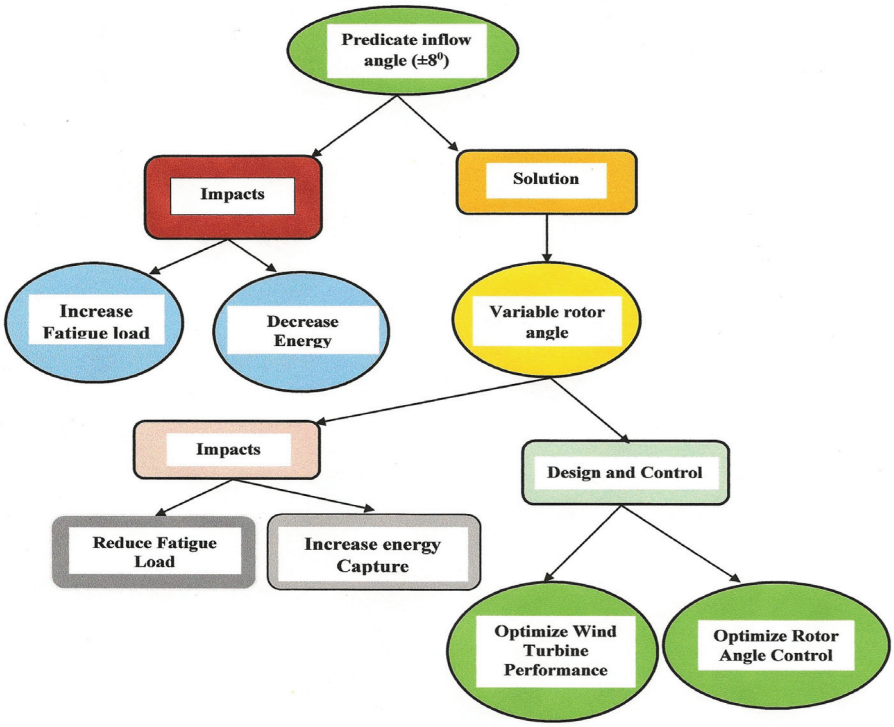

Figure 7.1: Proposed design and control of predicated inflow angle

7.1.1 Text explanations

Predicate inflow angle

1) Impacts
a) Increased fatigue load
b) Decreased energy capture
2) Solutions
a) Variable rotor angle
2a) Impacts
a) Reduced fatigue load
b) Increased energy capture
2b) Design and control
a) Optimize wind turbine performance
b) Optimize rotor angle control

7.2 Interrelated results

Figure 7.2 illustrates the relationships between energy capture, rotor angle and predicted inflow angle. We consider that the predicted inflow angle (according to the results of previous researchers) affects the wind turbine energy capture. Hence, we suggest the solution discussed in Chapter 6. Now, if we take the predicted inflow angle and rotor angle, the result is the rotor angle tracking the inflow angle. Furthermore, if we take the rotor angle and the energy capture, the result is increased wind passing through the rotor blades. The more important contribution of this thesis is the modified model can help the wind turbines increase energy capture which lead to enhanced wind turbine performance.

7.3 General specifications of wind turbines

Manufacturing companies develop their wind turbines for the market based on the values of customer satisfaction and operational reliability. Table 7.1 shows the main general specifications of wind turbines. We use the following wind turbine general specifications for V90 3.0 MW [50], with all data valid at air density ($\rho = 1.225kg/m^3$) and 60 Hz variable speed turbine at sea level.

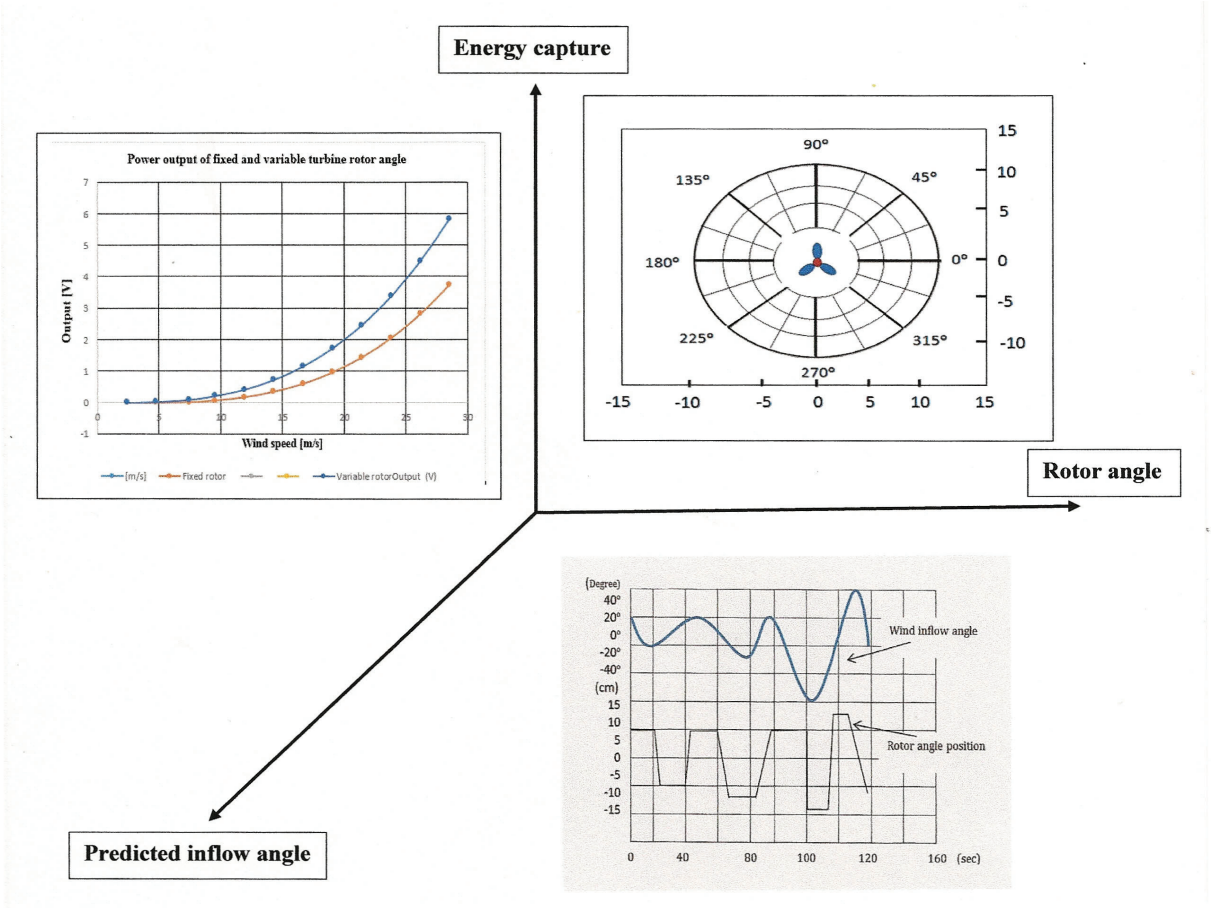

Figure 7.2: Predicted inflow angle, energy capture, and rotor angle relationship

Table 7.1: Technical specifications for wind turbine type V90 3.0 MW

1- Rotor		
	Diameter	90 m
	Swept area	6362 m2
	Speed, nominal power	16.1 RPM Speed, Dynamic operation range
	rotor	9.9 - 18.4 RPM
	Rotational direction	Clockwise (front view)
	Orientation	Upwind
	Number of blades	3
2- Hub		

	Type	SG Cast Iron
	Weight	8500 kg
3- Blades		
	Material	Fiberglass
	Length	44 m
4- Bearings		
	Type	4-point ball bearing
5- Sensors		
	Lightning Detector	Lightning detector
	Wind Sensor	Ultrasonic wind sensor
	Smoke	Smoke detector
6- Generator 60 Hz		
	Rated power	3.0 MW
	Type	Asynchronous with wound rotor, slip rings and VCRS
	Voltage	1000 VAC
	Frequency	60 Hz
	No. of poles	4
	Class of protection	IP54
7- Transformer	Type	Cast resin
	Rated Power	3160 kVA
	High voltage	10 34.5 kV
	Frequency	60 Hz
8- Yaw System		
	Type	Plain bearing system with built-in friction
9- Yaw Gears		
	Type	4-step planetary gear with motor brake
10- Gearbox		
	Type	2 planetary stage + 1 helical stage
11- Parking Brake		
	Type	PZ.I.4420.2802.10
12- Hydraulics		
	Pressure	250 bar

13- Cooling System		
	Gear oil cooling	
	Generator cooling	
	Water-cooling	
	Nacelle cooling	
	Transformer cooling	
14- Nacelle		
	Material	Fibre-glass
15- Tower		
	Type	Conical tubular

7.4 Optimize rotor angle control

We now begin to build a concept that can be used to solve the problem outlined, which is the movement of the rotor angle to track the predicate inflow angle under control. The main limitation of this objective is that we assume that the complete state $x(t)$ of the plant can be accurately measured at all times and is available for feedback. With the increase in the energy capture, the need to operate the wind turbine systems closer to their limits of stability requires optimal robust controls. To enhance stability and improve the dynamic response of the wind turbine systems to operate under safe conditions, the controller must be applied properly, as indicated in the thesis statement. The proposed approach different from the conventional approach it's have ability to change its rotor angle according to the changes inflow angle.

The three main recommendations of this strategy are:

1. Developing a rotor angle that can move in multidimensional directions.
2. Using the right controller to optimize the response of the rotor angle actuation.
3. Studying the response of the rotor angle movement under robust control.

According to the wind turbine mechanical power in Equation (7.0), the power coefficient (Cp) is dependent on tip speed ratio (λ) and pitch angle (β).

$$P_{mech} = 0.5\rho\pi C_p\left(\lambda, \beta\right)R^2V^3 \qquad (7.0)$$

The new technique, which allows the rotor to move in multidimensional directions to change its angle, leads to reformulating the wind turbine mechanical power equation. This is indicated in Equation (7.1), which shows that the power coefficient (Cp) depends on tip speed ratio, pitch angle, rotor yaw angle (φ) and rotor angular deflection (ϕ).

$$P_{mech} = 0.5\rho\pi C_p\,(\lambda, \beta\ , \varphi, \phi) R^2 V^3 \qquad (7.1)$$

As we see in Chapter 5, the impact of rotor angle on wind turbine energy capture shows that adjusting the rotor angle increases the energy capture. Now we are going to study how to achieve the movement of rotor angle in multidimensional directions with robust controls.

7.4.1 Desired rotor angle models

Figure 7.3 demonstrates that we can take the movements of desired 1 $(\varphi 1, \phi 1)$, which is the movement of the rotor angle from the $(\varphi 0, \phi 0)$ position to the desired 1 $(\varphi 1, \phi 1)$, as required by tracking the predicted wind inflow angle 1. This means it requires the rotor to move in the (-x) axis and move in the (y) axis to get the desired 1 $(\varphi 1, \phi 1)$. These movements should be under robust control to keep the operation of the wind turbines protected and to achieve the goal, which is to increase the energy capture without any damage to the wind turbines. We thus need to apply different controllers for the two actuations in order to find which controller achieves our goal.

Actuation control:

Control signal (t) = gain$\times(desired\ \ state(t) - actual\ \ state(t))$

7.4.2 Design and control

In order to minimize the deviation between the actual angle and the predicted angle, we must provide the proper inputs to the system. Physically, the correction actuation movement causes the disturbance affecting the wind turbine operation. As shown in Figure 7.4, adding a closed loop feedback control system using state space control systems reduces this disturbance and reduces the deviation between the actual rotor angle and the desired rotor angle. In this chapter, we begin to build a concept that can be used to solve the problems outlined, which are the movement of the rotor angle to beat the predicate inflow angle under control. The main limitation of this chapter is that we assume that the complete state x (t) of

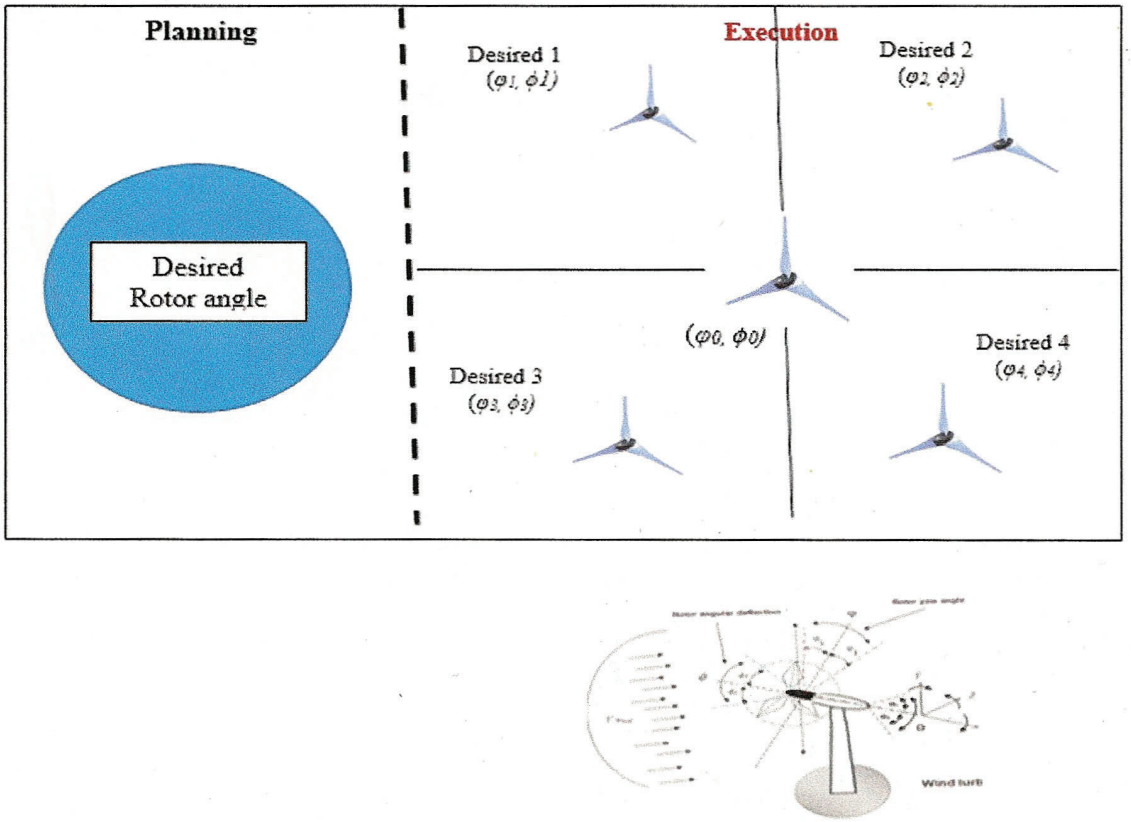

Figure 7.3: Movement of rotor angle multidimensionally

the plant can be accurately measured at all times and is available for feedback.

7.5 Optimal control method

To optimize the power produced in a wind turbine, the speed of the turbine should vary with the wind speed. An optimal control method is used that will allow the rotor speed to run a turbine at its maximum speed. This thesis presents a different control scheme, where the rotational speed is the controlled variable. Two controllers that can be used to achieve an optimal control design are a pole placement controller and a linear quadratic regulator controller.

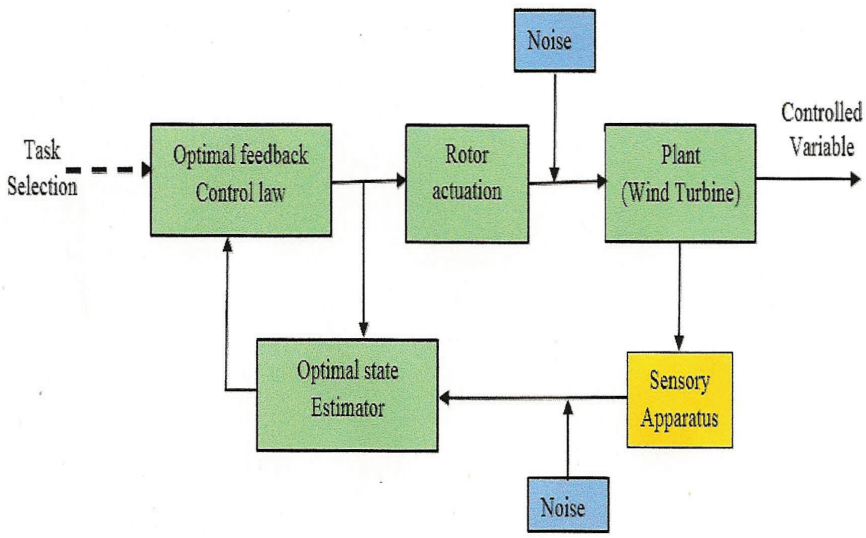

Figure 7.4: Rotor actuation control system

7.6 Proposed controller used for wind turbine, rotor angle and yaw direction

For state feedback and pole placement, let us consider a linear dynamic system in the state space form, as in state space Equation 4.22 and output Equation 4.23.

$$\dot{x} = Ax + Bu \tag{4.22}$$

The output equation

$$y = Cx + Du \tag{4.23}$$

To achieve the goal, we stabilize the system or improve its transient response by using the full state feedback, which represents a linear combination of the state variables.

$$u = -Fx \tag{7.1}$$

So, the closed-loop system is given by

$$\dot{x} = (A - BF)x \tag{7.2}$$

The main role of state feedback control is to stabilize a given system so that all closed-loop eigenvalues are placed in the left-half of the complex plane. The following theorem gives a condition under which it is possible to place system poles in the desired locations.

7.7 Controller via integral and pole placement

Figure 7.5 shows the simulator of the state space control loop of wind turbine and rotor angle that will represent the effect of the rotor angle in a wind turbine system by using an integral and pole placement controller.

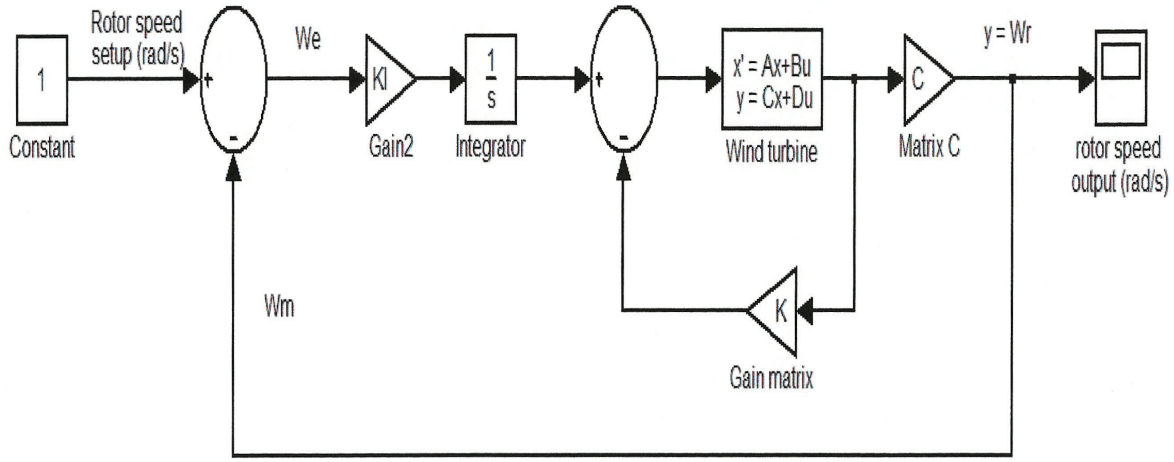

Figure 7.5: State space control loop of wind turbine and rotor yaw actuator

$$\dot{x} = Ax + Bu$$

The output equation

$$y = Cx + Du$$

Where

ω_{ref} reference speed (desired speed) [rad/s]

ω_r rotor speed output [rad/s]

ω_m measured rotor speed [rad/s]

$$\dot{\xi} = \omega_{ref} - y = \omega_{ref} - Cx \tag{7.3}$$

$$\dot{\xi} = \omega_{ref} - \omega_r$$

The augmented system is:

$$\begin{bmatrix} \dot{x} \\ \dot{\xi} \end{bmatrix} = \begin{bmatrix} A & 0 \\ -C & 0 \end{bmatrix} \begin{bmatrix} x \\ \xi \end{bmatrix} + \begin{bmatrix} B \\ 0 \end{bmatrix} u + \begin{bmatrix} 0 \\ 1 \end{bmatrix} \omega_r \tag{7.4}$$

let

$$\bar{A} = \begin{bmatrix} A & 0 \\ -C & 0 \end{bmatrix} \qquad \bar{B} = \begin{bmatrix} B \\ 0 \end{bmatrix} \qquad , \bar{x} = \begin{bmatrix} x \\ \xi \end{bmatrix}$$

Pole placement controller

The input equation:

$$u = -K\bar{x} \tag{7.5}$$

Closed loop system is:

$$\dot{\bar{x}} = \bar{A}\bar{x} + \bar{B}(-K\bar{x}) + G\omega_r$$

$$\dot{\bar{x}} = (\bar{A} - \bar{B}K)\bar{x} + G\omega_r \tag{7.6}$$

$$\left|sI - (\bar{A} - \bar{B}K)\right| = P_r = desired\ \ polynomial \tag{7.7}$$

Figure 7.6 shows a state space wind turbine with pole placement controller. We consider the response of the input actuator and pole placement controller of the wind turbine system, noting that the output tracks the change of the inflow angle in the horizontal direction until it reaches the set point.

Figure 7.7 shows the y-axis representing the rotor speed [rpm] and the x-axis representing time [sec]. We consider the response of the input actuator and the speed of the rotor of the wind turbine system and note that the rotor speed increases to steady state after 7 [sec].

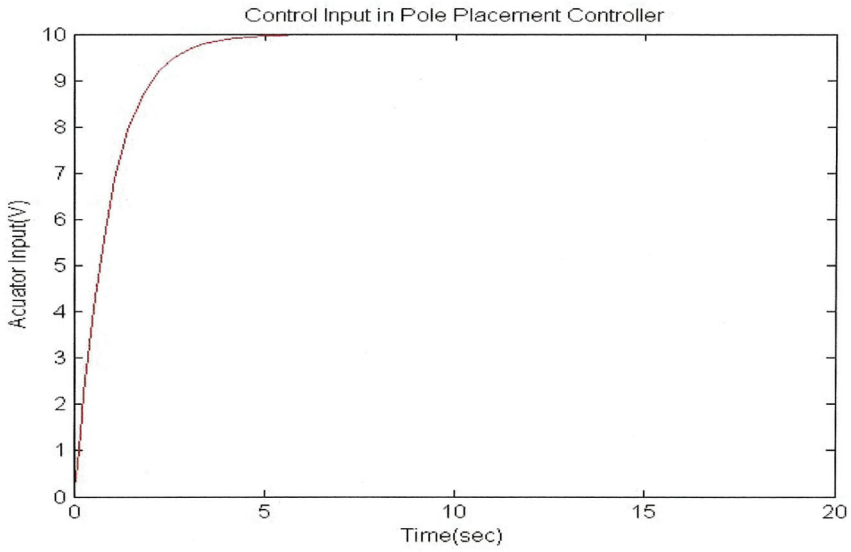

Figure 7.6: State space wind turbine with pole placement controller

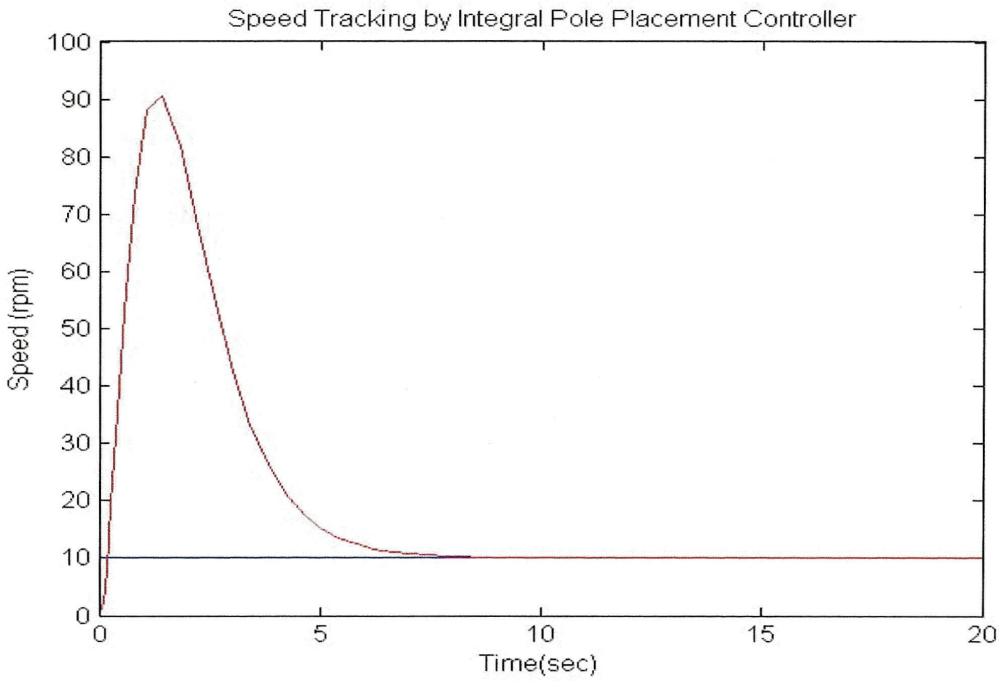

Figure 7.7: State space wind turbine with pole placement controller

Figure 7.8 shows the response of actuation. We consider the response of the yaw rotor angle $[\varphi]$ actuator moving in the x-axis direction to find the inflow angle at the x-axis point. We

note that the actuation response tracks the inflow angle until it gets to the setup position of the rotor angle.

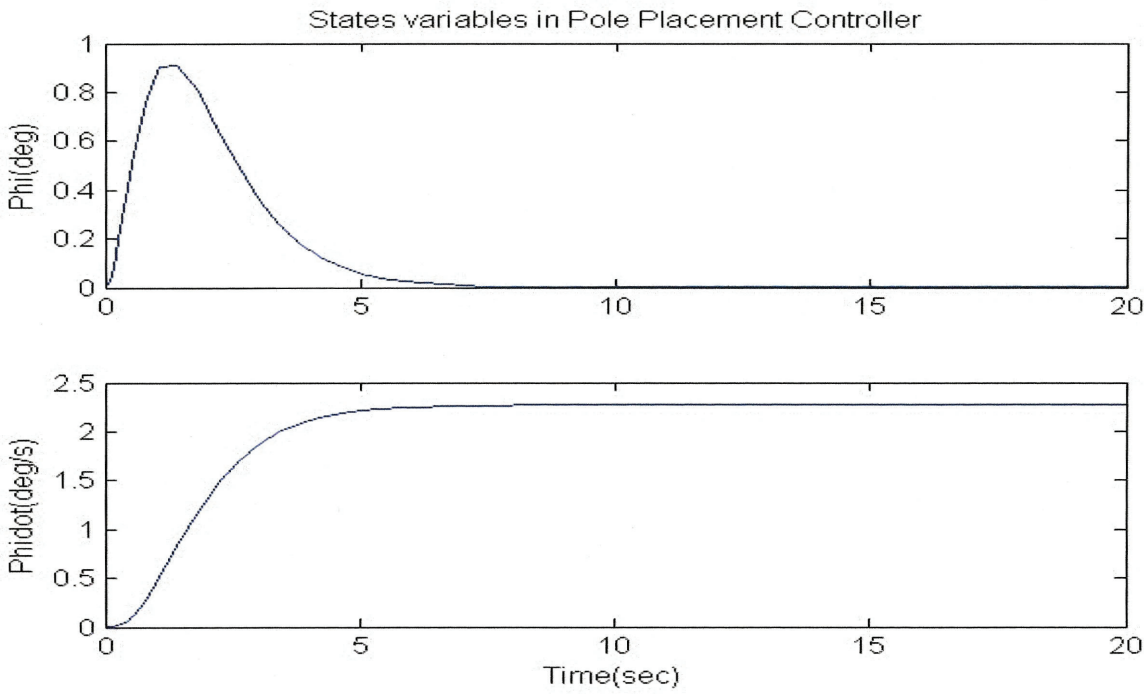

Figure 7.8: Actuation response

7.8 Controller by integral and Linear Quadratic Regulator (LQR)

Problem Background: The Q and R matrices of LQR are usually selected by trial and error. A simple guideline is to choose these matrices to be diagonal and make the diagonal entry positive large for any variable that needs to be small in the time domain. In two rotor angles (φ, ϕ), the most important variable to control is the rotor angle in order to match inflow angle.

Therefore, the value of Q is set first, followed by the R identity matrix. More weight is given to the diagonal term for good performance (i.e., small rise time and low overshoot for overall control). After getting a good value of Q, the feedback gain K is obtained [51]. Figure 7.9 shows a simulator of a state space wind turbine with integral and LQR controllers. In observing this simulator, we consider the effect of integral and LQR controllers on a wind

turbine with a rotor angle. The general idea of the LQR method is to minimize the cost function stated below in Equation (7.8).

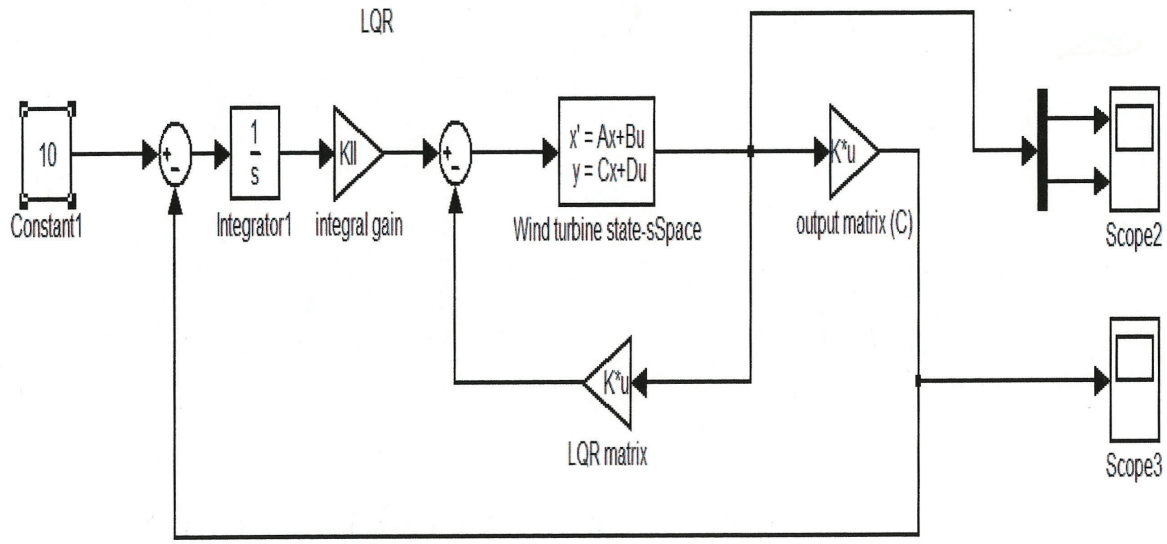

Figure 7.9: State space wind turbine with integral and LQR controllers

$$J = \int_0^\infty (x^T Q x + u^T R u) dt \qquad (7.8)$$

where:

J is the performance index

Q is the weighting matrix of the states

R is the weighting matrix of the control signals

x is the state vector

u is the control signal vector

Q_{ii} = 1/(maximum acceptable value of$[x_i^2]$)

R_{ii} = 1/(maximum acceptable value of $[u_i^2]$)

where:

Q_{ii} is the element at row i and column i of the Q-matrix

R_{ii} is the element at row i and column i of the R-matrix

x_i is the i'th element of the state vector

u_i is the i'th element of the input vector

Input equation (5.33)

$$u = -K\bar{x} \tag{7.9}$$

$$u = -K\bar{x} = R^{-1}\bar{B}^T P\bar{x} \tag{7.10}$$

where P is solution of following Algebraic Riccatti Equation (ARE)

$$\bar{A}^T P + P\bar{A} - P\bar{B}R^{-1}\bar{B}^T P + Q = 0 \tag{7.11}$$

By selecting the Q and R matrices and minimizing the performance index J, a balance between state deviation and control effort arises. The difference between the reference and the actual output is called state deviation, while the control effort is the amount of output the actuators need to provide. To choose the values of the weighting matrices Q and R, Brysons Rule is used. This rule is a reasonable method to start the LQR design, which is an iterative process. The entities of Q and R are selected to be:
Where Q and R are positive definite matrices for our problem, we choose Q and R as:
MATLAB code is used to find the parameter of the LQR controller linear quadratic regulator
Q = diag([10 10 10]);
R = 0.1;
Figure 7.10 shows the rotor speed tracking by integral and LQR controller at $R = 0.1\ and\ Q = 1$ Note that the settling time is 0.5 [sec]; if we compare this to the pole placement controller (which is 5 [sec]), the integral and LQR are much better (i.e., faster). Figure 7.11 shows the actuation response of the yaw rotor angle (φ) and rotor angular deflection (ϕ). Let us consider the effect of the outputs of both actuators on the wind turbine system. We note that the overshooting is less than the use of integral and pole placement controllers. Figure 7.12 shows the actuator input and its response. Let us now consider the effect of the actuator input on the wind turbine system. We see that the use of integral and LQR is reducing the overshooting of the startup point, as shown in the figure.

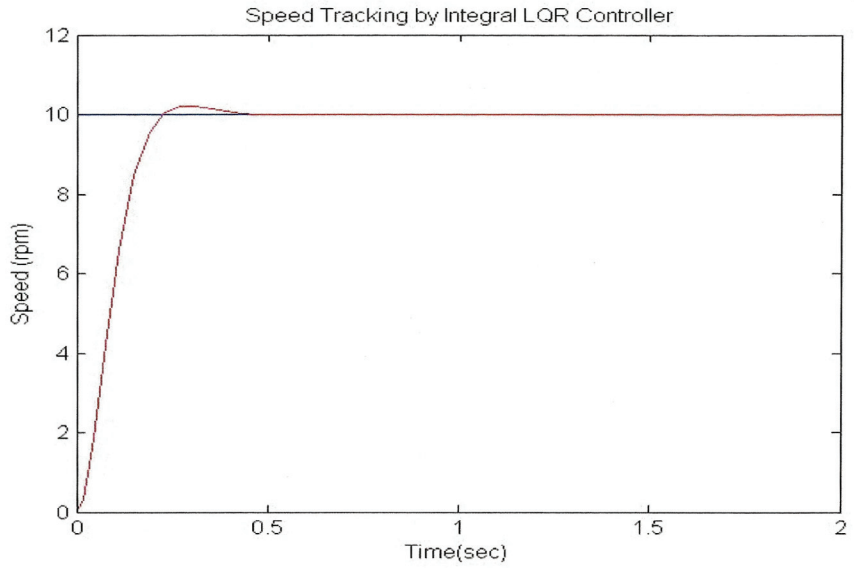

Figure 7.10: Speed tracking by integral LQR controller R=0.1 and Q=1

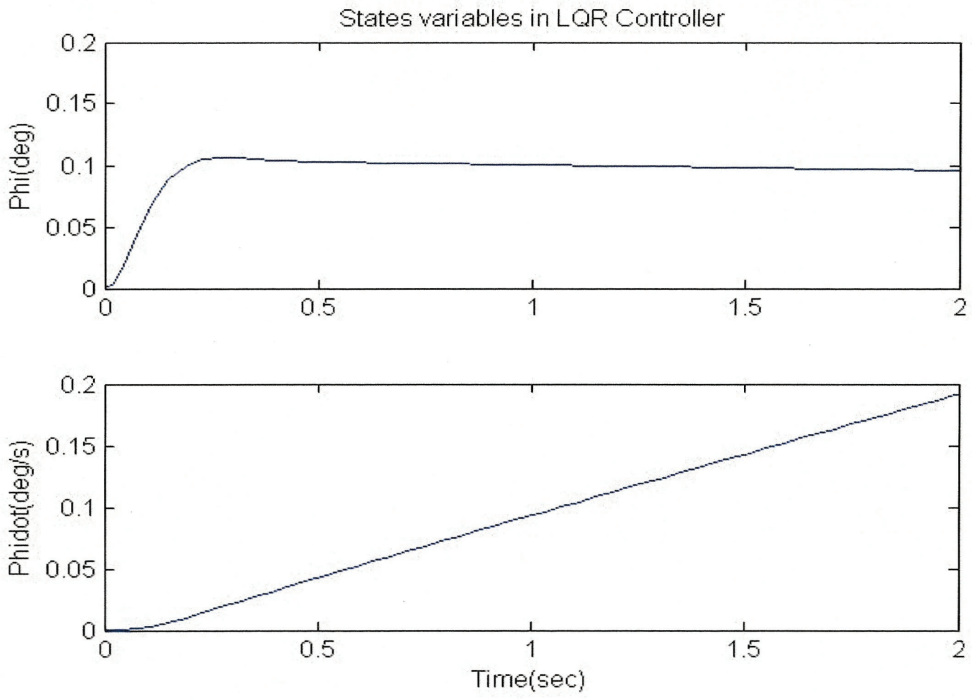

Figure 7.11: State variables in LQR controller at R=0.1 and Q=1

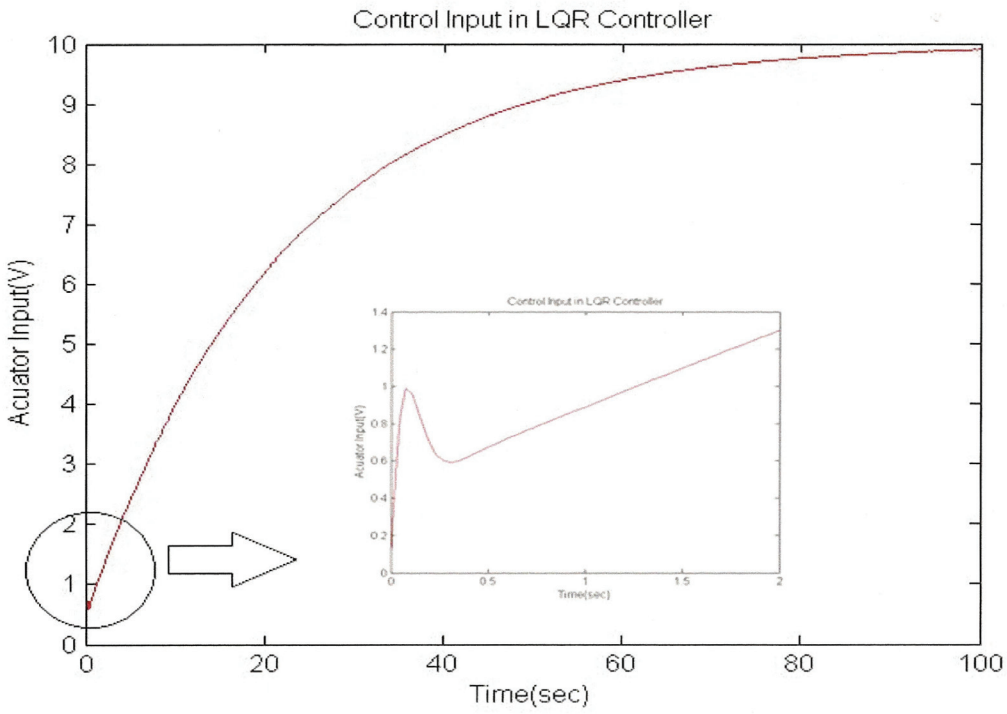

Figure 7.12: Control input in integral LQR controller at R=0.1 and Q=1

7.8.1 LQR controller parameters

The output of any control system designed using an LQR controller has percentage of errors and overshoots that are undesirable. Efforts have been made to tune LQR controller parameters for better system performance, since it is indispensable in the industry and yet very difficult to obtain as optimal parameters. The matrices Q and R should always be chosen as positive-definite. In this section, we consider the effect of the matrices Q and R on the LQR controller. As can be seen in Figures 7.13, 7.14 and 7.15, when the value of matrix Q goes up, its effect on the rotor angle actuators regarding the overshooting increases the effect of wind turbine stability.

7.9 Controller by Linear-Quadratic-Gaussian control

In control theory the Linear-Quadratic-Gaussian (LQG) control problem is one of the most fundamental optimal control problems. It concerns uncertain linear system disturbed by additive white Gaussian noise having incomplete state information (i.e. not all the state variables are measured and available for feedback) and undergoing control subject to quadratic

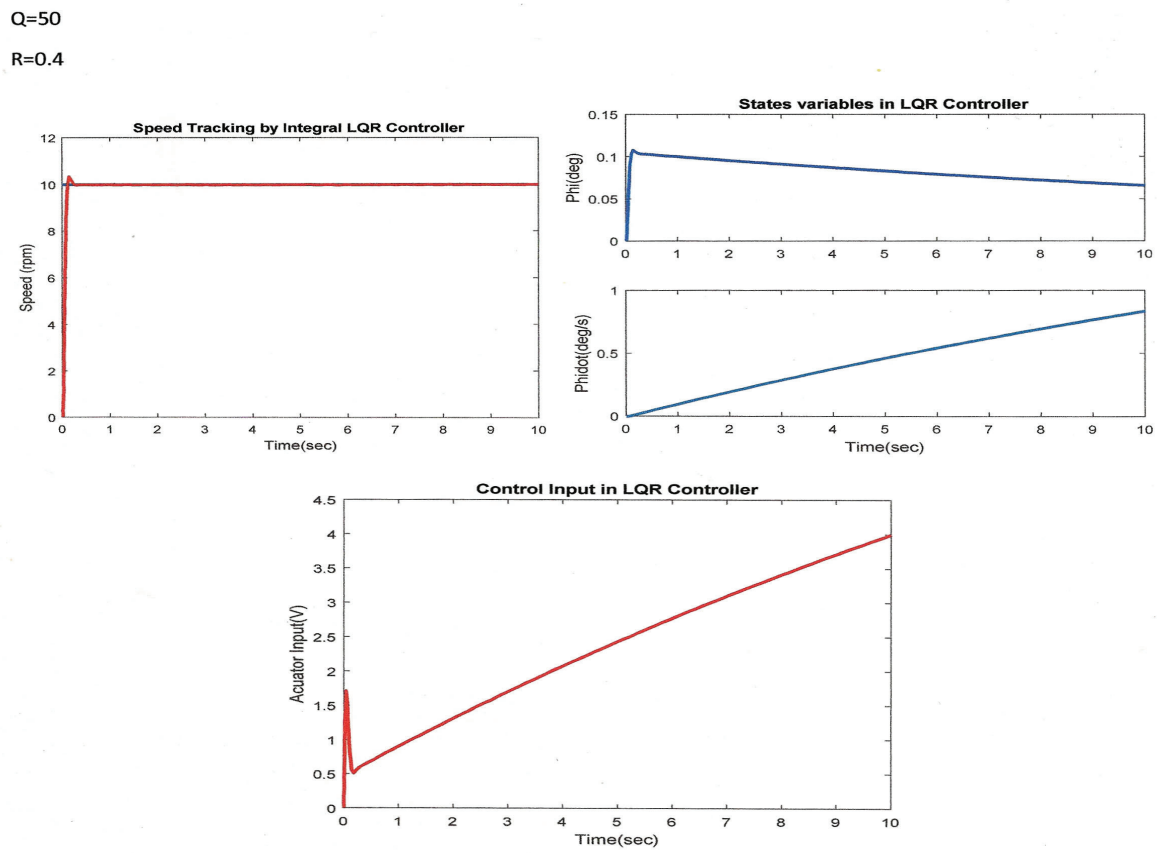

Figure 7.13: LQR controller at R=0.4 and Q=50

costs. Moreover, the solution is unique and constitutes a linear dynamic feedback control law that is easily computed and implemented [55, 56].

The LQG controller is simply the combination of a Kalman filter, i.e. a linear-quadratic estimator (LQE), with a linear-quadratic regulator (LQR). The separation principle guarantees that these can be designed and computed independently. LQG control applies to both linear time invariant system as well as linear time-varying systems. The application to linear time-invariant systems is well known. The application to linear time-varying systems enables the design of linear feedback controllers for non-linear uncertain systems [57].

7.9.1 Mathematical description

Continuous time

Consider the continuous-time linear dynamic system

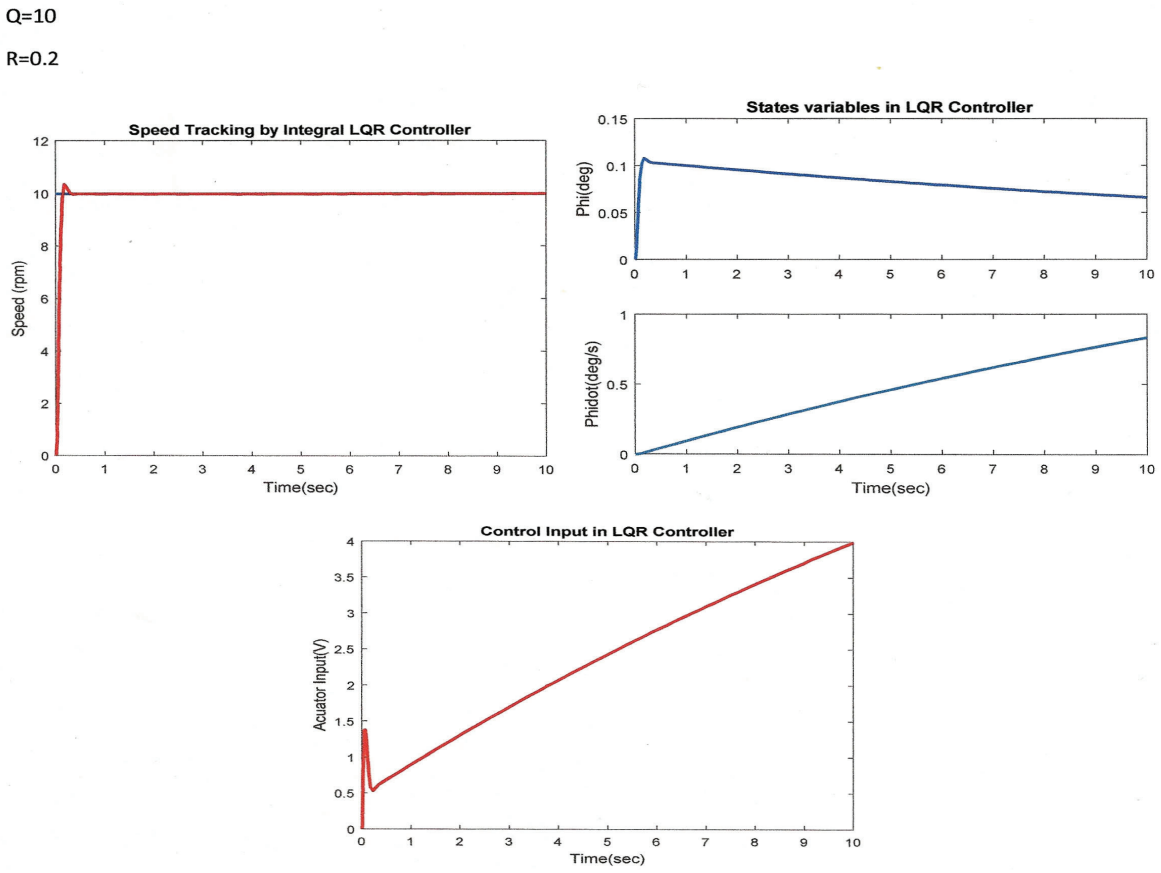

Figure 7.14: LQR controller at R=0.2 and Q=10

$$\dot{x}(t) = Ax(t) + Bu(t) + v(t) \quad (7.12)$$

The output equation

$$y(t) = Cx(t) + Du(t) + w(t) \quad (7.13)$$

where x represents the vector of state variables of the system, u the vector of control inputs, and y the vector of measured outputs available for feedback. Both additive white Gaussian system noise v(t) and additive white Gaussian measurement noise w(t) affect the system. Given this situation, the objective is to find the control input history u(t), which at every time t may depend only on the past measurements $y(t^{'}), 0 \leq = t' < t$, such that the following

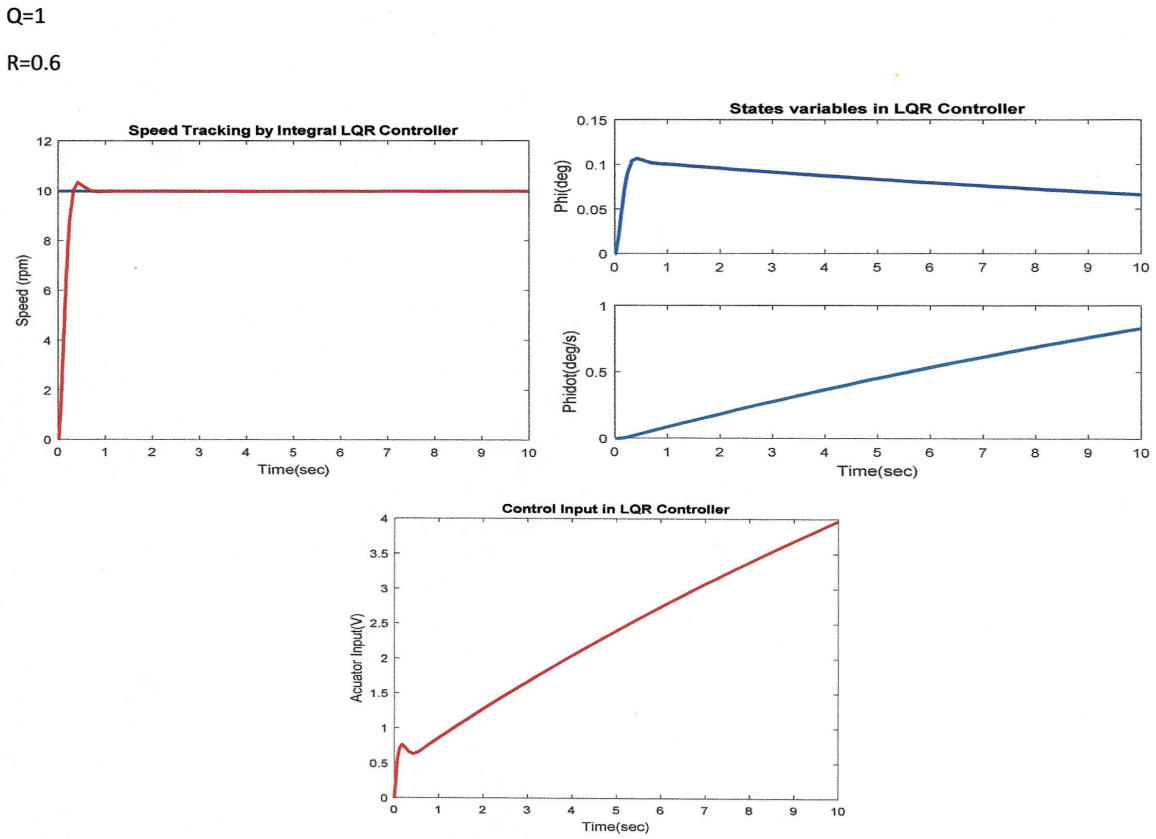

Figure 7.15: LQR controller at R=0.6 and Q=1

cost function is minimized:

$$J = E(x^T(T)FX(T) + \int_0^T (x^T Q(t)x(t) + u^T(t)R(t)u(t))dt) \qquad (7.14)$$

where

$F \geq 0, Q(t) \geq 0, R(t) > 0$

where E denotes the expected value. The final time $(horizon)$ T may be either finite or infinite. If the horizon tends to infinity the first term $x^T(T)Fx(T)$ of the cost function becomes negligible and irrelevant to the problem. Also to keep the costs finite the cost function has to be taken to be J/T.

The LQG controller that solves the LQG control problem is specified by the following equations:

$$\hat{x}' = A\hat{x}(t) + Bu(t) + K(t)(y(t) - C\hat{x}(t)) \qquad (7.15)$$

where:
$\hat{x} = 0 = E(x(0))$

$$u(t) = -L(t)\hat{x}(t) \qquad (7.16)$$

The matrix $K(t)$ is called the Kalman gain of the associated Kalman filter represented by the first equation. At each time t this filter generates estimates $\hat{x}(t)$ of the state $x(t)$ using the past measurements and inputs. The Kalman gain$K(t)$ is computed from the matrices $A(t), C(t)$, the two intensity matrices $V(t), W(t)$ associated to the white Gaussian noises v(t) and w(t) and finally $E(x(0)x^T(0))$. These five matrices determine the Kalman gain through the following associated matrix Riccati differential equation:

$$\dot{P}(t) = Ax(t)P(t) + P(t)A^T(t) - P(t)C^T(t)W^T(t)C(t)P(t) + V(t) \qquad (7.17)$$

$P(0) = E(x(0)x^T(0))$
Given the solution $P(t), 0 \leq t \leq T$ the Kalman gain equals

$$K(t) = P(t)C^{\mathrm{T}}(t)W^{-1}(t) \qquad (7.18)$$

The matrix is called the feedback gain matrix, which is determined by the matrices $A(t), B(t), Q(t), R(t)$ and F through the following associated matrix Riccati differential equation:

$$-\dot{S}(t) = A^{\mathrm{T}}(t)S(t) + S(t)A(t) - S(t)B(t)R^{-1}(t)B^{\mathrm{T}}(t)S(t) + Q(t) \qquad (7.19)$$

$S(T) = F.$
Given the solution $S(t), 0 \leq t \leq T$ the feedback gain equals

$$L(t) = R^{-1}(t)B^{\mathrm{T}}(t)S(t) \qquad (7.19)$$

7.9.2 Test turbine with LQG controller

Impulse input

We consider the effect of LQG controller function on wind speed with the variation of rotor yaw angle and rotor speed. Figure 7.16shows the impulse response for the test turbine with and without an LQG controller.

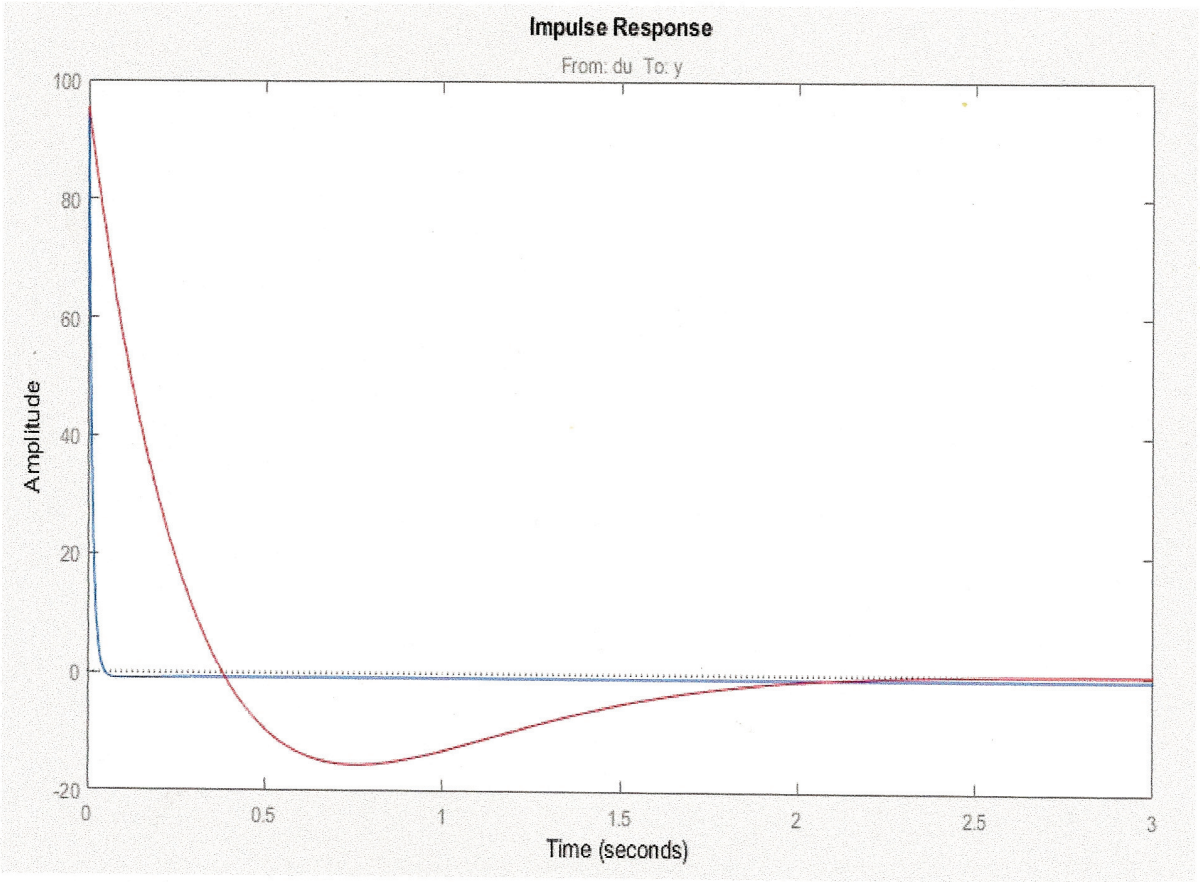

Figure 7.16: Impulse response of the system with LQGC

Step input

We consider the effect of the LQG controller function on wind speed with the variation of rotor yaw angle and rotor speed. Figure 7.17 shows the step response of the wind turbine with and without the LQG controller. We note that the output with the LQG is much better than without it. The reason for this is that with the LQG, the overshoot is smaller and the

settling $time = 4[sec]$ less than $6.1[sec]$ for the system without the controller, as shown in Figure 7.16. Here we use different test signals to see the performance of the controller on the system.

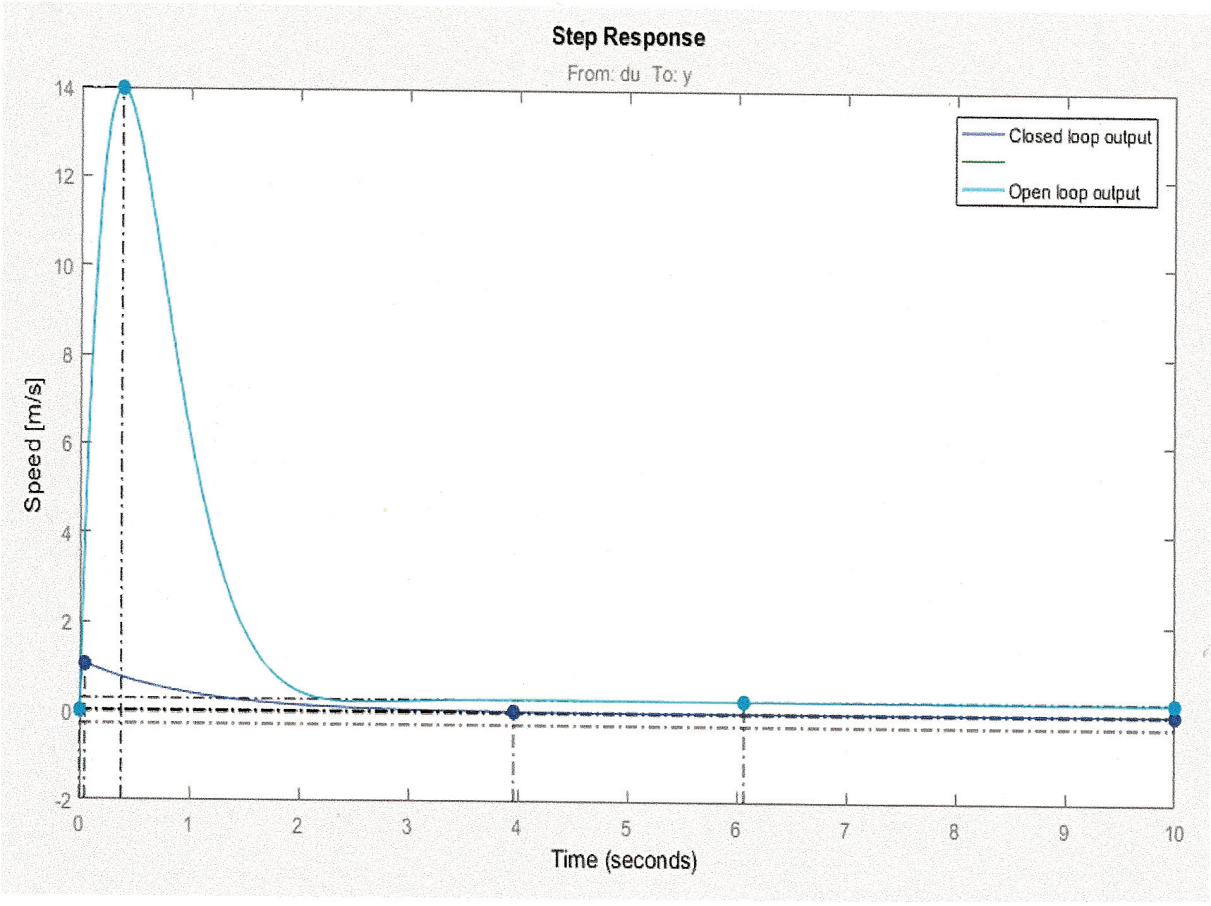

Figure 7.17: Step response of the system with LQGC

Stability

Let us consider the stability of the system with the LQG controller by $Pole-Zero$ mapping. The criteria of a pole-zero map are that all poles must be on the left-hand side of the S-plane, indicating stability. Figure 7.18 shows that all poles and zeros are on the left-hand side, so the system is stable. Note that if the system is unstable, we cannot work with it, so we need to adjust the system to become stable.

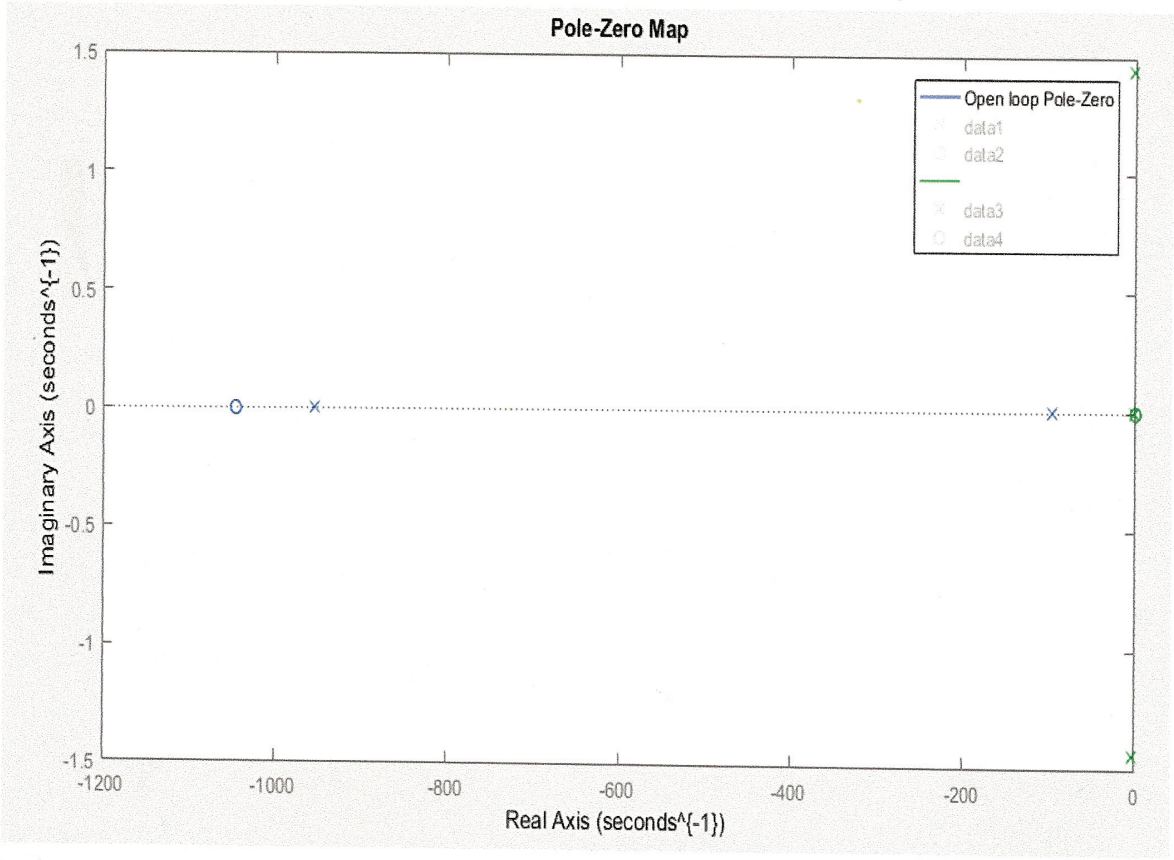

Figure 7.18: Pole-zero map of the system with LQGC

Bode diagram

Figure 7.19 depicts the Bode plot of frequency response of the transfer function of the system. In this figure, we illustrate one of the advantages of using a logarithmic frequency scale: We can without difficulty obtain a useful approximate bode plot for a continuous-time system.

Root locus

Figure 7.20 shows a root locus for a system which is able to use root locus information to predict aspects of the systems closed loop behavior, including speed of response.

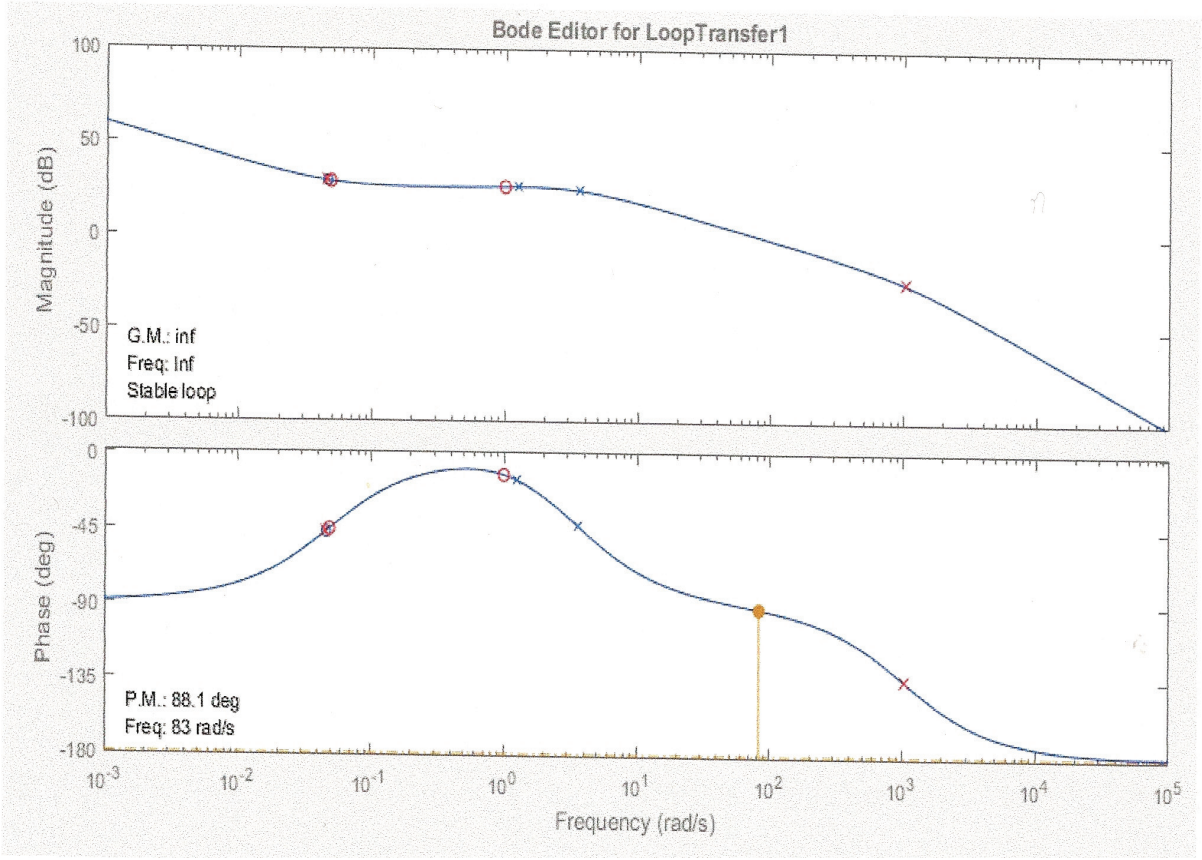

Figure 7.19: Bode diagram of system transfer function

7.9.3 Simulation results

To evaluate the performance of a variable speed wind turbine controller implemented in a power system simulation by MATLAB software, step response simulations with deterministic wind speeds are performed. Typical quantities versus time show the wind speed in [m/s], the rotor angle in [deg], and the rotor speed in [rpm].

7.9.4 Summary of results

The three controller designs presented show different impacts on the outputs of wind turbine and rotor angle in relation to rotor angle controller implementation and the design for tracking the inflow angle. First controller: The outputs of the integral and pole placement controllers show high overshooting and lengthy settling time duration. Second controller: The outputs of the integral and LQR controllers show better performance in overshooting

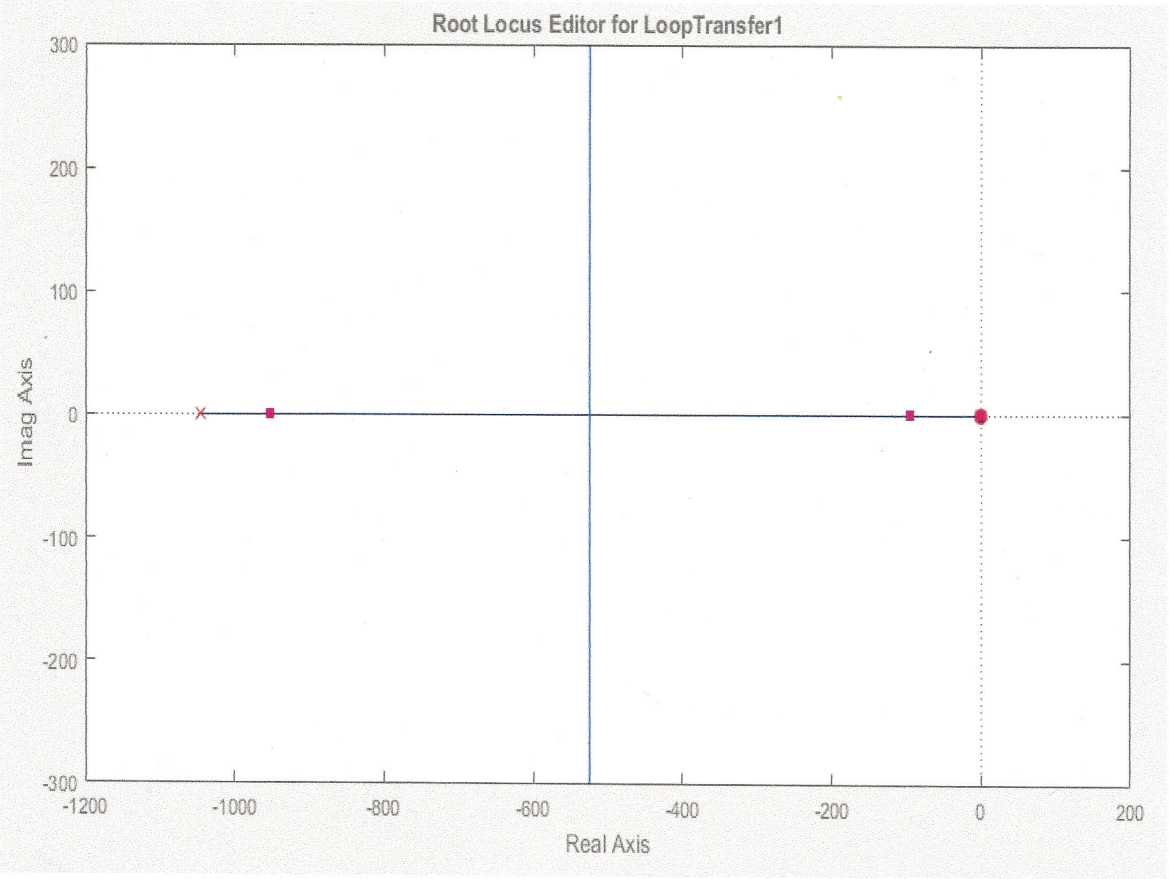

Figure 7.20: Root locus of system transfer function

and settling times than the integral and pole placement controllers because of changes we made to the Q and R matrices.

Third controller: The output of the LQG controller gives the best performance in overshooting and settling time. Moreover, in this controller we can adjust the settling time and create a compensator to adjust the parameter of the system automatically according to the settling time. It can also deal with the noise using the Kalman filter.

7.9.5 Compare the result of integral pole placement, integral LQR and LQG controllers

The optimal control outputs of pole placement and LQG controllers are shown in Figure 7.17. The LQG controller shows better results than the pole placement and LQGcontrollers, as seen in Table 7.2. Table 7.2: Comparing results between the outputs of pole placement

and the outputs of LQR and LQG controllers

Table 7.2: Compare the results between the output of poles placement, the output of LQR and LQG controllers

Property	Pole placement controller	LQR controller	LQG controller
Rise time Tr	5.67 sec	0.756 sec	0.16 sec
Steady state time Tss	5 sec	0.7 sec	0.1 sec
Peak time	1.3 sec	0.3 sec	0.02 sec
Over shooting	6.363%	0.9	0.00%

Chapter 8

CONCLUSIONS AND FUTURE WORK

8.1 Introduction

This research has contributed to the field of wind turbine generators by exploring the rotor angle and keeping track of the wind inflow angle. This is a relatively new area that has growing importance given the continual increase in energy capture from wind speed. This work is helping to provide a framework for future investigations of enhanced and optimized wind turbine mechanisms, as well as giving specific guidelines for large-scale wind turbine usage.

8.2 Summary of contributions

The main contributions of this work are as follows:

1. Identifying how characteristics of modified wind turbines can affect wind turbine performance

The modification of wind turbines through the addition of universal joint to its rotor allows it to change angles.

2. Creating a model that represents the rotor angle applications

This enables the relationship between variable rotor angles and wind inflow angles to be studied.

3. Providing additional support to continuing wind turbine energy capture

The work studies the impact of this new technique (rotor angle) on wind turbine energy capture.

8.3 Conclusion

The proposed optimization techniques are based on wind turbine rotor angles through the investigation of variations in wind turbine performance. This study demonstrates the effect of the proposed model on rotor angle and its angle changes in a multidimensional way.

The work both theoretically and experimentally studies the performances of wind turbines relating to variable rotor angles. As well, the study depicts variable and fixed rotor angles and confirms which rotor angle is the most practical for the design and optimization of energy captured from wind turbines. It shows that it is possible to adjust the rotor angle according to the incoming wind inflow angle. The study also shows several models demonstrating wind turbines with changeable rotor angles. Overall, the work focuses on the interaction between wind direction and rotor angle control system strategies and considers how multiple aspects of control systems are combined in a variety of ways to enhance the energy captured from wind turbines. Additionally, the study shows how a wind turbine with changeable rotor angles tracks the wind inflow angle. A new micro-controller is developed to organize and interconnect all models. Hence, this work is important in the investigation, modeling, and experimental analysis of various inflow angle solutions for the development of a new generation of wind turbines with variable rotor angles that can handle changes in wind inflow angles.

8.4 Future work

1. In the present work, the variable turbine rotor angle is used for small-scale wind turbines, showing positive results. However, future work will consider large-scale wind turbines.
2. The proposed system is tested under limited sources (fan), as the wind tunnel available at Dalhousie University was not large enough for the wind turbine. Future work will use wind tunnels to gain more accurate results from proposed wind turbines.
3. The micro-controllers will be modified by using the interlock system to protect the variable turbine rotor angle control from damage.
4. The variations in wind inflow angle will also be taken into consideration to increase the energy capture and reduce fatigue load.

8.4.1 Multi-Processor Controller (MPC)

Future work will use MPC for monitoring and controlling all functions of the wind turbines. The MPC controller serves the following functions:
1. Monitoring and supervising of the operation.
2. Operating of the turbine during various fault situations.

3. Automatic yawing of the nacelle in accordance to the wind direction.
4. Controlling the blade pitch.
5. Controlling the rotor yaw angle.
6. Controlling the rotor angular deflection.
7. Power control and variable speed.
8. Monitoring of ambient conditions (wind, temperature).
9. Monitoring of the grid.

8.4.2 Control and regulation

Different forms of wind turbine energy capture control need practical experimental setup model technologies like RAC and multidimensional optimal control mechanisms in order to optimize wind turbine operation and performance, after a link has made for the wind rotor by a universal joint. This thesis addressed the problem of wind speed inflow angles and how it varies wind turbine energy capture.

8.4.3 Meteorology dynamics (Meteodyn)

Meteodyn offers an accurate evaluation of wind characteristics data forecast on-line, which includes:
Wind speed and wind direction
Wind inflow angle
Ambient turbulence intensity
Vertical wind profile
Energy density
These data allow the user to connect the wind turbine with new techniques on-line to update its changes in yaw direction and rotor angle to continuously track wind direction and wind inflow angle.

Publication

Multidimensional Optimal Control of wind Turbine Generator

Abdulrazig Alarabi, Member, IEEE, and M. El-Hawary, Fellow, IEEE Department of Electrical and Computer Engineering
Dalhousie University Halifax, Nova Scotia, Canada, B3H 4R2
IEEE EPS (Nov. , 2014)

Rotor Angle Wind Turbine Energy Capture Control

Abdulrazig Alarabi, Member, IEEE and M. E. El-Hawary, Fellow, IEEE Department of Electrical and Computer Engineering
Dalhousie University Halifax, Nova Scotia, Canada, B3H 4R2
IEEE EPS (May ,2015)

Comparative Study of Reduced Order Model for Two and Three Area Interconnected Wind Turbines

Abdulrazig Alarabi Member, IEEE Department of Electrical and Computer Engineering
Dalhousie University, Halifax, Nova Scotia, Canada
IEEE Green Technologies Conference, Kansas City (Feb., 2016)

Bibliography

[1] http://www.nspower.ca/en/home/about-us/how-we-make-electricity/renewable-electricity/wind-farm-map.aspx(July,2015).

[2] http://www.windpowerengineering.com/construction/projects/developing-wind-projects-in-complex-terrain-using-wind-so (Augut,2015).

[3] http://www.nrcan.gc.ca/sites/www.nrcan.gc.ca/files/www/pdf/publications/emmc/renewable_energy_e.pdf(July,2015).

[4] http://www.energy.novascotia.ca/sites/default/files/renewable-electricity-plan.pdf(July,2015).

[5] http://www.google.ca/webhp?sourceid=chrome-instant&ion=1&espv=2&ie=UTF-8#q=upwind%20turbine%20design(July,2015).

[6] Ramesh C. Bansal Ahmed F. Zobaa. Handbook of Renewable Energy Technology, 2011.

[7] Mohammed Bezzazi Abdellatif Khamlichi, Brahim Ayyat and Carlos Vivas (2011). Control of Wind Turbines, Fundamental and Advanced Topics in Wind Power, 8,2011.

[8] http://www.renold.com/UploadedFiles/Brochure_UJ.pdf(2014, 7.

[9] https://colortheearthturquoise.files.wordpress.com/2012/03/horizontal-and-vertical-axis-wind-turbines-1.pdf (July, 2015).

[10] Omid Alizadeh. Electronic Thesis and Dissertation Repository,5, 2014.

[11] A. Miller, E. Muljadi, and D.S. Zinger. A variable speed wind turbine power control. *Energy Conversion, IEEE Transactions on*, 12(2):181–186, Jun 1997.

[12] R. Sakamoto, T. Senjyu, T. Kinjo, N. Urasaki, T. Funabashi, H. Fujita, and H. Sekine. Output power leveling of wind turbine generator for all operating regions by pitch angle control. In *Power Engineering Society General Meeting, 2005. IEEE*, pages 45–52 Vol. 1, June 2005.

[13] M. Mauri, I. Bayati, and M. Belloli. Design and realisation of a high-performance active pitch-controlled h-darrieus vawt for urban installations. In *Renewable Power Generation Conference (RPG 2014), 3rd*, pages 1–6, Sept 2014.

[14] N. Rosmin, S. Samsuri, M.Y. Hassan, and H.A. Rahman. Power optimization for a small-sized stall-regulated variable-speed wind turbine. In *Power Engineering and Optimization Conference (PEDCO) Melaka, Malaysia, 2012 Ieee International*, pages 373–378, June 2012.

[15] Ming-Shun Lu, Chung-Liang Chang, Wei-Jen Lee, and Li Wang. Combining the wind power generation system with energy storage equipments. In *Industry Applications Society Annual Meeting, 2008. IAS '08. IEEE*, pages 1–6, Oct 2008.

[16] D.L. Hoffman and T.S. Molinski. How new technology developments will lower wind energy costs. In *Integration of Wide-Scale Renewable Resources Into the Power Delivery System, 2009 CIGRE/IEEE PES Joint Symposium*, pages 1–1, July 2009.

[17] M.B. Kadri and S. Khan. Fuzzy adaptive pitch controller of a wind turbine. In *Multitopic Conference (INMIC), 2012 15th International*, pages 105–110, Dec 2012.

[18] Guo Peng. Nonlinear feed forward pitch controller for wind turbine based on rotor's aerodynamic characteristic. In *Machine Learning and Cybernetics (ICMLC), 2010 International Conference on*, volume 2, pages 879–883, July 2010.

[19] G. Banjac, V. Spudic, and M. Baotic. Tuning of model predictive controller for wind turbine load reduction. In *Information Communication Technology Electronics Microelectronics (MIPRO), 2013 36th International Convention on*, pages 919–924, May 2013.

[20] M. Fard, R. Rahmani, and M.W. Mustafa. Fuzzy logic based pitch angle controller for variable speed wind turbine. In *Research and Development (SCOReD), 2011 IEEE Student Conference on*, pages 36–39, Dec 2011.

[21] Lixun Zhang, Yingbin Liang, Erxiao Li, Song Zhang, and Jian Guo. Vertical axis wind turbine with individual active blade pitch control. In *Power and Energy Engineering Conference (APPEEC), 2012 Asia-Pacific*, pages 1–4, March 2012.

[22] Xue Xia, Yongzhi Qi, and Yutian Liu. Variable-speed variable-pitch coordinated control strategy of wind turbine ramping power. In *Power and Energy Engineering Conference (APPEEC), 2013 IEEE PES Asia-Pacific*, pages 1–5, Dec 2013.

[23] Yang Xiyun and Liu Xinran. A sliding mode control scheme for pitch angle in variable-pitch wind turbine. In *Control Conference (CCC), 2010 29th Chinese*, pages 2284–2288, July 2010.

[24] Ghanim Putrus, Mahinsasa Narayana, Milutin Jovanovic, and Pak Sing Leung. Maximum power point tracking for variable-speed fixed-pitch small wind turbines. In *Electricity Distribution - Part 1, 2009. CIRED 2009. 20th International Conference and Exhibition on*, pages 1–4, June 2009.

[25] Jiawei Chen, Jie Chen, and Chunying Gong. New overall power control strategy for variable-speed fixed-pitch wind turbines within the whole wind velocity range. *Industrial Electronics, IEEE Transactions on*, 60(7):2652–2660, July 2013.

[26] Jie Zhang, Min Wu, Jianqi An, and Jin hua She. Application of a disturbance rejection method based on equivalent-input-disturbance on a sealing machine. In *Digital Manufacturing and Automation (ICDMA), 2010 International Conference on*, volume 1, pages 252–255, Dec 2010.

[27] M. Mirzaei, M. Soltani, N.K. Poulsen, and H.H. Niemann. An mpc approach to individual pitch control of wind turbines using uncertain lidar measurements. In *Control Conference (ECC), 2013 European*, pages 490–495, July 2013.

[28] Chen Yan, Wang Xiang-dong, Li Shu-jiang, and Kong Li-xin. Optimal speed tracking for wind power generator via switching control. In *Industrial Electronics and Applications (ICIEA), 2011 6th IEEE Conference on*, pages 2283–2287, June 2011.

[29] Wei Qiao, G.K. Venayagamoorthy, and R.G. Harley. Design of optimal pi controllers for doubly fed induction generators driven by wind turbines using particle swarm optimization. In *Neural Networks, 2006. IJCNN '06. International Joint Conference on*, pages 1982–1987, 2006.

[30] A.G. Abo-Khalil and Dong-Choon Lee. Dynamic modeling and control of wind turbines for grid-connected wind generation system. In *Power Electronics Specialists Conference, 2006. PESC '06. 37th IEEE*, pages 1–6, June 2006.

[31] Shaolin Li, Xing Zhang, Zhen Xie, Shuying Yang, Chongwei Zhang, and Renxian Cao. A study on dynamic model and analyse of wind turbine generation system. In *Power and Energy Engineering Conference (APPEEC), 2010 Asia-Pacific*, pages 1–4, March 2010.

[32] O. Tutty, M. Blackwell, E. Rogers, and R. Sandberg. Iterative learning control for improved aerodynamic load performance of wind turbines with smart rotors. *Control Systems Technology, IEEE Transactions on*, 22(3):967–979, May 2014.

[33] J.H. VanZwieten, N. Vanrietvelde, and B.L. Hacker. Numerical simulation of an experimental ocean current turbine. *Oceanic Engineering, IEEE Journal of*, 38(1):131–143, Jan 2013.

[34] Dongliang Xie, Zhao Xu, Lihui Yang, J. Ostergaard, Yusheng Xue, and Kit Po Wong. A comprehensive lvrt control strategy for dfig wind turbines with enhanced reactive power support. *Power Systems, IEEE Transactions on*, 28(3):3302–3310, Aug 2013.

[35] S.M. Muyeen and A. Al-Durra. Modeling and control strategies of fuzzy logic controlled inverter system for grid interconnected variable speed wind generator. *Systems Journal, IEEE*, 7(4):817–824, Dec 2013.

[36] C. Eisenhut, Florian Krug, C. Schram, and B. Klockl. Wind-turbine model for system simulations near cut-in wind speed. *Energy Conversion, IEEE Transactions on*, 22(2):414–420, June 2007.

[37] C.G. Anderson, J.-B. Richon, and T.J. Campbell. An aerodynamic moment-controlled surface for gust load alleviation on wind turbine rotors. *Control Systems Technology, IEEE Transactions on*, 6(5):577–595, Sep 1998.

[38] S. Khan, A. Khan, M. Irfan, and S. Hussain. Aerodynamic analysis and dynamic modeling of small horizontal axis wind turbine. In *Robotics and Artificial Intelligence (ICRAI), 2012 International Conference on*, pages 117–124, Oct 2012.

[39] S.J. Schreck and M.C. Robinson. Horizontal axis wind turbine blade aerodynamics in experiments and modeling. *Energy Conversion, IEEE Transactions on*, 22(1):61–70, March 2007.

[40] Min Yang and Gang Xing. Research on individual pitch control based on inflow angle. In *Control, Automation and Systems Engineering (CASE), 2011 International Conference on*, pages 1–4, July 2011.

[41] T. Knudsen and T. Bak. Simple model for describing and estimating wind turbine dynamic inflow. In *American Control Conference (ACC), 2013*, pages 640–646, June 2013.

[42] Chenkai Zhang, Jun Hu, Delong Liu, and Chao Ma. A study of wind turbine blades optimization based on a rotational speed control model. In *World Non-Grid-Connected Wind Power and Energy Conference, 2009. WNWEC 2009*, pages 1–6, Sept 2009.

[43] V.D. Casas, F.L. Pena, and R.J. Duro. Automatic design and optimization of wind turbine blades. In *Computational Intelligence for Modelling, Control and Automation, 2006 and International Conference on Intelligent Agents, Web Technologies and Internet Commerce, International Conference on*, pages 205–205, Nov 2006.

[44] E. Muljadi, K. Pierce, and P. Migliore. Control strategy for variable-speed, stall-regulated wind turbines. In *American Control Conference, 1998. Proceedings of the 1998*, volume 3, pages 1710–1714 vol.3, Jun 1998.

[45] `http://beldenuniversal.com/cm/Universal-Joints/Home.html?gclid=CJ6myLXWsLUCFYtaMgodlkkA0Q(March,2013.`

[46] `http://en.wikipedia.org/wiki/Ball_joint(2,2014).`

[47] `http://www.annualreviews.org/doi/full/10.1146/annurev-fluid-122109-160634.`

[48] `http://www.freestudy.co.uk/control/t2.pdf-2016-03.`

[49] `http://learn.kidwind.org/files/manuals/ADVANCED_BLADE_DESIGN_MANUAL.pdf-2016-03,.`

[50] http://www.gov.pe.ca/photos/sites/envengfor/file/950010R1_V90-GeneralSpecification.pdf-2016-07.

[51] G. Shahgholian, P. Shafaghi, S. Moalem, and M. Mahdavian. Analysis and design of a linear quadratic regulator control for static synchronous compensator. In *Computer and Electrical Engineering, 2009. ICCEE '09. Second International Conference on*, volume 1, pages 65–69, 5, 2009.

[52] http://arduino.cc/en/Main/ArduinoBoardUno(April,2014).

[53] http://www.wind-solutions.com/(June,2016).

[54] http://www.control.aau.dk/~ms/project_proposals/11gr633-student_report.pdf(Sept.,2016).

[55] Athans M. The role and use of the stochastic Linear-Quadratic-Gaussian problem in control system design. In *IEEE Transaction on Automatic Control. AC-16 (6): 529552, (1971).*

[56] Van Willigenburg L.G.; De Koning W.L. algorithms and issues concerning the discrete-time optimal projection equations In European Journal of Control. 6 (1): 93100.8, (2000)

[57] Van Willigenburg L.G.; De Koning W.L. Optimal reduced-order compensators for time-varying discrete-time systems with deterministic and white parameters In *Automatica. 35: 129138.8, (1999)*

Appendices

Appendix A

The wind turbine models for wind turbine direction and turbine rotor angle simulations, developed at Dalhousie University in Electrical and Computer Engineering lab represent those mechanisms of wind turbine, which have the most observable influences on wind turbine system operation. Also, these models are explained widely in a number of publications.
1) Electric part of a variable wind direction model
2) Electric part of a variable turbine rotor angle model
3) Controls wind turbine rotor speed model controller models that work for the determination of wind direction and turbine rotor angle through energy capture and wind turbine performance stabilization, are discussed in chapter 4 and 5 respectively.

Micro-controller

The Arduino Uno is a micro-controller board based on the ATmega328 (data sheet). It has 14 digital input/output pins (of which 6 can be used as PWM outputs), 6 inputs, a 16 MHz ceramic resonator, a USB connection, a power jack, an ICSP header, and a reset button.
The Arduino Uno contains everything needed to support the micro-controller; simply connect it to a computer with a USB cable or power with an AC-to-DC adapter or battery to get started.
The Uno differs from all preceding boards in that it does not use the FTDI USB-to-serial driver chip. Instead, it features the Atmega16U2 (Atmega8U2 up to version R2) programmed as a USB-to-serial converter. ”Uno” means one in Italian and is named to mark the upcoming release of the Arduino 1.0. The UNO and version 1.0 will be the reference versions of the Arduino, moving forward. The UNO is the latest in a series of USB Arduino boards, and the reference model for the Arduino platform [52].

Micro-Controller data sheet

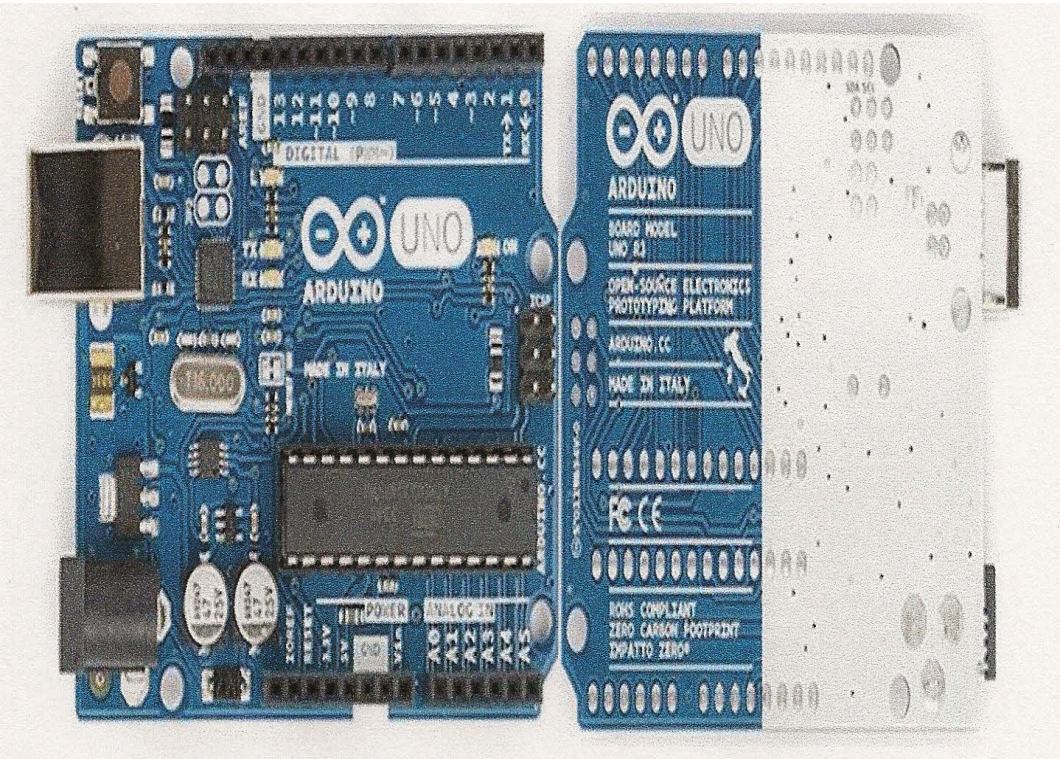

Figure 8.1: The arduino uno micro-controller board

Table 8.1: Micro-controller data sheet

Micro-controller	ATmega328
Operating Voltage	5V
Input Voltage (recommended)	7-12V
Input Voltage (limits)	6-20V
Digital I/O Pins	14 (of which 6 provide PWM output)
Analog Input Pins	6
DC Current per I/O Pin	40 mA
DC Current for 3.3V Pin	50 mA
Flash Memory	32 KB (ATmega328) of which 0.5 KB used by bootloader
SRAM	2 KB (ATmega328)
EEPROM	1 KB (ATmega328)
Clock Speed	16 MHz

Appendix B

Input and output

Each of the 14 digital pins on the Uno can be used as an input or output, using pinMode (), digitalWrite (), anddigitalRead () functions. They operate at 5 volts. Each pin can provide or receive a maximum of 40 mA and has an internal power supply.

Choose arduino uno (micro-controller) as controller for experimental set-up

The Arduino Uno is the chosen micro-controller as it is programmable, able to receive and transmit signals for inputs and outputs. Moreover, it can control the DC motor driver to drive the actuation which represent the rotor angle position.

Appendix C

Arduino motor shield motor driver

Overview

The Arduino Motor Shield is based on the L298 (datasheet), which is a dual full-bridge driver designed to drive inductive loads such as relays, solenoids, DC and stepping motors. It lets you drive two DC motors with your Arduino board, controlling the speed and direction of each one independently.

You can also measure the motor current absorption of each motor, among other features. The shield is TinkerKit compatible, which means you can quickly create projects by plugging TinkerKit modules to the board.

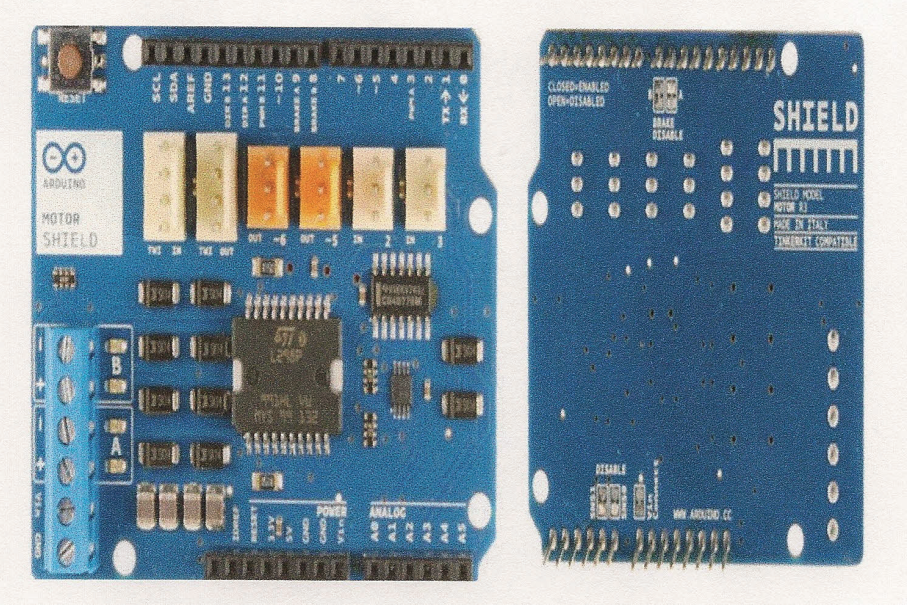

Figure 8.2: Shows Arduino Motor Shield R3 Front and Back

Arduino motor shield R3 data sheet

Table 8.2: Arduino motor drive data

Operating Voltage	5V to 12V
Motor controller	L298P, Drives 2 DC motors or 1 stepper motor
Max current	2A per channel or 4A max (with external power supply)
Current sensing	1.65V/A

Appendix D

Input and output

This motor shield has two separate channels, called A and B, that each use 4 of the Arduino pins to drive or sense the motor. In total there are 8 pins in use on this shield. You can use each channel separately to drive two DC motors or combine them to drive one bipolar stepper motor. The shield's pins, divided by the channel are shown in table **??**

- D12 motor driver out used for driving rotor in vertical direction
- D13 motor driver output used to drive the rotor in horizontal direction
- A2, A3, A4 and A5 are analog inputs
- A2 and A3 used for measuring wind inflow angle
- A4 used for feedback shown in the rotor vertical angle position
- A5 used for feedback shown in the rotor horizontal angle position

Appendix E

Micro controller operation program code:

The following is the program code used to operate the micro-controller, motor drive: wind turbine rotor angle, controller.
July, 2014 Abdulrazig Alarabi
Cotroller Two Motors
Start Matlab Controller

Start-up program

```
clc
close all
clear all                          delete(instrfind('Port''COM5'))
a = arduino('COM5')
```

Controller Two Motor Part A

displacement1 =0	Set point
displacement2 =0	Set point
m=1	
potPin2 = 0	select the input pin for the potentiometer
potPin3 = 1	select the input pin for the potentiometer
sensor1= 0	variable to store the value coming from the sensor
sensor2=0	
senor3=0	
sensor4=0	
Setup Channel A	
a.pinMode (12,OUTPUT)	Initiates Motor Channel A pin
a.pinMode (9, OUTPUT)	Initiates Brake Channel A pin
Setup Channel B	
a.pinMode(13, UTPUT)	Initiates Motor Channel B pin
a.pinMode (8,OUTPUT)	Initiates Brake Channel B pin
for m=1:2000	
displacement1= a.analogRead(2)	read the value from the sensor
sensor1= a.analogRead(3)	read the value from the sensor
displacement2= a.analogRead(4)	read the value from the sensor
sensor2= a.analogRead(5)	read the value from the sensor
displacement Pos1= displacement1 + 10;	
displacement Neg1 =displacement1 -10	
displacement Pos2 = displacement2 + 10	
displacement Neg2 = displacement2 - 10	
sen1(m) = sensor1;	
sen2(m) = sensor2;	
data = [sensor1 sensor2]	Start Motor A Controller
Start Motor A Controller	
if (displacement Pos1 $\leq sensor1)$	
a.digitalWrite(9, 0)	Disengage the Brake for Channel A
a.digitalWrite(12, 1)	Establishes forward direction of Channel A
a.analogWrite(3, 255)	Spins the motor on Channel A at full speed
end	

Controller Two Motor Part B

if (sensor1 $\geq displacement\ \ Neg1$)	
if (sensor1 $\leq displacement\ \ Pos1$)	
a.digitalWrite(9, 1)	Disengage the Brake for Channel A
a.analogWrite(3, 0)	Spins the motor on Channel A at full speed
end	
end	
if (displacement Neg1 $\geq sensor1$)	
a.digitalWrite(9, 0)	Disengage the Brake for Channel A
a.digitalWrite(12, 0)	Establishes forward direction of Channel A
a.analogWrite(3, 255)	Spins the motor on Channel A at full speed
end	
End Motor A Controller	
Start Motor B Controller	
if (displacement Neg1 $\geq sensor2$)	
a.digitalWrite(9, 0)	Disengage the Brake for Channel A
a.digitalWrite(12, 0)	Establishes forward direction of Channel A
a.analogWrite(3, 255)	Spins the motor on Channel A at full speed
end	
End Motor A Controller	
Start Motor B Controller	
if (displacement Pos2 $\leq sensor2$)	
a.digitalWrite(8, 0)	Disengage the Brake for Channel A
a.digitalWrite(13, 1)	Establishes forward direction of Channel A
a.analogWrite(11, 255)	Spins the motor on Channel A at full speed
end	
if (sensor2 $\geq displacement\ \ Neg2$)	
if (sensor2 $\leq displacement\ \ Pos2$)	
a.digitalWrite(8, 1)	Disengage the Brake for Channel A
a.analogWrite(11, 0)	Spins the motor on Channel A at full speed
end	
end	

Controller Two Motor Part C

if (displacement Neg2 $\geq sensor2$)	
a.digitalWrite(8, 0)	Disengage the Brake for Channel A
a.digitalWrite(13, 0)	Establishes forward direction of Channel A
a.analogWrite(11, 255)	Spins the motor on Channel A at full speed
end	
End Motor B Controller	
end	
plot(sen1)	
hold on	
plot(sen2)	
plot(MotorA)	
hold on	
plot(MotorB)	

Appendix F

Matlab code for integral pole placement controller:

MATLAB has been used to determine $A_{dash}, B_{dash}\ and\ gain\ matrix$

$A_{dash} = [Azeros(2,1); -C\ \ 0]$

$$A_{dash} = \begin{bmatrix} -4.8045 & -4.4037 & 0 \\ 1.0000 & 0 & 0 \\ -95.3629 & -4.4037 & 0 \end{bmatrix}$$

$B_{dash} = [B; 0]$

$$B_{dash} = \begin{bmatrix} 1 \\ 0 \\ 0 \end{bmatrix}$$

$Desired\quad poles$

$$d_{poles} = \begin{bmatrix} -2 & -2 & -1 \end{bmatrix}$$

$Matrix\ \ gain = Kgp$

$Kgp = acker(A_{dash}, B_{dash}, d_{poles})$

$$Kgp = \begin{bmatrix} 0.1955 & -83.0237 & -0.9083 \end{bmatrix}$$

$KgIp = Kgp(1:2)$

$$KgIp = \begin{bmatrix} 0.1955 & -83.0237 \end{bmatrix}$$

$The\ integral\ \ gain = KIp$

$KIp = -Kgp(3)$

$KIp = -0.9083$

The poles of the closed-loop system is the eigenvalues of the closed-loop system. The eigenvalues shows all poles in lift side of s-plane that is mean the system is stable:

$$eig(A_dash - B_dash \times Kgp) = \begin{bmatrix} -14.6328 + 9.3462i \\ -14.6328 - 9.3462i \\ -0.0462 \end{bmatrix}$$

sim('new$_r aziq'$)

figure(1);

plot(ttime,ref,'b');

hold on;

plot(ttime,Speed,'r');

xlabel('Time(sec)');

ylabel('Speed (rpm)');

title('Speed Tracking by Integral Pole Placement Controller');

figure(2);

subplot(2,1,1);

plot(ttime,Phi,'b');

ylabel('Phi(deg)');

title('States variables in Pole Placement Controller');

subplot(2,1,2);

plot(ttime,Phidot);

xlabel('Time(sec)'); ylabel('Phidot(deg/s)');

figure(3);

plot(ttime,act$_i nput,' r')$;

$xlabel('Time(sec)')$;

$ylabel('AcuatorInput(V)')$;

$title('Control\ Input\ in\ Pole\ Placement\ Controller')$;

Appendix G

Matlab code used to operate the simulation of integral and LQR controller:

clear all;

close all;

A=[-4.8045 -4.4037;1 0];

B=[1;0];

C=[95.3629 4.4037];

D=[0];

Adash=[A zeros(2,1);-C 0];

Bdash=[B;0];

Q=eye(3);

R=0.1;

k=lqr(Adash,Bdash,Q,R);

Linear quadratic matrix gain

Kgl = lqr(A$_{dash}$, $B_{dash}, Q, R)$

$Kgl = [22.0334 \quad -2.9698 \quad -3.1623]$

$Kg1l = Kgl(1:2)$

$Kg1l = [22.0334 \quad -2.9698]$

$KIl = -Kgl(3)$

$KIl = 3.1623sim$('new$_r aziq')$

figure(1)

plot$(ttime, ref,' b')$

hold on

plot$(ttime, Speed,' r')$

xlabel$('Time(sec)')$

ylabel$('Speed(rpm)')$

title$('Speed\ Tracking\ by\ Integral\ LQR\ Controller')$

figure(2)

subplot$(2,1,1)$

plot$(ttime, Phi,' b')$

ylabel$('Phi(deg)')$

title($'States\ variables\ in\ LQR\ Controller'$);

subplot$(2,1,2)$

plot$(ttime, Phidot)$

xlabel$('Time(sec)')$

ylabel$('Phidot(deg/s)')$

figure(3);

plot$(ttime, act_input,'r')$

xlabel$('Time(sec)')$

ylabel$('AcuatorInput(V)')$

title$('Control\ Input\ in\ LQR\ Controller')$